Erika Jahaira Góngora Muñoz

Development of LC-MS/MS method for the determination of glutamine and GABA in CSF - case study on Alzheimer's disease patients

Dissertação apresentada para provas de mestrado em Química Forense, orientada pelos Senhores Doutor Bruno José Fernandes Oliveira Manadas, Doutor João Eduardo Aleixo Rodrigues, e Professor Doutor Jorge Luís Gabriel Ferreira da Silva Costa Pereira, apresentada ao Departamento de Química da Faculdade de Ciências e Tecnologia da Universidade de Coimbra.

Setembro de 2021

Faculdade de Ciências e Tecnologia
da Universidade de Coimbra

Development of LC-MS/MS method for the determination of glutamine and GABA in CSF - case study on Alzheimer's disease patients

Erika Jahaira Góngora Muñoz

Dissertação apresentada para provas de mestrado em Química Forense, orientada pelos Senhores Doutor Bruno José Fernandes Oliveira Manadas, Doutor João Eduardo Aleixo Rodrigues e Professor Doutor Jorge Luís Gabriel Ferreira da Silva Costa Pereira, apresentada ao Departamento de Química da Faculdade de Ciências e Tecnologia da Universidade de Coimbra.

September, 2021

1 2 9 0

UNIVERSIDADE D
COIMBRA

The present work was performed in the Life Sciences Mass Spectrometry group of Center for Neuroscience and Cell Biology (University of Coimbra, Portugal), and under scientific guidance of Doctor Bruno Manadas and Doctor João Rodrigues.

The work was supported by Fundação para a Ciência e Tecnologia (FCT), Portugal, PTDC/MED-NEU/27946/2017, POCI-01-0145-FEDER-007440 (UIDB/04539/2020 and UIDP/04539/2020), POCI-01-0145-FEDER-016428 and the National Mass Spectrometry Network (RNEM) under the contract POCI-01-0145-FEDER-402-022125 (Ref. ROTEIRO/0028/2013).

Este projeto foi realizado no grupo Life Sciences Mass Spectrometry do Centro de Neurociências e Biologia Celular (Universidade de Coimbra, Portugal), orientado pelo Doutor Bruno Manadas e Doutor João Rodrigues.

O trabalho foi financiado pela Fundação para a Ciência e Tecnologia (FCT), Portugal, com os projetos PTDC/MED-NEU/27946/2017, POCI-01-0145-FEDER-007440 (UIDB/04539/2020 and UIDP/04539/2020), POCI-01-0145-FEDER-016428 e pela Rede Nacional de Espectrometria de Massa (RNEM), sob o contracto POCI-01-0145-FEDER-402-022125 (Ref. ROTEIRO/0028/2013).

Agradecimentos

A realização deste trabalho de tese não teria sido possível sem a colaboração de muitas pessoas a quem desejo expressar a minha gratidão.

Em primeiro lugar, quero agradecer ao Dr. Bruno Manadas pela oportunidade de realizar este trabalho e por contribuir ativamente no desenvolvimento deste. Gostaria também de expressar um enorme agradecimento ao Dr. João Rodrigues, por toda a paciência em dissipar as minhas dúvidas, bem como pelo apoio e disponibilidade demonstrados ao longo de cada uma das etapas deste projeto, obrigado pela orientação e todos os conhecimentos transmitidos.

Agradeçer ainda a todo o grupo do Life Sciences Mass Spectrometry, principalmente à Vera, por todo o conhecimento que ela compartilhou comigo e pelo apoio na realização do trabalho. Agradeço também a Maria pela colaboração demonstrada nesta fase, e também a Margarida, Inês e Miguel. Eu não teria conseguido chegar a esses resultados se não fosse por sua ajuda incondicional. Agradeço também ao Dr. Jorge da Costa Pereira, pelo seu contributo neste trabalho.

Gostaria também de agradecer às minhas colegas de mestrado a Melissa Moniz e a Rita Gastão pelos bons momentos e pela cumplicidade que tivemos nesta etapa.

Por fim, à minha família, principalmente ao meu esposo, por seu total apoio em todas as fases da minha vida. Às minhas filhas, por serem o meu impulso para a concretização dos meus objetivos. Aos meus pais, irmãs e amigos por encorajarem-me nos momentos de decaimento e sempre acreditar em mim.

Não poderia deixar de agradecer à cidade que me acolheu nestes anos e a todas as pessoas que, de uma forma ou outra, tornaram a minha estadia mais confortável. Eu levarei cada pessoa no meu coração e estarei eternamente grata.

Mais uma vez, muito obrigada a todos.

Contents

List of Figures

List of Tables

Nomenclature

3-MT 3-Methoxytyramine

5-HIAA 5-Hydroxyindoleacetic acid

5-HT 5-Hydroxytryptamine

5-HTP 5-Hydroxytryptophan

%RE Percentage relative error

AAAD Aromatic amino acid decarboxylase

AB Amyloid B protein

ACh Acetylcholine

AChE Acetylcholinesterase Enzyme

AChE-Is Acetylcholinesterase inhibitors

ACN Acetonitrile

ACo-A Acetyl coenzyme A

AD Alzheimer´s disease

ADRDA Alzheimer's disease and related disorders association

ALDH Aldehyde dehydrogenase

ALR Aldehyde reductase

AMPA Alpha-amino-3-hidroxi-5-metilo-4-isoxazolpropiónico

ANOVA Analysis of variance

APOE Apolipoprotein E gen

ApoE Apolipoprotein E

APP Amyloid Precursor Protein

ATP Adenosine triphosphate

BH4 Tetrahydrobiopterin

C-PiB C-Pittsburgh compound B

CE Collision energy

CES Collision energy spread

chAT Choline Acetyltransferase

CNS Central nervous system

COMT Catechol-o-methyltransferase

CRM Charge residue model

CSF Cerebrospinal fluid

CT Computed tomography

CUR Curtain gas

CV Coefficient of variation

DA Dopamine

DAD Diode array detector

DC Direct current

DNA Deoxyribonucleic acid

DOPAC 3,4- Dihydroxyphenylacetic acid

DOPAL 3,4- Dihydroxyphenylacetaldehyde

DOPET 3,4-Dihydroxyphenylethanol

DP Declustering potential

ELISA Enzyme-linked immunosorbent assay

EMA European Medicines Agency

EO-FAD Early-onset familial Alzheimer's disease

EOAD Early-onset Alzheimer's disease

ESI Electrospray ionization

FA Formic acid

FAD Familial Alzheimer's disease

FDA Food and Drug Administration

FDG Fluorodeoxyglucose

GABA gamma-aminobutyric acid

GAD Glutamic Acid Decarboxylase

GC Gas chromatography

GLT-1 Glutamate transporter 1

Glu Glutamate

HPLC High performance liquid chromatography

HRMS High-resolution mass spectrometry

HVA Homovanillic Acid

ICH International Conference on Harmonization

IEM Ion evaporation model

IS Internal standard

ISO International Organization for Standardization

ISVF Ion spray voltage floating

IT Ion trap

IUPAC International Union of Pure and Applied Chemistry

L-DOPA L-dihydroxyphenylalanine

LC Liquid chromatography

LLOQ Lower limit of quantification

LO-FAD Late-onset familial Alzheimer's disease

LOAD Late-onset Alzheimer's disease

LOD Limit of detection

LOQ Limit of quantification

LTP Long-term potentiation

m/z Mass-to-charge ratio

MAO Monoamine oxidase

MB-COMT Membrane-bound catechol-o-methyltransferase

MeOH Methanol

MOPAL 3-Methoxy 4-hydroxyphenylacetaldehyde

MRI Magnetic resonance imaging

MRM Multiple reaction monitoring

MS Mass spectrometer

MS/MS Mass spectrometer in tandem

NCI National Cancer Institute

NE Norepinephrine

NEP Neutral endopeptidase

NFL Neurofilament light chain

NFs Neurofilaments

NFT Neurofibrillary tangles

NIA-AA National Institute on Aging and the Alzheimer's Association

NINCDS National Institute of Neurological and Communicative Disorders and Stroke

NMDA N-methyl-D-aspartate

NMDAR N-methyl- D-aspartate receptor

NMR Nuclear magnetic resonance

OLS Ordinary least squares

PEEK Polyether ether ketone

PET Positron emission tomography

pH Potential of hydrogen

PS1 Presenilin-1

Q-TOF Triple quadrupole time of flight

QC Quality control

QqQ Triple quadrupole mass spectrometer

r Coefficient of correlation

RF Radio frequency

RI Refractive index

RNA Ribonucleic acid

ROS Reactive Oxygen Species

RSD Relative standard deviation

S-COMT Soluble catechol-o-methyltransferase

S/N Signal-to-noise

SAD Sporadic Alzheimer's Disease

SFC Supercritical fluid chromatography

SPECT Single-photon emission computed tomography

SRM Selective reaction monitoring

SS Sum of squares

TH Tyrosine hydroxylase

TOF Time-of-flight

TPH Tryptophan-Hydroxylase

Trp L-tryptophan

TV Test value

Tyr L-tyrosine

USP United States Pharmacopoeia

UV-Vis Ultraviolet-visible

WLS Weighted least squares

XIC Extracted-ion chromatogram

Resumo

A doença de Alzheimer (DA) é uma doença neurodegenerativa progressiva caracterizada pela morte de neurónios em uma região específica do cérebro, condicionando a pessoa afetada à degeneração da memória, comprometimento cognitivo grave e deficiência funcional. O número de pessoas que sofrem de demência relacionada à DA é de cerca de 50 milhões, com este número aumentando rapidamente à medida que aumenta o envelhecimento da população em todo o mundo. O envolvimento de vários sistemas neurotransmissores (dopamina, glutamato, GABA, acetilcolina e serotonina) tem sido progressivamente associado a vários distúrbios neurológicos, incluindo a doença de Alzheimer. Portanto, a medição e avaliação desses neurotransmissores tornaram-se imperativas para múltiplos propósitos, incluindo o diagnóstico da doença na fase pré-clínica, previsão/monitorização do comprometimento cognitivo e o desenvolvimento da terapia farmacológica. Aqui é descrito um método de cromatografia acoplada ao método de espectrometria de massa (LC-MS/MS) utilizando um equipamento híbrido (quadropolo - tempo de voo Qq-TOF) para a separação e (semi) quantificação de glutamina, glutamato, ácido aminobutírico (GABA), acetilcolina (Ach), e colina (Cho) em amostras de líquido cefalorraquidiano (LCR). O método não usa derivatização; apenas um padrão interno marcado para cada analito e tem um tempo de execução de 15 min. Para atingir este objetivo, a injeção direta de analitos individuais no sistema MS e LC-MS/MS foi realizada como parte de uma etapa de otimização do método, sendo possível estimar as condições ótimas para cada analito em termos de separação cromatográfica e fragmentação adequada no MS, configurando o experimento em modo HR-MRM.

Após a otimização do método analítico, foi realizado um procedimento de validação para testar a capacidade do método ser aplicado na gama estabelecida. O método foi validado quanto à linearidade, precisão, exatidão, limite de detecção e limite de quantificação.

Em testes preliminares para ambos os analitos do metabolismo colinérgico, ACh e Cho, foi observado um comportamento não linear do sinal de resposta produzido em relação à concentração, gerando picos intensos a partir de baixas concentrações e mantendo valores aproximados em toda a faixa de concentração. Por conta disso, a validação foi realizada com foco nos analitos do metabolismo glutamatérgico, sendo demonstrada a linearidade do método para glutamato, glutamina e GABA. Uma regressão linear ponderada foi necessária devido à heterocedasticidade dos resultados.

Os limites inferiores de quantificação (LOQ) foram estabelecidos em 0.02, 0.03, and 0.002 pmol/µM para glutamato, glutamina e GABA, respectivamente, e a precisão e exatidão foram determinadas para os três compostos em termos de desvio padrão relativo (% RSD) e erro relativo (% RE).

Depois da validação, o método foi aplicado para medir os compostos em amostras de LCR de pacientes com DA pertencentes a 2 grupos diferentes Aβ- e Aβ+. Diferenças significativas foram encontradas entre as mulheres dos grupos Aβ+ e Aβ- para as quantidades obtidas da glutamina, indicando aumento significativo deste analito nas mulheres com Aβ+. No entanto, não foram encontradas diferenças significativas entre os pacientes com Aβ+ e Aβ-.

Encontramos ainda uma diminuição significativa nos níveis de GABA no LCR em Aβ+ em pacientes com mais de 60 anos de idade. Em contraste, não foram observadas alterações significativas nos pacientes com Aβ+ e Aβ-, nem nos dados baseados no sexo. No caso do glutamato, os

efeitos da matriz afetaram a capacidade do método de mensurar esse analito, não sendo possível sua medição.

Além disso, um aumento significativo nas medições de razão de GABA/glutamina foi encontrado nas mulheres do grupo Aβ-, é provável que a produção de glutamina aumentou enquanto GABA diminuiu em pacientes Aβ+ do sexo feminino, como um reflexo dos níveis aumentados de glutamato neste grupo. No entanto, para sugerir isso, é necessário ter medições de glutamato e estudos de várias vias metabólicas.

Palavras-chave: Doença de Alzheimer, LCR, biomarcadores, neurotransmissores, LC-MS/MS, validação.

Abstract

Alzheimer's disease (AD) is a progressive neurodegenerative disorder characterized by the death of neurons in a specific brain region, conditioning the affected person to memory degeneration, severe cognitive impairment, and functional disability. The number of people suffering from AD-related dementia is around 50 million, with this number rapidly rising as increase the aging of the population worldwide. The involvement of several neurotransmitter systems (dopamine, glutamate, GABA, acetylcholine, and serotonin) has been progressively linked to several neurological disorders, including Alzheimer's disease. Therefore, the measurement and evaluation of these neurotransmitters have become imperative for multiple purposes, including the diagnosis of the disease in the preclinical stage, prediction/monitoring of the cognitive impairment, and the development of pharmacologic therapy. Here is described a chromatography method coupled with the mass spectrometry (LC-MS/MS) method using a hybrid equipment (quadrupole - time of flight Qq-TOF) for the separation and (semi) quantification of glutamine, glutamate, aminobutyric acid (GABA), acetylcholine (Ach), and choline (Cho) in cerebrospinal fluid (CSF) samples. The method does not use derivatization; only a labeled internal standard for each analyte is used and has a run time of 15 min. To achieve this purpose, the direct injection of individual analytes into the MS and LC-MS/MS system was carried out as part of a method optimization stage, it was possible to estimate the optimal conditions for each analyte in terms of chromatographic separation and an adequate fragmentation in the MS, setting up the experiment in an HR-MRM mode.

After the optimization of the analytical method, a validation procedure was carried out in order to test the ability of the method to be applied in the established range. The LC-MS/MS method was validated with respect to linearity, precision, accuracy, the limit of detection, and the limit of quantification.

In the preliminary tests for both analytes of cholinergic metabolism, ACh and Cho, a non-linear behavior of the response signal produced with respect to concentration was observed, generating intense peaks from low concentrations and maintaining approximate values throughout the concentration range. Because of this, validation was performed with a focus on glutamatergic metabolism analytes, being demonstrated the linearity of the method for glutamate, glutamine, and GABA. A weighted linear regression was required due to the heteroscedasticity of the results.

The lower limits of quantification (LOQ) were established at 0.02, 0.03, and 0.002 pmol/µM for glutamate, glutamine, and GABA, respectively, and the precision and accuracy were determined for the three compounds in terms of relative standard deviation (% RSD) and relative error (% RE).

Once the method was validated, it was applied to measure the compounds in CSF samples from patients with AD belonging to 2 different groups Aβ- and Aβ+. Significant differences were found between the females of Aβ+ and Aβ- groups for the measurements obtained from glutamine, indicating a significant increase in the females with Aβ+. However, no significant differences were found between the AD patients with Aβ+ and Aβ-.

We further found a significant decrease in CSF GABA levels in Aβ+ from patients older than 60 years old. In contrast, no significant changes were observed in patients with Aβ+ and Aβ-, nor in the data based on gender. In the case of glutamate, the effects of the matrix affected the ability

of the method to measure this analyte, so its measurement was not possible.

Furthermore, a significant increase in the ratio measurements of GABA/glutamine was found in the Aβ- group of females, it is likely that glutamine production increased while GABA decreased in Aβ+ female patients, as a reflection of the increased glutamate levels in this group. Nevertheless, to suggest this it is necessary to have glutamate measurements and studies of various metabolic pathways.

Keywords: Alzheimer's disease, CSF, biomarkers, neurotransmitters, LC-MS/MS, validation.

Chapter 1

Introduction

1. Introduction

1.1 Alzheimer's disease

Alzheimer's Disease (AD) is a chronic, progressive and, until now, incurable disorder [1–4]. AD is one of the most common neurodegenerative diseases, characterized by conditioning the affected person to memory degeneration, severe cognitive impairment and functional disability [2, 5].

AD is an important health problem with a significant economic impact on health care systems, families, and society, being referred to as the prime cause of dementia, a term used to describe different diseases marked by a progressive deterioration in brain functions [6–9].

The number of people living with this disease is rapidly rising as increase the aging of the population worldwide [7, 10, 11]. According to Alzheimer's Disease International in the World Alzheimer Report 2019, worldwide, about 50 million people are living with AD-related dementia, being expected that in 2050 they will increase to around 152 million [4].

In Europe, around 10 million people suffer from AD, being Italy the country with the highest incidence, 2.37% of its population. In Portugal, the presence of this disease is increasing, representing 2.11% of the population [12]. Comparing the rates by sex and age, it stands out that women have approximately 1.5- to 3-fold the incidence concerning men in all European countries, and the number of people with AD increases with age [12].

AD was first described by psychiatrist Alois Alzheimer in 1906 when the first case was reported. A 51-year-old German woman named Auguste Deter with symptoms including hallucinations, disorientation, loss of language and memory [9, 13, 14]. The woman died at 55 years old, and her autopsy described what is currently considered the main characteristics of AD in her brain [1, 14, 15]. These main pathological hallmarks of AD include the formation of extracellular senile plaques caused for the deposition of amyloid β (Aβ) peptides and intracellular neurofibrillary tangles (NFT) at the microscopic level, causing progressive degeneration of synapsis and neuronal loss [9, 16–20]. In terms of macroscopic level, it is characterized by a notable atrophy of the brain (figure 1.1) [9].

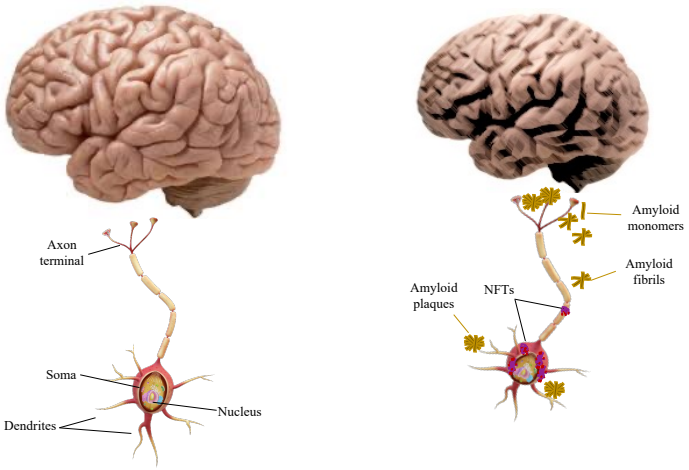

Figure 1.1: Diagram illustrating pathological hallmarks of AD

Representation of a healthy brain section (left) compared with a brain presenting hallmarks of AD (right), manifesting intracellular NFT and Aβ aggregates in the extracellular space in the form of amyloid fibrils and plaques.

These pathological changes that trigger AD can begin years and even decades before the first symptoms appear [21–24]. Symptoms at the onset of the disease tend to be diffuse and overlap with other disorders or typical deterioration with age [25].

The onset of the disease is distinguished by an inability to encode information, difficulty holding or understanding a conversation, and memory loss. But, as the disease progresses, the cognitive impairments related to synaptic loss manifest as: significant memory loss, hallucinations, learning problems, difficulty learning new things, and making decisions. Finally, functional impairment affects self-care activities, leading to permanent dependence on family care [2, 9, 17, 21, 22, 26–29]. Although AD is a complex and irreversible disease, a healthy lifestyle such as, the practice of physical activities, a balanced diet, keep learning constantly, not smoking, and an adequate sleep cycle can delay and even prevent the development of AD [7, 10, 13, 30–37].

1.1.1 Alzheimer's disease aetiology

AD may be subcategorized based on age at symptom onset and heritability. The former category is, in turn, divided into early-onset (EOAD) and late-onset (LOAD), based on an arbitrary cut-off that is typically 65 years old, but a 60-year cut-off is also used [38]. EOAD represents approximately 5% of AD cases, and typically occurs in people between the ages of 30 and 50, but around 10-15% of cases are related to a genetic cause [1, 13, 38–41].

Based on heritability (genetic predisposition), it is classiffied as familial (FAD) and sporadic (SAD) [1, 39, 41, 42]. FAD is caused by the inherited mutations in three genes: amyloid precursor protein (APP; chromosome 21), presenilin-1 (PS1; chromosome 14), and presenilin-2 (PS2; chromosome 1) [1, 13, 15, 28, 43–45]. Mutation in these genes affects the synthesis and proteolysis of APP, leading to increased production of toxic Aβ and Aβ42/Aβ40 ratio, which promotes the aggregation of Aβ into oligomers, amyloid fibrils and plaques (more details in the section 1.1.2.1). [28, 40, 41, 43].

People with FAD generally develop symptoms before 60 years old, being considered as early-onset familial Alzheimer's disease (EO-FAD). However, when the onset of symptoms is after this age, it is known as late-onset familial Alzheimer's disease (LO-FAD)[1, 38, 46].

Most people with AD (95% prevalence) have the SAD form, and it occurs mainly in people older than 60 or 65 years, know as LOAD. This type of AD is believed to be caused by defective clearance of toxic Aβ from the brain, subsequent by a combination of environmental and genetic factors [13, 38, 46–49].

In the development of the disease, the heritability of AD is considered the second factor of risk, after age [2, 5, 6, 10, 13, 41]. Although, a specific gene that directly causes SAD has not yet been found, there is one gene that has been consistently found to be associated as a risk, as the apolipoprotein E (APOE) gene, located on chromosome 19 (19q13.2) [13, 41].

APOE gene codes for making the apolipoprotein E (ApoE) , which is involved in clearance functions of Aβ such as: cholesterol metabolism, transport and storage in the brain and plasma, and also have roles in the process of neuroplasticity [13, 41, 50–53].

The APOE gene exists as three different types, called alleles, namely: ε2, ε3, ε4. APOE ε2 is relatively rare, around 8% of the general population, and it is associated with some protection or decrease in the risk for SAD. APOE ε3 is the most common, around 78% of the population; however, it is considered that it does not play a crucial role in the development of this disease [49, 50]. On the other hand, APOE ε4 is described as increasing the risk of developing SAD and

LO-FAD in people who carry one or more copies of this allele, with a higher incidence in women [50].

Unlike FAD, where the mutations in one of the three genes (APP/PS1/PS2) that are sufficient to cause AD, some people carrying the APOE ε4 allele never develop the disease, so inheriting that gene is not definitive for the development of AD [13, 41, 44, 49, 54].

1.1.2 Alzheimer's disease pathogenesis

The principal hallmarks lesions of AD at the neuropathological level are extracellular amyloid plaques and intracellular NFT [55, 56]. Both lesions are distributed throughout the hippocampus, amygdala, and certain areas of the neocortex [49]. The consequences of these pathological processes include synaptic dysfunction and neurodegeneration, which may lead to progressive atrophy of the hippocampus [13, 15, 55, 57, 58].

In this work, the hypotheses of the amyloid cascade and tau aggregation are considered as the main pathogenesis mechanisms of AD. Other hypotheses are also detailed here, namely the cholinergic hypothesis, glutamatergic hypothesis, mitochondrial dysfunction, and oxidative stress. Moreover, there are others processes involved in the development of the disease, such as metal intoxication, microglial activation, and neuroinflammation [13, 59, 60].

1.1.2.1 Amyloid cascade hypothesis

Amyloid plaques consist primarily of the extracellular accumulation of Aβ peptide, derived from APP processed by β and γ secretase in the amyloidogenic way, as shown in figure 1.2 [19, 31, 52, 61]. During this process, high amounts of insoluble fragments of Aβ with 40 and 42 amino acids (Aβ40-Aβ42) are produced, the latter being more toxic due to its potential to promote Aβ aggregates and form oligomers, protofibrils, fibrils, and finally senile plaques [9, 13, 17, 31, 59, 61, 62].

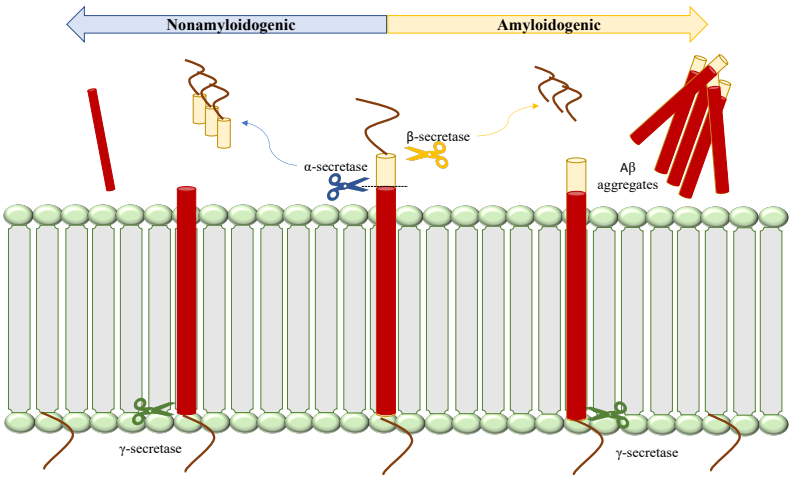

Figure 1.2: Pathways of APP metabolism.

APP is a natural protein produced in large quantities in neurons, in normal conditions is processed by α and γ-secretase in the non-amyloidogenic route, a process that does not generate Aβ, shown on the left. But, due to alterations, the metabolism of APP is altered, causing aggregation of neurotoxic Aβ through the amyloidogenic pathway, shown on the right, in which the enzymes β and γ secretase are involved. In the metabolic alteration of APP, the genetic factors, already mentioned in the Alzheimer's aetiology, are involved in the generation of Aβ and its clearance. The secretase cleavage sites are represented by colors (yellow, β-secretase; blue, α-secretase; green, γ-secretase). Adapted from: [14].

In addition to its presence in extracellular aggregates, Aβ40 and Aβ42 can be found in different regions of the brain, in intra- and extraneuronal compartments, in cerebrospinal fluid (CSF), and plasma [63]. In a normal brain, lower amounts of Aβ40 and Aβ42 are released, being Aβ40 more abundant than Aβ42 [13, 17–19, 64, 65]. But, in the early stage of AD, Aβ42 levels in the brain increase, while CSF Aβ42 levels decrease by approximately 50%. A hypothesis suggests that this may reflect the sequestration of soluble brain Aβ42 in insoluble plaques with a resulting decrease in the transport of Aβ42 from the brain [7, 58, 61, 66, 67]. However, the lack of information on the ranges of Aβ present in the brain represents a challenge in the study of the Aβ role in the normal brain [65].

The amyloid cascade hypothesis suggests amyloid plaques as the initiator and main event of AD pathology [9, 59]. They exert a toxic effect that leads to AD through some mechanisms such as hyperphosphorylation of tau, increased oxidative stress, mitochondrial dysfunction, synaptic disruption, and neurotransmitters system dysfunction, trigger neuronal disruption and death of the brain tissue [7, 17, 35, 48, 58, 61, 68]. Aggregation of Aβ could also trigger an innate immune action that causes inflammatory response (neuroinflammation) by activation of microglia and astroglia [2, 35]. In the figure 1.3 the relationship of several pathogenic mechanisms associated with the disease is represented.

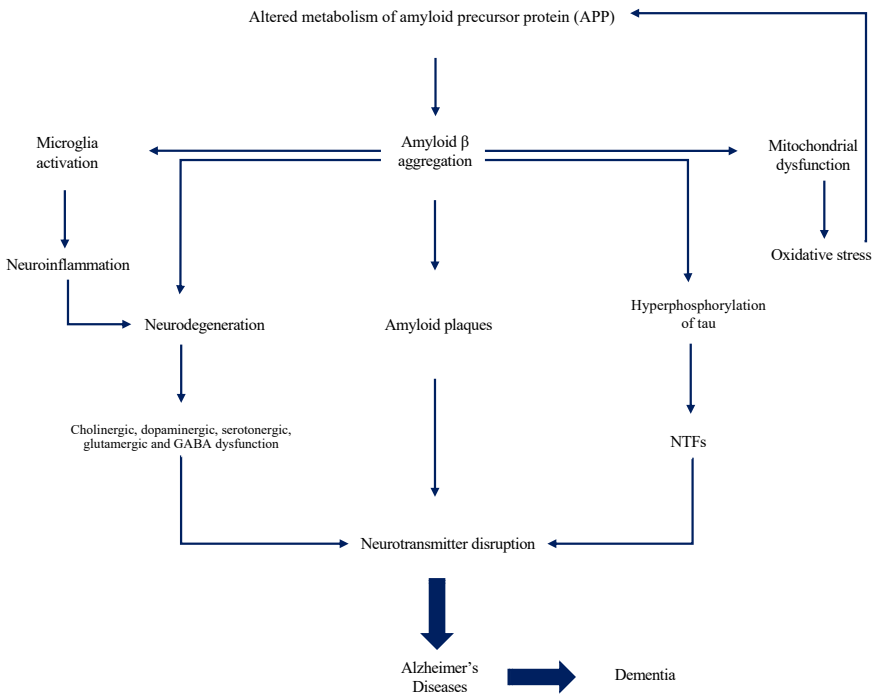

Figure 1.3: Scheme of pathogenesis

In this scheme is postulated that the accumulation of Aβ caused by an alteration in its metabolism triggers the activation of microglia and astroglia as an innate immune action which in turn causes an inflammatory response, neurodegeneration, and dysfunction of several neurotransmitters. On the other hand, the formation of NTFs can contribute to the dysfunction and loss of neurons and lead to various alterations in neurotransmitter signaling systems, typical in AD and dementia. Furthermore, Aβ aggregation is related to mitochondrial dysfunction, and this in turn to increased oxidative stress that can alter the metabolism of APP.

Neuroinflammation is also associated with as an accelerating event of AD progression. During the initial stages of AD, the activation of microglia and astroglia could be the key to generating a set of complex neuroprotective reactions involved in the clearance of Aβ. However, with the progression of the disease, this response leads to a self-perpetuating cycle of inflammatory processes that decreases the clearance of Aβ; consequently, the accumulation of Aβ in the brain increases, resulting in neurodegeneration and neuronal loss [2, 35, 60, 62, 69]. In turn, the dysfunction and loss of neurons lead to several alterations in the neurotransmitter signaling systems, typical in AD [70, 71].

As another alternative explanation to Aβ accumulation, disturbances of Aβ-related molecules in the brain, such as ApoE, can result in a deficient clearance of these oligomers.

In patients with AD the rate of clearance was 5.2% per hour, while in control subjects, it was 7.6% in the same period. The clearance of Aβ in the brain involves some proteases and enzymes; among these, neprilysin, also known as neutral endopeptidase (NEP), is identified as the most efficient extracellular proteases [61, 72].

1.1.2.2 Tau hypothesis

Tau is a microtubule-associated protein synthesized in all healthy neurons. As main function, tau promotes microtubule stability [73–75]. Microtubules are filamentous intracellular structures that are part of the cytoskeletons, assist in supporting structure, movements, shape, and especially the transport of nutrients, organelles, and products from the soma to the axon terminal and back [18].

The physiological functions of tau are regulated by various post-translational modifications through interaction with other proteins. Therefore, a disruption of these modifications can affect their functioning and even allow the development of pathological conditions [75, 76].

Phosphorylation is the principal modification of tau, which is a result of dynamic regulation in the activity of protein kinases and phosphatases [18, 73, 76]. In pathological conditions, an increase in the phosphorylation of tau is produced, probably caused by a deterioration of the activity of the enzymes mentioned above. This hyperphosphorylation reduces the affinity of tau for microtubules, resulting in detachment of microtubules, promoting the collapse of the cytoskeleton, and the formation of new tau filaments structures as straight and paired helical filament, which forms the NFT [13, 18, 58, 73–76].

The intracellular presence of NFT disrupt the interaction with other proteins by interrupting transport and their normal functions, and outside of the cell, senile plaques block neural synaptic junctions causing the neuron to become dysfunctional and leading to neuronal loss [13, 18, 19, 58, 59, 73–76].

Studies showed that in the early stage of AD, NFTs are found in the transentorhinal cortex or the entorhinal cortex in the medial temporal lobe. NFTs are spread throughout the cerebral cortex through areas of the hippocampus and finally reach the main areas of the neocortex. The spread of tau pathology occurs in a stereotyped pattern throughout a neural network, probably by interneuronal transfer [75].

There is a direct connection between Aβ aggregation and tau hyperphosphorylation in the development of AD. Hyperphosphorylation occurs after the generation of Aβ, which suggests that Aβ aggregation could initiate this process, as expressed in the amyloid hypothesis. However, the tau hypothesis suggests tau as an essential element for pathological Aβ because high concentrations of tau become neurons more vulnerable to the damage caused by Aβ aggregation [13, 59, 76].

1.1.2.3 Cholinergic hypothesis

Acetylcholine (ACh) is a neurotransmitter found primarily in the synapses of the central nervous system CNS, allowing communication between neurons. ACh is involved in a variety of functions, including learning, memory and motor functions [59, 77].

Under normal conditions, cholinergic neurons release ACh by exocytosis into the synaptic cleft during neurotransmission [59, 77]. The enzyme choline acetyltransferase (chAT) catalyzes the synthesis of ACh from two precursors acetyl coenzyme A (ACoA) and choline within the presynaptic endings [77, 78].

ACh interacts with cholinergic receptors (nicotinic and muscarinic) present in the pre-and postsynaptic membranes. Then, signal transmission is interrupted by rapid hydrolyzation of the acetylcholinesterase enzyme (AChE) into choline and acetate [77, 78].

The cholinergic hypothesis of AD suggests that the affection of the cholinergic synapse results in the onset of AD, caused by Aβ aggregation. Having as main alterations the decrease in the activity of chAT, decrease of choline uptake, deficiency in the expression of receptors, and loss of cholinergic neurons [4, 59, 71, 79–81].

The decrease and dysfunction of cholinergic neurons in the brain, especially those located in the nucleus basalis of Meynert, has been detected in AD patients, causing low levels of ACh [11, 59, 64, 82–84]. Regarding ACh receptor systems, they appear relatively unchanged in patients with AD [80]. Recent studies suggest that an increase in AchE activity can lead to a lack of Ach as well [85].

1.1.2.4 Glutamatergic hypothesis

Glutamate (Glu), is the most important excitatory neurotransmitter in the CNS and plays a crucial metabolic role in the brain. Also, it has a vital role in synaptic plasticity, as a mediator of excitatory signals in memory and learning. One of the fundamental mechanisms is through long-term potentiation (LTP) [21, 29, 86].

A disruption in the mechanism of glutamatergic has been demonstrated in AD patients, especially at the point of glutamate reuptake, which may be associated with a decrease of glutamate transporter 1 (GLT-1). Also, the increased levels of glutamate and N-methyl-D-aspartate (NMDA) receptors can be caused by a significant decline in glutamine synthetase (synthesize glutamate to glutamine) activity affected by increased oxidative stress [87].

The glutamatergic hypothesis suggests that high levels of glutamate can cause excitotoxicity in the brain [21, 29, 87]. Neurotoxicity leads to an increase in intracellular calcium followed by the activation of a cascade of enzymes with consequent cell death by necrosis or apoptosis [87]. This neuronal death appears to depend primarily on NMDA receptor overactivation, and this could lead to excessive Aβ production [29].

In vivo ante-mortem studies have been reported low glutamate levels in the temporal cortex, but lower than postmortem levels, suggesting that the damage to the glutamatergic system proceeds in parallel with the severe cognitive impairment, typical in the terminal stage of AD. However, not all reports agree with this hypothesis; several autopsies of AD patients showed lower levels of glutamate and NMDA receptors compared to healthy control subjects [88].

1.1.2.5 Mitochondria dysfunction and oxidative stress

Mitochondria are cytoplasmic organelles made up of about 1200 proteins. Although these proteins are synthesized mostly by nuclear genes, mitochondria also contain their mitochondrial genomes [89–91]. In coordination, both determine mitochondrial function and durability [69, 91–94].

Mitochondria are responsible for multiple biological processes, including intracellular calcium homeostasis, steroid synthesis, production of reactive oxygen species (ROS), and apoptosis [90, 95]. Also, it fulfills functions associated with membrane excitability and performance of neurotransmission and plasticity processes [90]. The principal function of the mitochondria is to provide the cell with adenosine triphosphate (ATP) through oxidative phosphorylation [90, 95].

Accumulation of Aβ can directly alter the functionality of the mitochondria. This alteration could potentially affect the integrity of the cell by promoting the deficiency of energy metabolism. Therefore, it can be involved in aging and the development of several common neurological disorders, including AD [91, 96].

Oxidative stress is caused by an imbalance between the production of ROS and antioxidant systems, causing free radical damage [29, 69, 93–95]. Numerous studies have suggested that oxidative stress can promote the amyloidogenic pathway of APP (which alters its normal metabolism) by decreasing the activity of α secretase activity while promoting β and γ-secretase expression [29, 93, 94].

In AD brains, some manifestations of oxidative stress have been found, like increased production of free radicals, markers of oxidative damage to DNA and RNA, decreased ATP production and cell viability [97].

1.1.3 Alzheimer's disease diagnosis

In 1984, it was established the first set of criteria for the AD diagnosis by the National Institute of Neurological and Communicative Disorders and Stroke (NINCDS) and the Alzheimer's Disease and Related Disorders Association (ADRDA). At that time, a probable diagnosis, with 90% confidence was based on medical records, neuroimaging tests, laboratory tests, family medical history, and physical-mental evaluations according to the criteria [25, 58, 98]. In contrast, a definitive diagnosis was possible only through autopsy with neuropathological confirmation of the presence of senile plaques and neurofibrillary tangles in the hippocampus [17, 48, 99, 100].

These criteria were revised in 2011 by the National Institute on Aging and the Alzheimer's Association (NIA-AA). The new guidelines identify three stages: early or preclinical stage with no symptoms, middle stage or mild cognitive impairment (MCI), and the final stage, dementia. In addition to this, biomarker tests (see section 1.3) and the use of tools to diagnose AD were incorporated [101].

The use of neuroimaging techniques provide a relevant aid for the probable diagnosis of AD, and these are classified into two categories: structural and functional neuroimaging [17, 102].

Structural imaging techniques are widely used to detect and identify structural and morphology changes in the brain, like magnetic resonance imaging (MRI) and computed tomography (CT) [17, 102, 103]. MRI is generally used to monitor hippocampal atrophy (reductions in AD patients are around 15-40% of hippocampal volume). However, this decrease can be related to the aging process and co-existing conditions [103, 104].

Functional imaging, such as fluorodeoxyglucose (FDG)-positron emission tomography (PET) and brain perfusion single-photon emission computed tomography (SPECT) offer a more accurate

diagnosis [17, 102, 103].

Amyloid PET (Aβ-PET) imaging has been incorporated into the research criteria for the diagnosis of AD, fulfilling an emerging role in the management of the disease [105]. This technique uses amyloid radiotracers that cross the blood-brain barrier and bind to aggregated Aβ, providing a virtual histopathological portrait of the burden and distribution of Aβ in the living human brain. Among these tracers, carbon-11-labeled Pittsburgh compound B (C-PiB) was the first Aβ-PET tracer used in humans and is the most extensively used and validated [102, 103, 105–110]. C-PiB was the prototype in the development of many fluoride-18 (F-18)-labeled tracers, three of which were approved by the US Food and Drug Administration (FDA) and the European Medicines Agency (EMA): florbetapir, flutemetamol and Florbetaben [105, 107, 108, 111, 112].

1.1.4 Alzheimer's disease therapy

Although many promising approaches are being explored, currently, there are no medications that slow down the progression of the disease. The development of drugs to reduce the burden of brain Aβ by reducing its production and improving its clearance process has been the main focus in recent decades. However, these have failed in clinical trials having as main hypotheses that drug administration did not start early enough to be effective or the doses used were inappropriate [2, 62, 77, 113, 114].

Currently, only four medical treatments approved by the FDA provide symptomatic relief in the early stage of AD: donepezil, rivastigmine, galantamine, and memantine [2, 8, 115]. These drugs have shown high safety and efficacy, complying with certain guarantees necessary to be commercialized internationally, focused on the correction of dysfunctional neurotransmission typical of the disease [77].

These treatments are classified into two main classes: donepezil, rivastigmine and galantamine as acetylcholinesterase inhibitors (AChE-Is) for mild to moderate stages of the disease, and the memantine as an N-methyl- D-aspartate (NMDA) receptor antagonist for moderate to severe stages, as depicts in the figure 1.4 [2, 4, 17, 59, 62, 116].

The rationale for AChE-Is is based on the cholinergic hypothesis, thus increasing synaptic ACh levels is the basis of treatment for AD patients, being the most successful to date [17, 62]. Reversible AChE-Is block the enzyme AChE delaying the hydrolysis of ACh and consequently improving cholinergic transmission [59, 77, 117].

NMDA receptor antagonist is a class of drugs that acts inhibiting the NMDA receptors. Therefore, it works as a neuroprotective agent against excess glutamate [118]. This type of drug shows therapeutic effects in a short time of treatment achieving improvements in cognitive abilities. The effectiveness of memantine in cognitive enhancement may be due to a decrease in synaptic noise caused by the overactivation of NMDA receptor activation, the inhibition of Aβ production or toxicity, and the readjustment of the balance between inhibition and synaptic excitation [118].

The efficacy of this drug was evidenced by research conducted on glutamate-injected rats [119]. The rats presented various alterations and pathological behaviors, which were significantly abrogated with the use of memantine [119].

Other antagonists that inhibit NMDA receptor activation have failed as therapeutic agents due to side effects related to the inability to fulfill their brain functions, including learning and memory. It is believed that the mechanism of action of memantine, although it consists in inhibiting the overactivation of NMDA receptors, allows its physiological activation at the same time [118].

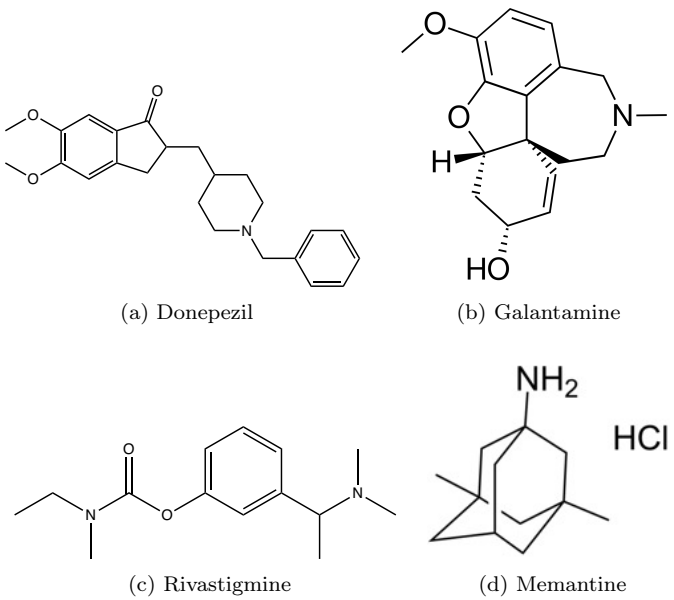

(a) Donepezil (b) Galantamine

(c) Rivastigmine (d) Memantine

Figure 1.4: Chemical structure of drug therapy approved by the FDA for the treatment of AD

To date, possible treatments are still under investigation, such as anti-inflammatory agents, antioxidants, and free radical scavengers [17]. The development of new therapeutic approaches to prevent the typical pathogenesis of AD is essential. Therapeutic goals include prevention of Aβ oligomerization at an early stage, modulation of APP/Aβ pathways, modulation of tau phosphorylation and tau aggregation [4, 11].

The use of non-pharmacological therapies, such as cognitive training, stimulation therapy, and rehabilitation, can improve the quality of life of patients with AD. Natural compounds, such as plants, could also be used because they provide abundant pharmacological effects [17, 60].

1.2 Neurotransmitters role in Alzheimer's disease

Neurotransmitters are endogenous chemicals synthesized and released by brain cells that use them to communicate with each other. Formerly, it was believed that neurons transmitted information by themselves to others through the movement of an electrical charge, but currently, neurotransmitters are known to be the central mode of synaptic transmission between adjacent nerve cells [120–122].

At a chemical synapse, neurotransmitters are released from vesicles into the synaptic cleft after exocytosis and bind to receptors on the postsynaptic cell [123]. The neuron sending the signal is called a presynaptic neuron and the receptor is called a postsynaptic neuron [123, 124]. Once the actions of neurotransmitters are completed, in most cases, it is stored in the vesicles and reuptake in the presynaptic neuron where it can be reused. However, in other cases, it is broken down into its initial components by enzymes and returned to the presynaptic neuron [123–125].

There are more than 100 different neurotransmitters, of which some of them are the ones who perform most of the body's functions. These neurotransmitters can be classified based on their molecular structure into biogenic amine, cholinergic and amino acids [126, 127].

There are five biogenic amine neurotransmitters: histamine, serotonin, and catecholamines,

namely: epinephrine, norepinephrine, and dopamine. All of them have in their structure one or more amine functional groups [120, 123, 126].

The cholinergic group is formed only by acetylcholine since it does not fit structurally in the other groups. ACh was the first neurotransmitter identified in several peripheral synapses, however, its identification in the CNS was a challenge that was overcome with the development of electrophysiological and neurochemical techniques [77, 120].

Finally, the group of amino acids neurotransmitters, glutamate, γ-aminobutyric acid (GABA), and glycine [120, 127].

Neurotransmitters have a pivotal role in regulating many brain functions, including cognition, behavior, mood, appetite, and sleep [128]. Minor imbalance in the normal levels of neurotransmitters in the CNS can affect the fulfillment of their functions, causing several neurological disorders [21, 129]. In the specific case of AD, has been evidenced the alteration in the normal functioning of cholinergic, glutamatergic, dopaminergic, serotonergic, and GABAergic systems [21, 71, 80, 130–133].

The neurotransmitter receptors associated with the clinical manifestations of AD include the cholinergic receptors α7 nicotinic and muscarinic M1 or M2, the glutamatergic receptors NMDA and AMPA, the dopamine D2 receptors, the serotonergic 5-HT6 receptors, and for GABA, the ionotropic and metabotropic receptors [130, 132–134]. Probably the alterations in their function are caused by the deterioration of the brain pathways. These brain pathways modulate the receptors in response to pharmacological treatments, pathological state, or physiological adaptations [134].

1.2.1 Dopamine

Dopamine or 3,4-dihydrophenylethylamine (DA), is the principal neurotransmitter in the family of catecholamines. It is composed by a catechol nucleus, a benzene ring with two hydroxyls groups in its structure [123, 135].

DA is synthesized in the CNS and at several peripheral sites. In the CNS, dopamine is present primarily in the substantia nigra, the ventral tegmental area of the midbrain, and the hippocampus. Among its functions, DA is responsible for communication between the substantia nigra and other brain regions associated with movement control, it has a vital role in processes of motivation, reward, and various cognitive functions as synaptic plasticity and memory [125, 136–139]. In the peripheral areas, DA acts as a modulator of vascular tone, cardiac, endocrine, and renal function, blood pressure, glucose metabolism, immune regulation, and gastrointestinal motility [125, 140].

Tyrosine hydroxylase (TH) is the rate-limiting enzyme for DA synthesis [136, 141, 142]. TH catalyzes the hydroxylation of L-tyrosine (Tyr) to L-dihydroxy-phenylalanine (L-DOPA), it uses oxygen and tetrahydrobiopterin (BH4) in equimolar amounts as cosubstrate and cofactor, respectively (see figure 1.5) [123, 143]. Individuals with a mutation in the TH gene cause a deficiency of the TH enzyme that is related to early Parkinson's disease [142].

L-DOPA is rapidly converted to DA in CNS by decarboxylation mediated by the enzyme action of L-aromatic amino acid decarboxylase, also called DOPA decarboxylase [123]. After being synthesized in the cytosol of neurons, DA can be transported and stored in synaptic vesicles. In a few minutes, DA is released by exocytosis or directly into the synaptic space, where it can interact with the post and presynaptic dopamine receptors [139, 144].

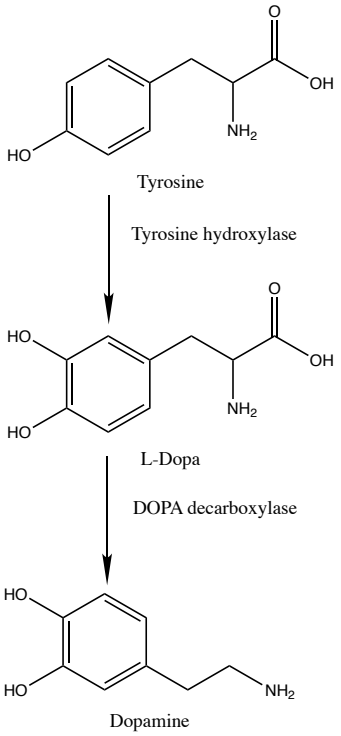

Figure 1.5: Biosynthesis of dopamine

Synthesis of the dopamine begins with the conversion of L-tyrosine to L-dihydroxy- phenylalanine (L-DOPA) by tyrosine hydroxylase (TH), and then is converted to Dopamine by DOPA decarboxylase.

Through enzymatic catabolism and reuptake, the inactivation of dopamine is achieved [143, 144]. Reuptake is the principal mechanism of DA inactivation by the action of monoamine transporters or dopamine transporter that carry it from the synaptic space to the cytosol in presynaptic neurons [145].

Catabolism of DA occurs rapidly in the neuron. It occurs by two enzymatic pathways, via monoamine oxidase (MAO) and catechol-o-methyltransferase (COMT) (figure 1.6) [143]. MAO is an enzyme located in the outer membrane of the mitochondria. MAO has two isoenzymes: MAOA and MAOB, found mainly in catecholaminergic neurons and astrocytes, respectively [136, 144]. Even when both act on dopamine, MAOA is most related to norepinephrine and serotonin, instead, MAOB is more associated with phenylethylamine and benzylamine [136, 144, 146]. The increase in MAOB activity is related to age, so inhibitors have been used as neuroprotective agents in the treatment of AD [147].

MAO catalyzes the oxidative deamination of DA to an aldehyde forming 3,4- dihydroxyphenylacetaldehyde (DOPAL) and by-products with neurotoxic potential such as hydrogen peroxide and ammonia [147, 148]. DOPAL is commonly processed to 3,4- dihydroxyphenylacetic acid (DOPAC) . By oxidation of its aldehyde to a carboxylic acid mediated by the enzyme aldehyde dehydrogenase (ALDH) with NADH as a cofactor of this reaction. But also DOPAL may be converted to 3,4-dihydroxyphenylethanol (DOPET) by aldehyde reductase (ALR) [138, 143, 147]. DOPET can be catalyzed by COMT, to form homovanillyl alcohol (HVAL), and DOPAC via COMT is converted in the final metabolite homovanillic acid (HVA) [139, 149].

Regarding the other pathway, COMT is a cytoplasmic enzyme, found mainly in the CNS and expressed by glial cells [120, 136, 143, 150]. COMT is encoded by the COMT gene, located in

the 22 chromosomes. It is expressed in two isoforms: a soluble form (S-COMT) and a membrane-bound form (MB-COMT), which is only found in the brain [144, 150]. A common functional polymorphism of this gene is Val158Met. This polymorphism reduces the enzyme activity and hence the metabolism of dopamine. Val158Met is associated with the characteristic cognitive impairment in AD and other disorders [150].

A small fraction of dopamine is modulated by COMT, through the transfer of a methyl group to the hydroxyl group in position 3 of dopamine from S-adenosylmethionine (a co-substrate) to generate 3-methoxytyramine (3-MT) [32, 144]. In turn, 3-MT can be converted to 3-methoxy 4-hydroxyphenylacetaldehyde (MOPAL) by the enzyme MAO, and this is converted to HVA by the enzyme ALDH [138, 148].

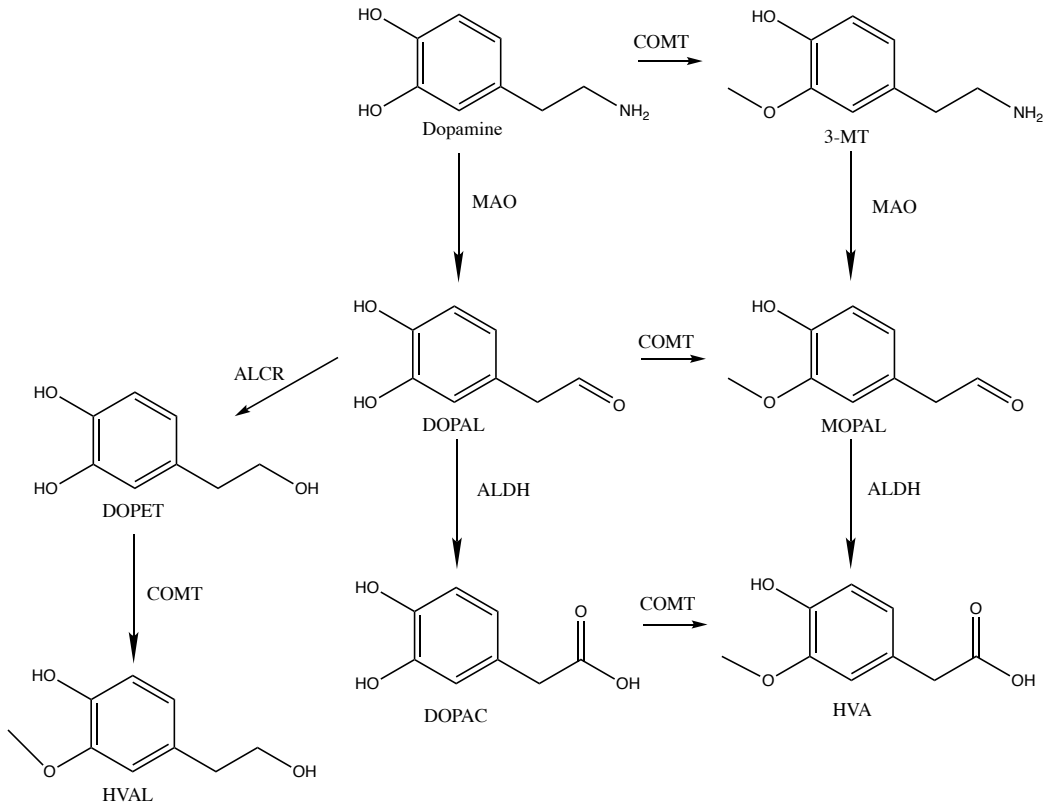

Figure 1.6: Dopamine metabolism

Dopamine is catabolized by monoamine oxidase (MAO) or catechol-O-methyl transferase (COMT), resulting in 3-methoxytyramine (3-MT) or 3,4-dihydroxyphenylacetaldehyde (DOPAL). In turn, 3-MT can be converted to 3-methoxy 4-hydroxyphenylacetaldehyde (MOPAL) by the enzyme MAO and finally converted to HVA by the enzyme ALDH. Through DOPAL, the end product is homovanillic acid (HVA). MAO: monamine oxidase; 3-MT: 3-methoxytyramine; DOPAL:3,4- dihydroxyphenylacetaldehyde; COMT:catechol-o-methyltransferase; MOPAL:3-methoxy4-hydroxyphenylacetaldehyde; DOPET: 3,4-dihydroxyphenylethanol; ALR: aldehyde reductase; ALDH: aldehyde dehydrogenase; DOPAC: 4- dihydroxyphenylacetic acid; HVA: homovanillic acid; HVAL: homovanillyl alcohol. Adapted from: [138].

DOPAC is the principal intraneuronal metabolite of the DA from MAO pathway, which then is finally metabolized to HVA, the main metabolite in urine, via COMT [139, 144]. DOPAC and HVA leave the neuron (where they are formed) crossing the neuronal membranes to enter the interstitial space where they can then diffuse into the CSF being transported out of the brain to the bloodstream or merely through the blood-brain barrier [144, 149].

Plasma DOPAC levels are approximately 50 times higher than dopamine levels due to the slow DA clearance from the circulation [151]. HVA levels are used as an indicator of dopaminergic activity since there is a concordance between the HVA concentration found in the CSF and the DA [143, 149].

3-MT is the O-methylated metabolite of the dopamine [152]. Found in low concentrations in the synaptic cleft, suggesting that 3-MT is rapidly metabolized from dopamine. Unlike DOPAC and HVA, 3-MT can be biologically active, having a vital role in the regulation of excessive stimulation of catecholaminergic neurons in the striatum by acting as an inhibitor [144, 153].

Patients with AD showed a reduction in the levels of striatal dopamine D1 receptors in PET studies that used the D1 receptor antagonist 11C-NNC756. In the same study, no change was observed in D2 receptor levels when the D2 antagonist 11C-raclopride was used [130]. Reports suggest that dopamine levels were higher in AD patients than in controls subjects [133].

Peripheral dopamine is metabolized in the kidneys, liver, gastrointestinal tract, and plasma by MAO and COMT [151]. In the kidneys, DA production depends mainly on L-DOPA uptake from the circulation, and the concentration of DA in the urine is mainly due to its uptake and decarboxylation. The decarboxylation of L-DOPA in kidneys is regulated by salt intake [152, 154].

DA also plays the role of an immediate precursor to the synthesis of norepinephrine (NE). This, in turn, is the precursor to the synthesis of epinephrine in the periphery [138].

1.2.2 Serotonin

Serotonin, or 5-hydroxytryptamine (5-HT), is a monoamine neurotransmitter of the biogenic amine group. 5-HT and its receptors are key in the coordination of food intake, body weight, temperature regulation, sexual behavior, regulation of the sleep-wake cycle, and fundamental in learning mechanisms where it plays an essential role in energy homeostatic actions [53].

The synthesis in the serotonergic neurons begins with the conversion of L-tryptophan (Trp) to 5-hydroxytryptophan (5- HTP). Mediated by the action of the enzyme L-tryptophan-5-Monooxygenase, also known as tryptophan-hydroxylase (TPH) (figure 1.7) [1, 155]. Then 5- HTP is converted to 5-HT by enzyme action of 5-hydroxytryptophan decarboxylase, also called aromatic amino acid decarboxylase (AAAD) .

As DA, 5-HT in the brain is regulated by reuptake and metabolism [156]. 5-HT is metabolized to 5-hydroxyindoleacetic acid (5-HIAA), catalyzed by the enzyme MAO, also involved in the dopamine catabolism as was described above [155].

TPH is the limiting step in the synthesis and metabolism of 5-HT. Its activity is influenced by diverse factors, such as the expression of the TPH gene, post-translational modification of proteins, and the availability of the substrates required for hydroxylation (oxygen and tryptophan). TPH also determines the production of 5-HTP and the metabolite 5-HIAA [72].

Some authors have suggested that 5-HT may also be involved in the metabolism of APP, since the activation of its serotonergic receptors seems to lead to an increase in the cleavage of α-secretase and reduction of γ-secretase, thus decreasing the reduced load of Aβ in the brain and Aβ production [21, 33]. Serotonergic neurons are among the first affected in the brain of patients with AD, even before the symptoms appear. AD patients show signs of degeneration in the serotonergic dorsal raphe nucleus, which causes a decrease in the serotonin content of the CSF and the neocortex [33].

The decrease in serotonergic neurons occurs as the reduction of 5-HT and consequently its metabolite 5-HIAA. This reduction is at least partially caused by chronic inflammation that pro-

duced degradation in the channeling of tryptophan and thence may reduce the activity of the NEP in the brain and therefore altering the clearance of Aβ [72].

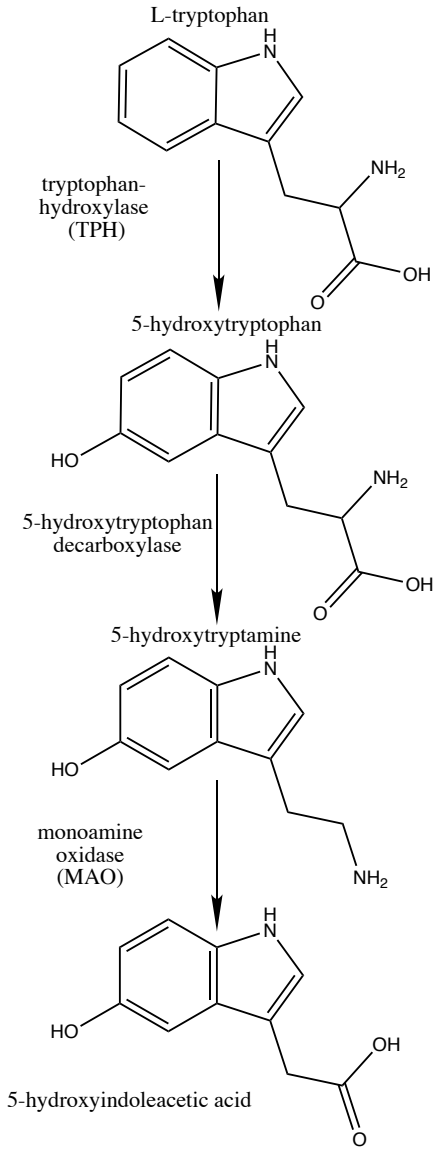

Figure 1.7: Serotonin synthesis

Serotonin is synthesized from the amino acid tryptophan to 5-hydroxytryptophan (5- HTP) by action of the enzymes tryptophan hydroxylase. This is then converted to serotonin by aromatic L-amino acid decarboxylase. Serotonin is metabolized by MAO to 5-hydroxyindoleacetic acid (5-HIAA).

Even though 5-HIAA does not have an established functional role, measurement of its levels in the CSF can indicate the status of the serotonergic system in the CNS. If 5-HTP is included in these measurements, a more in-depth study of this system can be obtained [157].

Although 5-HT is predominantly known in the CNS, it is found mostly in the gastrointestinal tract. It is also present in blood platelets, and the pineal gland, where it is a precursor to the hormone melatonin [120].

1.2.3 Acetylcholine

Acetylcholine (ACh) is a cholinergic neurotransmitter that plays a prime role in the process of memory and learning [70, 77, 80]. It is diffused in many synapses in the CNS, parasympathetic ganglia and postganglionic parasympathetic nerves, and peripherical nervous system [77, 78, 158].

ACh synthesis occurs in the nerve terminal cytoplasm in a single step, with the transfer of the acetyl group from acetyl-CoA to choline mediated by the enzyme ChAT, as shown in figure 1.8 [78, 80, 122, 159, 160].

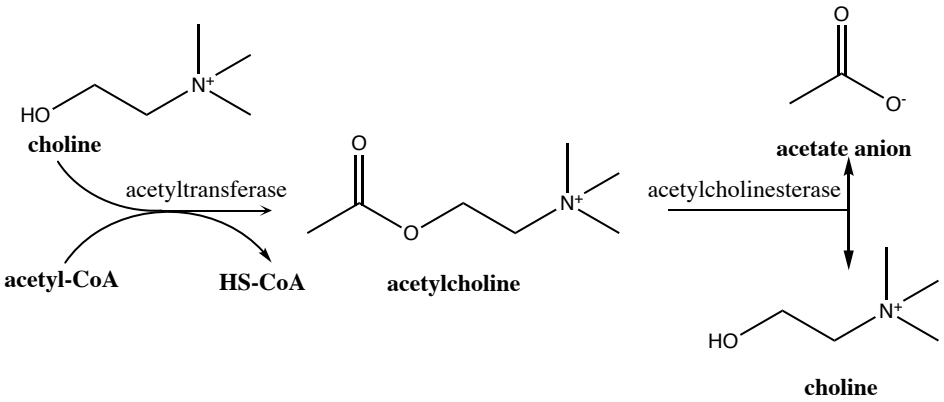

Figure 1.8: Acetylcholine synthesis and metabolism

Acetylcholine is synthesized from choline and acetyl-CoA by the action of the enzyme acetyltransferase. Then is metabolized to acetate anion and choline by the acetylcholinesterase.

Most of the ACh synthesized is transported from the cytosol to synaptic vesicles, and a small part remains free in the cytosol [77, 78]. ACh is released by exocytosis into the synaptic cleft during neurotransmission, where it interacts specifically with the cholinergic receptors (nicotinic and muscarinic) present in the pre-and postsynaptic membranes. Signal transmission is interrupted by a rapid hydrolyzation of the acetylcholinesterase enzyme (AChE) into choline and acetate [77, 78, 161]. Approximately 50% of this choline is reuptaked by the nerve terminal and reused in the synthesis of ACh [78]. AChE belongs to the group of cholinesterase, mainly distributed in the brain and neuromuscular junctions in the muscles, liver, spleen, and erythrocytes [77, 162].

The choline necessary for the synthesis of ACh comes from various sources, it can be synthesized in the liver, brain, and from reuptake, but most of it is obtained exogenously through food and supplements [159, 161]. Choline is present in the cell and nuclear membrane, as well as in the membrane of the endoplasmic reticulum and the myelin sheath. Likewise, it is found in most tissues, such as nervous tissue, plasma, liver, and CSF. Concentration levels of choline found in CSF are lower compared to plasma but accurately reflect the composition in the brain [161]. While, the acetyl-CoA is synthesized in the mitochondria by a series of reactions that begin with the oxidative decarboxylation of pyruvate, derivated from glycolysis. Acetyl-CoA is found in several areas of the brain and also in many non-neuronal tissues, such as the liver and the heart [78, 81, 122, 161, 163].

In a meta-analysis made by Maneyevitchm et al., (2018), the decrease of ACh levels found in CSF of AD patients compared to healthy control subjects was attributed to a probable reduction in the concentrations of the precursor acetyl-CoA, synthesized predominantly from pyruvate, which also registered lower levels [81]. In another study reported, an increase in the concentration of choline in CSF was determined, which could imply an alteration in its use in the ACh synthesis process [71].

1.2.4 Glutamate and gamma-aminobutyric acid (GABA)

Glutamate (Glu) is the main fast excitatory neurotransmitter in the CNS and the spinal cord, involved in various aspects related to cognitive functions [87]. Glu plays an important role in nitrogen trafficking, ammonia homeostasis in the brain, as well as linking carbohydrate and amino acid metabolism through the tricarboxylic acid (TCA) cycle [164]. The alteration of their normal levels have been associated with excitotoxicity in several neurological disorders such as AD, as already mentioned in the glutamatergic hypothesis [120, 165].

The glutamatergic neurotransmission cycle typically begins in the mitochondria of neurons in the hippocampus. Glutamate is produced in the brain by different metabolic pathways, but this work is focused on the routes from glutamine by deamidation and from α- ketoglutarate by transamination, as depicted in figure 1.9 [80, 81, 87, 120].

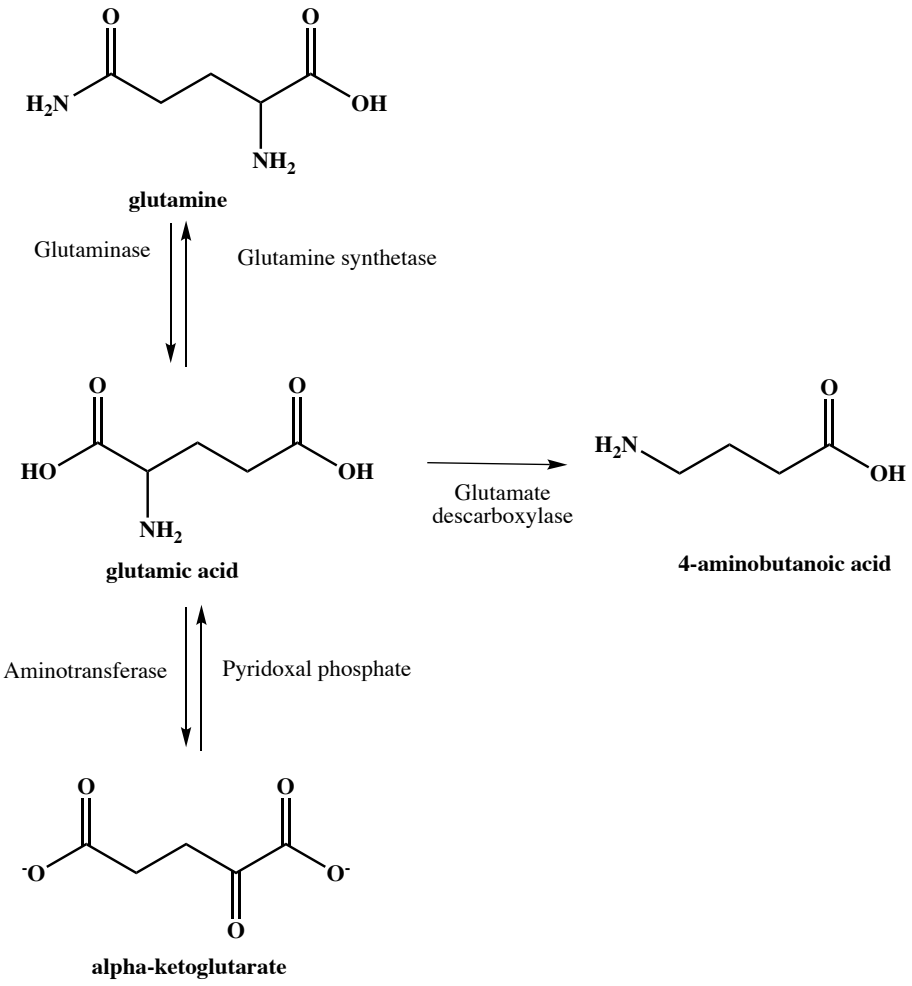

Figure 1.9: Glutamate metabolism

Glutamate is synthesized by two major pathways, from α-ketoglutarate by the action of the enzyme pyridoxal phosphate, and from glutamine by the action of the enzyme glutaminase. Glutamate is then converted to GABA by the enzyme glutamate decarboxylase.

Glutamate is packaged into vesicles mediated by the vesicular glutamate transporter molecule, then is released in the synaptic cleft and can transmit neural signals by interacting with glutamatergic receptors in postsynaptic neurons [87]. By the action of glutamine synthetase, glutamate is converted into glutamine, a nonessential amino acid widely found in plasma [120, 164, 166].

Aminotransferase is the enzyme responsible for converting glutamate back to ∝-ketoglutarate, a crucial dicarboxylic acid intermediate in the TCA cycle [120, 164, 167].

There are no glutamate-degrading enzymes in the synaptic cleft. Therefore, high-affinity presynaptic and glial transporters are responsible for clearing glutamate from the synapse after release. Glutamate transporter 1 (GLT-1) is the major glial transporter associated with this function [29].

Glu is the foremost precursor to GABA, converted by decarboxylation under the enzymatic action of glutamic acid decarboxylase (GAD) [120, 164, 165]. In contrast to glutamate's effects, GABA is the primary inhibitory neurotransmitter in the brain and plays an essential role in its metabolism [120, 165, 168]. Glutamate and GABA have important effects on sleep, learning, memory, and LPT [33, 70, 87, 120].

Although initial studies indicated that AD did not alter GABAergic receptors and neurons [169, 170], recent studies have shown that the GABAergic transmission system undergoes significant pathological changes due to AD [81, 131, 171]. Low levels of GABA in CSF and the temporal cortex were measured in patients with AD in these studies [81, 131].

1.3 The search for biomarkers

According to the National Cancer Institute (NCI), biomarkers are defined as biological molecules that could be an indicator of normal or pathogenic biological processes. Biomarkers can reflect molecular, cellular, or biochemical alterations. It can be found or measured in tissues and body fluids such as saliva, serum, plasma, CSF, urine, and bile [15, 172]. The alteration of the biomarkers caused by any pathology can be reflected with a strong level of imbalance in the affected patient, but it could also be reflected in the absence of the biomarker [172].

The measurement and evaluation of AD biomarkers has become imperative for multiple purposes, mainly for the diagnosis of the disease in the preclinical stage and the prediction/monitoring of the progression of cognitive impairment [7, 17, 21, 48, 100, 173, 174]. The ability to diagnose AD in the preclinical stages would provide a crucial opportunity for effective treatment before cognitive functions deteriorate and damage to neurons and synapses becomes irreversible [58, 175]. In clinical trials of novel drugs, biomarkers make it possible to classify the population to be studied, monitor the therapeutic response, and identify side effects [100, 176].

Biomarkers are also used in medical research to better understand disease pathogenesis, identify genetic and environmental risk factors, and use them to assess populations where biomarker data exist to attribute whether those factors contribute to AD development [174].

In the NIA-AA 2018 update guidelines, the core AD biomarkers are divided into three categories (the A/T/N system). In this classification "A" represents Aβ biomarkers, "T" tau, and "N" refers to neurodegeneration biomarkers or neuronal injury and dysfunction (table 1.1). Each category is binarized as positive or negative, being the measurement and evaluation of the AT (N) profile mainly carried out in CSF and neuroimages [23, 24, 100, 101, 173, 177, 178].

According to this categorization, the term "AD" would be applied to an individual with Aβ and tau neuropathologies, reflected either by a positive amyloid PET, decreased levels of Aβ42 in CSF, decreased Aβ42/Aβ40 ratio, positive tau PET, or increased levels of T in CSF-tau or P-tau (for details see next section) [101, 179].

Neurodegeneration is characterized by neuronal injury in specific areas of the brain or hypometabolism, measured by MRI or FDG-PET, respectively. Neurodegeneration is not a specific

marker of AD, as it can reveal any other disease, but, the combination of the three biomarkers is admitted as biological predictors of MCI conversion [23, 101, 113, 180, 181].

CSF has been considered the key source in the search for biomarkers because it has proven to be much more reliable and attractive than other sources to detect changes that occur in AD patients [23, 113, 175]. AD biomarkers can also be measured in the blood (plasma/serum), being his collection done routinely, minimally invasive, and cheap. However, a limitation in identifying AD biomarkers in blood resides in the fact that it is a complex matrix, so standardized protocols are needed to prepare the sample and analyze it [182].

In the future, when these adversities are overcome, it will be possible to apply tests for biomarkers in the blood as a screening tool in primary care [178].

Table 1.1: AT(N) classification of biomarkers in the detection of AD.

	Amyloid (A)	Tau (T)	Neurodegeneration (N)
CSF	Aβ42 or Aβ42/Aβ40	P-tau and T-tau	T-tau
Imaging	Amyloid PET, MRI, Computerized tomography	Tau PET	MRI; FDG-PET

Aβ40-Aβ42: Amyloid-beta protein with 40-42 amino acids; T-tau; total tau; P-tau: phosphorylated tau; MRI: magnetic resonance imaging; FDG-PET: fluorodeoxyglucose - positron emission tomography. Adapted from: [23, 101].

1.3.1 Biomarkers of AD in CSF

CSF is a body fluid produced mainly by a specialized structure called choroid plexus within the cerebral ventricles, about 20% of the CSF is formed extrachoroidal by the interstitium and the meninges [183, 184]. CSF not only provides physical protection and buoyancy for the CNS, but also carries nutrients to neurons and transports by-product of the metabolism of the brain and toxins acting as a lymphatic system [172, 175, 185–187].

Neurotransmitters have a pivotal role in regulating many brain functions, including cognition, behavior, mood, appetite, and sleep. Most of the compounds present in cerebrospinal fluid come from the blood. Substances such as electrolytes, soluble lipids, and water, easily cross the blood-brain barrier, so they are at roughly the same levels in both fluids. However, other compounds such as sugar, amino acids, and cations cannot move freely through this barrier, requiring specific transporters, so there is a difference between these substances in CSF and blood [172, 185, 188].

Normally, CSF is collected by lumbar puncture, in which a needle is inserted into the subarachnoid space of the lumbar region (L3/L4 or L4/L5) [100, 187, 189]. Even though lumbar puncture is a safe and routine procedure, it is a highly invasive method that requires a certain experience on the part of the medical team [149, 187, 189].

The main advantage of CSF is to be in direct contact with the extracellular space of the brain, so it reflects its composition very well. CSF is an appropriate matrix for the evaluation of different biomarkers in order to detect lesions caused by pathological processes [21, 71, 129, 187, 189–191].

Three classic CSF biomarkers have been used during the last 25 years for the diagnosis of AD: Aβ, total tau (T-tau), and phosphorylated tau (P-tau) [23, 58, 100, 113, 180]. Enzyme-linked immunosorbent assay (ELISA) is the antibody-dependent technique most commonly used to measure these markers [58, 66, 100, 180].

Increased levels of T-tau and P-tau in CSF have been measured in AD patients. In the case of P-tau, the increment has been approximately 2-3 times more than in healthy control subjects [58]. Furthermore, P-tau is considered substantial for differentiating AD from other types of dementia, because it reflects NFT load and phosphorylation status. On the other hand, even thouth T-tau is not specific to AD, it is considered as an expression of neurodegeneration [58, 100, 179, 180].

Within amyloid plaques, Aβ42 is more abundant than Aβ40, on the contrary to what was observed in the brains of healthy subjects (Aβ40 > Aβ42). Therefore, a variation in the Aβ42/Aβ40 ratio is a relevant indicator of amyloid pathology [13, 178, 180]. Studies have shown that the Aβ42/Aβ40 ratio as an indicator of amyloid pathology, it has shown higher performance than using only CSF Aβ42 as a biomarker. Nevertheless, there is still no reliable explanation for better performance using this ratio in identifying AD [13, 178, 180].

The decreased CSF levels of Aβ42 are believed to reflect the sequestration of Aβ in senile plaques of the brain, since an inverse association has been found in multiple autopsies between the CSF levels of Aβ42 and the brain amyloid load [67, 180]. ELISA can distinguish between Aβ peptides of different lengths, which makes it possible to focus on Aβ40 peptide since the variation of this fragment could represent the compensation produced by the variation of Aβ42 [113, 180].

It was not until the use of Aβ-PET scan, that relationship between brain Aβ deposit and Aβ42 in CSF was demostrated in *in vivo* studies [67]. CSF Aβ42 and Aβ-PET scan are used to define an amyloid-positivity, based on low CSF Aβ42 and presence of Aβ plaques [67]. Amyloid positivity scan indicates the presence of Aβ plaque but does not establish the diagnosis of AD or another cognitive disorder [108, 109]. A negative Aβ-PET scan, indicate there is little or no neuritic plaque at the time of image acquisition, it can be used to rule out the disease, so correlation studies between scans and CSF biomarkers have been studied, proving to be good, but does not have a complete concordance [103, 192]. In a study developed by Hansson et al. (2018), high levels of concordance between CSF Aβ42 and amyloid positive and negative PET scans was demonstrated. Cutoffs for CSF Aβ42 at 1100 pg/mL was established, [Aβ42 ≤1100 pg/mL: test positive; ≥1100 pg/mL: test negative] [192]. However, a negative Aβ-PET scan does not give 100% confidence that an AD diagnosis is rejected [111]. Nevertheless, a meta-analysis of patients with clinically diagnosed AD has shown 12% of negative on amyloid PET [193]. Another study established that the risk of developing AD was elevated 1.9-fold in amyloid-positive vs amyloid-negative participants [194].

Recently, new biomarkers have been described in the literature, such as neurofilament light chain NFL and neurogranin, proposing that they can be included as putative biomarkers of axonal and synaptic degeneration, respectively [23, 179, 195, 196].

NFL is a subunit of neurofilaments (NFs), which are cylindrical proteins that confers structural stability to neurons [23, 195, 196]. The measurement of NFL can be performed in both CSF and blood (50 times lower than in CSF). In CSF, it can be easily performed with ELISA, letting, together with classical biomarkers, better diagnostic precision up to 10 years before symptoms, differentiating AD from other neurodegenerative disorders [23, 179, 197]. Both, CSF and blood NFL levels have been shown to have increased in AD patients [180, 197].

Neurogranin is a neural-specific postsynaptic protein, expressed in hippocampus, amygdala and basal forebrain [23, 179]. Like NFL, neurogranin can be quantified in CSF. Its levels in AD patients are higher than in control patients, which could help in the identification of early symptomatic AD [180, 197].

1.3.2 Biomarkers-targeted and untargeted approaches

The lack of adequate diagnostic tests for neurological disorders has motivated the continuous search for reliable biomarkers as a valuable early diagnostic tool [198]. Neurotransmitters and their metabolites are used as biomarkers in CNS disorders at early stages [21]. Since neurotransmitter dysfunction has been linked to these disorders, it is imperative to develop reliable analytical methods to detect and monitor them [155, 199–201].

Metabolomics has emerged as a high-throughput tool in the search for predictive biomarkers [175, 201, 202], allowing the identification of alterations in metabolic function, often indicative of disease, through measurements of small molecules or metabolites resulting from a cellular metabolic process [202–205].

Metabolomics studies can be performed by two different approaches untargeted and targeted analysis [200, 206, 207]. Metabolomics approaches have become an optimal strategy to evaluate neurotransmitters [202–204, 208].

The most widely metabolomic platforms used in these approaches are nuclear magnetic resonance (NMR) and mass spectrometry [200, 206–209].

In the untargeted approach, the aim is to detect the maximum number of metabolites present in a biological sample, due to the huge amount of data collected after the analysis, it requires the use of chemometric techniques for the management of the results [202, 206, 210, 211].

In contrast, the targeted approach is used to accurately determine the quantification of specific proteins or metabolites, since it is possible to optimize not just the chromatographic separation but only the sample preparation protocol [202, 207, 212, 213]. Consequently, the use of a targeted metabolomics strategy is the favorite for studying a specific metabolic pathway or a particular class of metabolites [211].

In quantitative procedures of many fields, including biological sciences and medicine, biostatistics is used for evaluating the quality of the data acquired. Its use allows making inferences about the population and thus generates hypotheses [214, 215].

Since neurotransmitters are present in low concentrations in some biological samples, being their detection and selective measurement still a challenge, even with the use of techniques such as PET, fluorescence, chemiluminescence, colorimetry, microdialysis, and HPLC [84, 200, 216–222]. Some relevant reports of detection and quantification of neurotransmitters in biological samples based on LC-MS/MS techniques are summarized in table 1.2.

Table 1.2: Methods for detection and quantification of neurotranmitters in biological samples.

Analyte	Sample volume (μL); matrix	Equipment;run time (min)	LOD or LOQ (ng/L)	Linearity (ng/ml)	Ref.
ACh, Cho	15 ; H.CSF	UPLC-QTOF-MS; Acquity UPLC BEH amide column;18	LOQ: 5 for all analytes	5-200 (Ach); 5-1000 (Cho)	[223]
Trp,5-HTrp, E, HVA,NE,5-HIAA,Try, VMA,DA, 3MT, LDOPA,DOPAC, 5-HT,	10; H.P	LC-MS/MS; Acquity UPLC BEH HILIC column;20	3;10 (Trp, VMA, 5-HT, 5-HIAA,DA,3-MT, E); 10;30 (5-HTrp, HVA,NE, DOPAC,L-DOPA)	10-500 (5-HT, Trp,5-HIAA, Ty, DA,VMA, -3-MT, E); 30-500 (5-HTrp,HVA, L-DOPA, DOPAC, NE)	[216]
5HT,HVA,NE, 5HIAA,DOPAC, Glu,GABA,DA, HIS	80; R.CSF	LC-MS/MS; XBridge Amide BEH column;13.3	0.03;0.15 (5-HT) 1; 5 (5-HIAA) 1; 5 (HVA) 0.05;0.2 (NE) 0.02; 0.15 (DA) 20;100 (Glu) 2;4 (GABA) 0.5;1 (DOPAC) 0.03;0.12 (HIS)	0.25-4000 for all analytes	[20]
5-HT,DA, HVA,5-HIAA,DOPAC	5-10; H.CSF	UPLC-MS/MS; Acquity UPLC BEH C18 column ;25	0.2 ; 1 nM (5-HT) 0.2; 0.5 nM (DA) 6.2; 25 nM (5-HIAA) 10; 50 nM (DOPAC) 25;100 nM (HVA)	1–25nM (5-HT) ; 0.5–25 nM (DA); 25–1000 nM (5-HIAA); 50-1000 nM (DOPAC); 100-1000 nM (HVA)	[156]
DA, 5-HT, NE	10; R.BT	UPLC-MS/MS; Acquity UPLC BEH C18 column;21	LOD: 25 (DA), 5 (NE) and 2.5 (5-HT) pg/mL	25 - 5000 pg/mL (DA); 2.5 - 500 pg/mL (5-HT); 5-1000 pg/mL (NE)	[218]
ACh, Cho	10 mL; R.BT	LC-MS/MS; Lichrospher diol 100 column;14	Ach (LOD: 0.02 nM (0.2 fmol), LOQ: 0.1 nM (1 fmol)); Cho (LOD: 1 nM (10 fmol), LOQ: 3.5 nM (35 fmol))	Ach (0.1–50 nM); Cho (100–3500 nM)	[84]
Glu, Glu-d5,Gln, Gln-d6,GABA, GABA-d6	50; H.CSF	LC/MS/MS; Synergi Polar-RP column ;5	LOQ: 7.8 ng/ml for all analytes	7.8-2000 for all analytes	[165]
Asp, 5-HT, Gly, GABA,NE, E, DA, Ach,5HT, HIS, Glu	5–15; R.CSF	UPLC-MS/MS; ACE Excel 2 C18-AR column ;6	LOQ: 1 μM (Asp, 5-HT,Gly,Glu), 0.1 μM (GABA,NE,E,DA, ACh, 5HT,HIS)	0.1-10 for all analytes	[124]

H.CSF:human CSF; H.P:human plasma; R.CSF: rat CSF; R.BT: rat brain tissue; ACh: acetylcholine; Arg: arginine; Asp: aspargine; Cho: choline; E: epinephrine; Gly: glycine; Glu: glutamate; Gln: glutamine; GABA:γ-aminobutyric acid ; HIS: histamine; HVA: homovanilic acid; Trp: L-tryptophan; Tyr: L-tyrosine; Pro: proline; 5-HT: serotonin; 5HT: 5-hydroxytryptamine; 5-HIAA: 5-hydroxyindoleacetic acid; NE: norepinephrine.

Chapter 2

Analytical methodologies

2. Analytical methodologies

2.1 Techniques

2.1.1 Chromatographic techniques

Chromatography is a term applied to a group of various separation techniques based on the same principle, separating the components of a mixture according to the different speeds at which they are transported through a fixed stationary phase by a mobile phase [224–227].

Chromatographic techniques are commonly classified according to the nature of the mobile phase in three general categories: gas chromatography (GC), liquid chromatography (LC), and supercritical fluid chromatography (SFC) if the mobile phase is a gaseous, liquid, and supercritical fluid, respectively, and further by the nature of the stationary phase and the types of chemical equilibrium between both phases [224, 228, 229]. Chromatographic techniques are also classified by the physical setup in which both phases are brought into contact. When the stationary phase is fixed in a column, and the mobile phase passes through the column by pressure or gravity force, it is called column chromatography. When the stationary phase is fixed on a flat surface, and the mobile phase passes through it either by capillarity or by the influence of gravity, it is called planar chromatography [224, 228, 229].

2.1.1.1 High-performance liquid chromatography

High-performance liquid chromatography (HPLC) is a chromatographic technique widely used in the analysis of complex mixtures to separate, identify and quantify its components [226, 230, 231]. HPLC has particular advantages compared to GC in the analysis of non-volatile and thermally sensitive substances making it one of the most used techniques in chemical, pharmaceutical and food industries, and even for environmental purposes [230, 232–234].

The HPLC system typically consists of a mobile phase delivery system, sample injector, column, detector, and software for data storage and analysis figure 2.2 [230, 235].

The mobile phase delivery system is made up of reservoirs that containing the mobile phases or solvents from which the mobile phases are mixed, as well as a degassing system to eliminate gas bubbles in the solvent, and one or more pumps capable of generating high pressures and low flow rates of the mobile phase [226, 230, 236, 237]. The sampling system can be entered manually through a micro syringe or automated from vials. Both allow the introduction of tiny sample volumes with high precision into the column [226, 228, 230, 235].

The stationary phase is packed on a chromatographic column. It is used to separate the components of a sample, based on the interaction of each of them with the column, leading to different elution times (figure 2.1) [236, 237]. The components with the highest affinity adhere for the longest time and elute at the end carried by a current of the mobile phase [227, 237, 238].

The column is usually made of stainless steel tubes, since it is an inert material, resistant to high pressures, although there are also columns of glass, PEEK , and even flexible polyethylene [228, 230, 237].

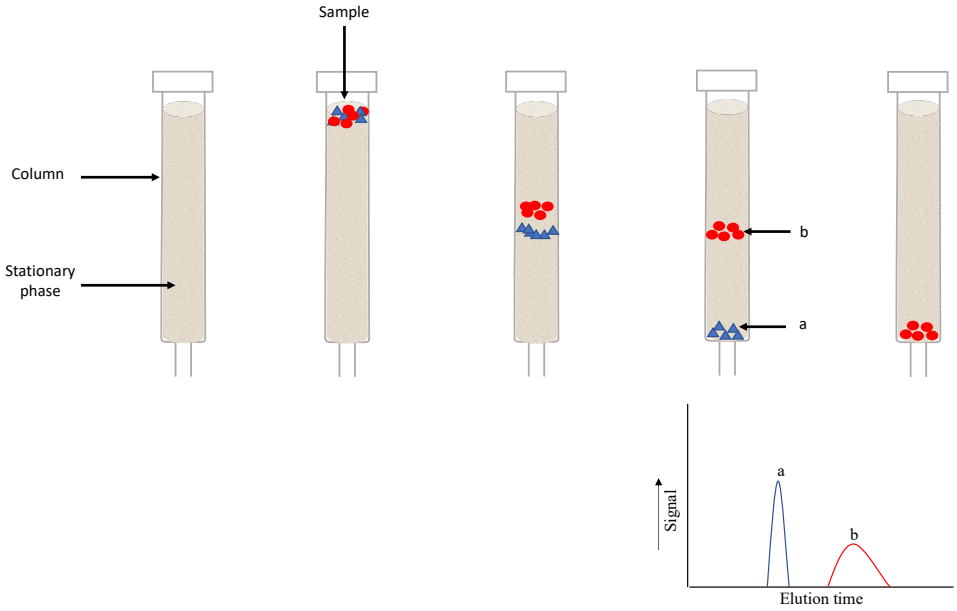

Figure 2.1: Elution of components in a mixture from a chromatographic column

Once the sample is injected and interacting with the stationary phase located on the chromatography column, components of a mixture begin and elute at different times according to their affinity for the stationary phase.

The temperature of the column affects the retention time and its selectivity. Because of this, the column is typically placed in an oven at 30-50 °C to improve its precision. Temperatures are usually not higher to avoid thermal degradation of its components [226]. The use of guard columns, a small column located between the injector and the analytical column, allows increasing its half-life by preventing impurities from entering the column [224, 228].

The HPLC separation mechanisms, in addition to being influenced by the physicochemical properties of the sample, the polarity, pH, composition, and nature of the mobile and stationary phases are also important [235, 238]. In addition to the above, some variables of the column can influence the chromatographic separation, including length, diameter, particle size, pore diameter, and homogeneity between the particles [228, 237]. Therefore, the optimization of the chromatographic method used to achieve a better separation of each compound is usually achieved by modifying specific experimental conditions, such as varying polarity, pH or flow rate of the mobile phase and reducing the diameter of the column [229].

According to the polarity of the phases, chromatography can be classified into normal and reverse phases. Chromatography in the normal phase was the first to be developed, it is characterized by non-polar mobile phase, while the stationary phase is very polar, such as silica [229, 231, 235]. Reversed-phase chromatography was developed later and is currently the most widely used. In this type of chromatography dissimilar to the normal phase, stationary phases with apolar properties are used, accompanied by polar mobile phases such as water or methanol [229, 235]. Mixtures of solvents with different polarities can change the polarity of the mobile phase. If these changes are desired to occur during the chromatographic run, gradient elution can be used. Otherwise, if no changes are required during the run, an isocratic elution can be used [235, 239].

Finally, the detector is probably the second most relevant component of an HPLC, after the column chromatography. The detector establishes the information to be acquired from the separated components and allows the identification of the components under study.

The most used detector in an HPLC are UV/Vis, diode array detector (DAD), refractive index (RI) , fluorescence, conductivity, and MS [230, 235, 240].

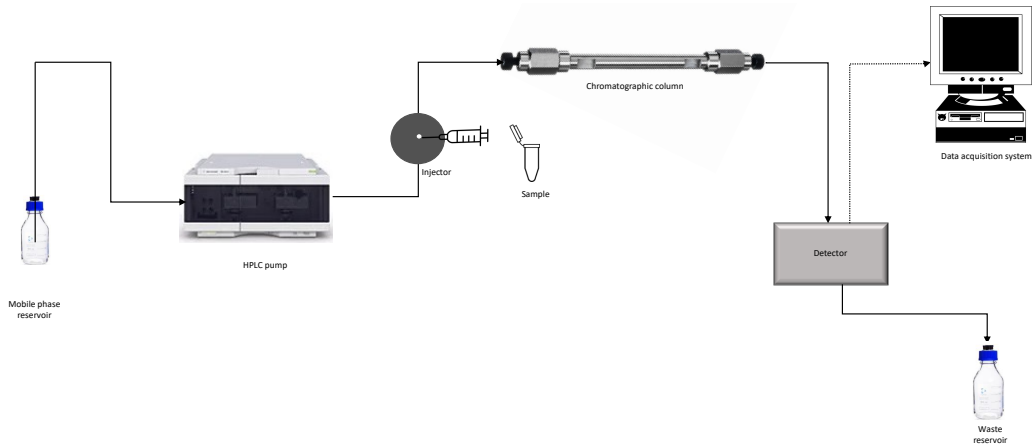

Figure 2.2: Scheme of the HPLC instruments

This scheme gives an overview of the HPLC system, which consists of mobile phase reservoirs, HPLC pumps, sample injector, chromatographic column, detector, and data acquisition system.

2.1.2 Mass spectrometry

Mass spectrometry (MS) is a sensitive and specific instrumental technique based on the production of ions from molecules or atoms. The ions generated are separated according to their mass-to-charge relationship m/z and then measured by their abundance [241–244].

Originally, mass spectrometry was used only for the analysis of small inorganic molecules. But currently, it is widely employed in qualitative and quantitative analysis of a lot of complex molecules, since it provides important information, such as the masses and structure of the molecules [242, 244–247].

Mass spectrometers are constituted of three principal components: an ion source, a mass analyzer, and a detector (see figure 2.3) [243, 244, 248, 249].

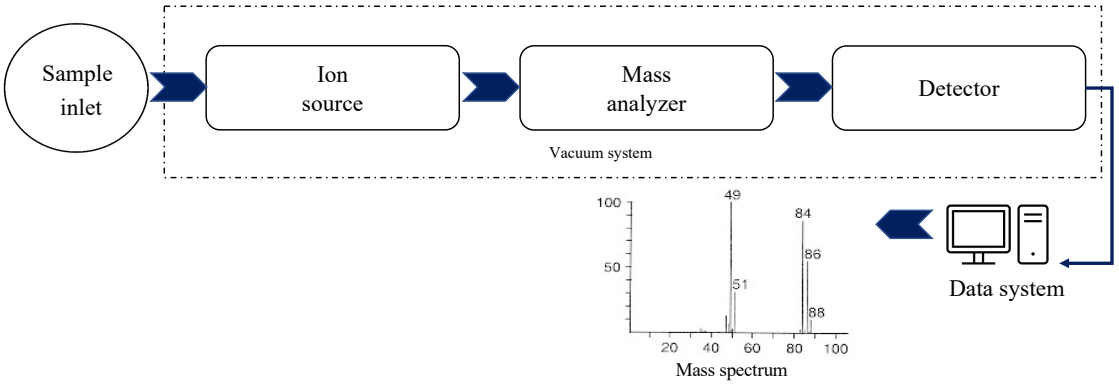

Figure 2.3: Scheme of a mass spectrometer

Mass spectrometers mainly consist of an ion source, a mass analyzer, and a detector, the last two must operate under high vacuum conditions. Once the sample mixture is introduced, the molecules or atoms are immediately converted into ions by the ion source, pass through a mass analyzer where they are classified according to their mass-to-charge ratio (m/z), and finally reach the detector. Results are recorded and displayed on a mass spectrum, a plot of signal intensity versus m/z.

The ion source is where the ionization of molecules or atoms occurs. There is a wide variety of ionization techniques available for mass spectrometry [242]. In terms of the internal energy transferred in the ionization process, hard and soft ionization methods that cause extensive and limited fragmentation, respectively, of the sample molecule [242, 250].

The development of sources like electrospray ionization (ESI) and matrix-assisted laser desorption/ionization (MALDI) allowed the ionization of small and thermostable compounds and the development of new mass analyzers and complex multi-stage instruments [251].

The ESI ion source, presented in the figure 2.4 is the most commonly method used in mass spectrometry [243, 252]. It is a soft ionization technique with high sensitivity for polar and non-volatile molecules, providing limited fragmentation [247, 253, 254]. The term electrospray refers to the dispersion of a liquid into small charged droplets by strong electric fields [242, 255].

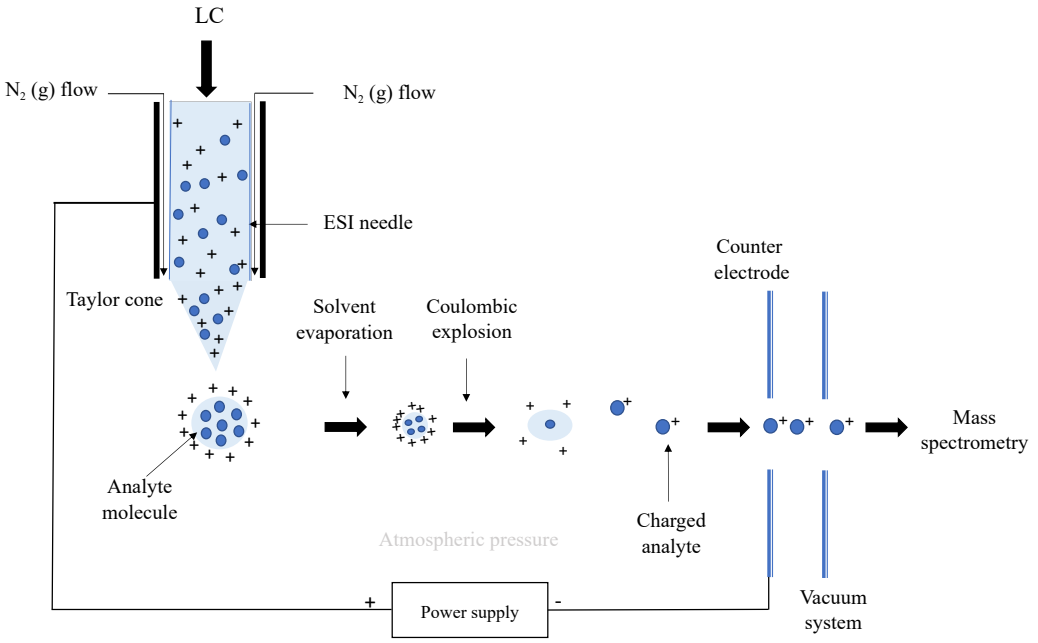

Figure 2.4: Scheme representation of the electrospray process in the positive mode

In the electrospray process, in the positive ionization mode, a weak flux is introduced in the ESI needle. Positive ions migrate towards the tip of the capillary caused by an electric field, forming analyte droplets charged with positive ions after the formation of a Taylor cone and the Coulombic explosion. Once the ions are released, some of them pass through skimmers or a heated capillary and travel toward the mass analyzer. Adapted from [256].

ESI source consists of a narrow stainless steel capillary and a counter-electrode. A high potential difference of 3-6 kV is applied (positive or negative according to the type of sample) between the tip of the capillary and the counter-electrode (detached by 0.3–2 cm), forming electric fields of the order of $10^6\ Vm^{-1}$. As a consequence of an accumulation charge generated by this electric field, the liquid emerging from the capillary assumes a Tylor cone shape at the end of the needle producing a jet of tiny charged droplets with the same charge from the needle [150, 213, 242, 244, 257]. A coaxial low gas flow around the capillary (most often dry nitrogen) allows to keep in a limited space the spray and support the nebulization [255, 256]. The droplets are repelled from the needle towards the source sampling cone on the counter electrode and drawn to the cone of MS, which is heald to opposite charge to the droplets [213].

When the surface tension of the drop cannot withstand the repulsion caused by similar loads on the surface (Rayleigh limit), the drops break into much smaller ones. This process is known as the Coulombic explosion, and consequently of this repeated process the ejection of ions from the droplet is obtained [150, 213, 256]. The process of formation of ions from small droplets has not been completely solved, but two methods have been proposed: the ion evaporation model (IEM) and the charge residue model (CRM) [213, 256].

Once the ions are released, some of them pass through skimmers and a curtain gas, such as nitrogen, or through a heated capillary and finally, they are accelerated to the mass analyzer where they are sorted according to their m/z [150, 213, 256, 258]. The result is displayed on a mass spectrum, a plot of signal intensity versus m/z of the sample [244, 259].

Since the ions generated are very reactive, the mass analyzer and detector must be operated at a high vacuum to avoid that the ions collide with other gaseous molecules in the mass analyzer on the way to the detector, because this would alter the trajectory of the ions, losing sensitivity, and increasing the complexity of the mass spectrum [242–244, 256].

Once the ions are formed, they are accelerated to the mass analyzer for sorting according to their m/z. As it happens with ionization sources, a wide variety of mass analyzers have been developed which carry out the separation of ions based on different principles [244, 248]. Two of the most common types of mass analyzers are quadrupole and time-of-flight (TOF) [246, 248].

A quadrupole mass analyzer is constituted by four cylindrically shaped rods extending in the z-direction and arranged in parallel [247, 248]. Quadrupole acts as a mass filter, separating the ions based on the stability of their flight trajectories through an oscillating electric field, as it is shown in figure 2.5 [247].

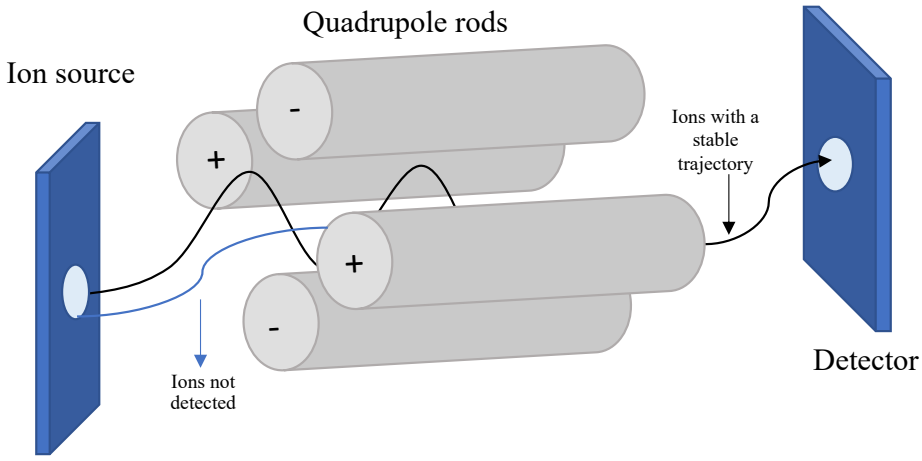

Figure 2.5: Scheme representation of a quadrupole mass analyzer

A quadrupole is constituted by four cylindrically shaped rods, connected to RF and DC, generating an electrical field. Only ions with a stable trajectory will pass through the quadrupole, whereas ions with unstable trajectories will be lost by colliding with the rods.

This field is generated when a radio frequency (RF) potential is applied in one pair of opposite rods and then is superimposed a direct current (DC) to the other pair [243, 247–249]. Therefore, depending on the electric field generated, only ions of a particular m/z will have a stable trajectory and will pass through the quadrupole, while, ions of different values of m/z (higher or lower) will have an unstable trajectory and will not reach the detector since they will collide with the rods

[241, 247, 248]. If only the RF voltage is applied to the rods, all the ions with a wide range of m/z will pass through the quadrupole [248].

Essentially, TOF is based on the principle that the ions generated in the ionization source are accelerated with the same kinetic energy through a flight tube in a drift field-free region. Therefore, ions of different m/z will take different in transit times to pass through the drift region and reach the detector that will measure the flight time [213, 248, 260]. Ions with lower m/z have a higher velocity; hence, they will reach the detector first than those with higher m/z [213, 244].

2.1.2.1 Tandem mass spectrometry

MS can be configured in tandem (MS/MS) , meaning that two or more stages of mass analyzers are arranged sequentially, usually separated by a collision cell [261–263].

This powerful arrangement has become one of the most popular techniques given its high capacity for structural identification and sensitivity of complex structures [216, 241, 242, 261–263].

In tandem MS/MS, the ions created in the ion source termed as "precursor ions" are selected on the first stage of mass analyzer, then are fragmented in a collision cell, and finally the fragments are analyzed in the second stage to generate a spectrum of the product ions [262, 264–267].

Accordingly if these events are performed separated spatially or temporally, the MS/MS instruments can be classified into tandem-in-space or tandem-in-time [242, 244, 264, 266, 268].

For tandem-in-time, the process is performed in the same physical space separated only by time, e.g. ion trap (IT) [242, 243, 264, 267, 269, 270].

Tandem-in-space is also known as beam techniques. In this configuration, all the events occur sequentially in different mass analyzers on the same instrument e.g., triple quadrupole (QqQ) [243, 254, 262, 264–266, 270].

The QqQ is obtained by placing an RF-only quadrupole that allows ions to pass and acts as a collision cell with an inert gas (such as helium, nitrogen, or argon) between two quadrupoles [241, 243, 244, 247, 249]. The main scan modes available to tandem MS are summarized in the figure 2.6 [241, 244, 249, 269].

Since tandem MS/MS is not limited to the same type of mass analyzers, the combination of two or more different types of mass analyzers is called hybrid MS. This arrangement allows obtaining better characteristics such as better resolution and precision [150, 254, 261, 266].

One typical configuration is achieved by replacing the last quadrupole of a QqQ by a TOF analyzer to produce a triple quadrupole-time-of-flight (Q-TOF) mass spectrometer [150, 249, 254, 266].

Q-TOF is a high-resolution mass spectrometry (HRMS) system, widely used in LC-MS applications [271–273]. These instruments are considered a powerful and robust tool used as an alternative to conventionally QqQ approaches for identifying and quantifying target compounds [211, 272].

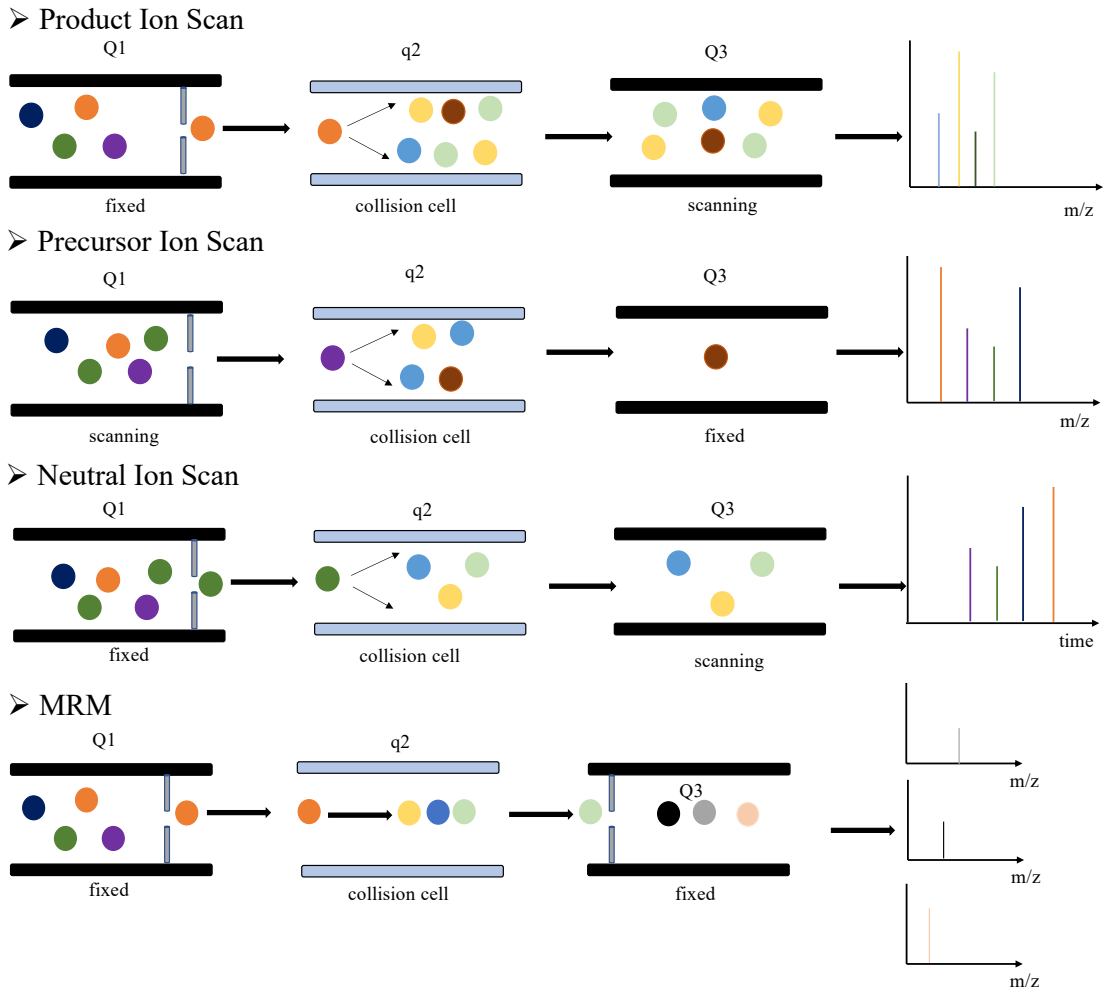

Figure 2.6: Schematic representation of the main scan modes of tandem-in-space instrument

Product ion is the mode scan more widely used in the analysis of target components in a complex mixture to generate feature fragment ions. This mode consists of the selection of a particular value of m/z in the first quadrupole (Q1), then is direct into q2 (act as a collision cell) to be fragmented, and finally in the third quadrupole (Q3) all the product ions are scanned. This process can be repeated for different precursors throughout the chromatographic run.

In precursor scan mode, the product ion with a specific value of m/z is fixed by Q3 and in Q1 are scanned all the molecules to establish which molecule can produce that product ion after the fragmentation in q2.

The neutral loss scan consists of choosing a neutral fragment that cannot be detected as it has no charge by a difference in the masses of the ions passing through Q1 and Q3. In this experiment Q1 is configured to scan all ions, fragmented into Q2, and finally, all fragmentations that lead to the loss of that neutral mass are scanned in Q3.

Multiple-reaction monitoring (MRM) mode, also known as Selective reaction monitoring (SRM), is widely applied using QqQ or QTRAP in the validation of biomarkers and for absolute quantification of low abundant molecules in biological samples. In this mode acquisition, predefined precursors and products ions (represent a transition) are simultaneously screened, in Q1 specific ions with m/z of interest are selected, fragmented in the collision cell and then one of the resulted fragments preselected are monitored by Q3. Usually, three to five transitions of the same parent ion are monitored for qualitative and quantitative methods.

A schematic of the LC-QTOF-MS instrument it is shown in figure 2.7. HRMS instruments are distinguished by providing high resolution and high mass accuracy, which allows differentiating compounds with the same nominal mass, identify unknown compounds and also establish the elemental composition [272].

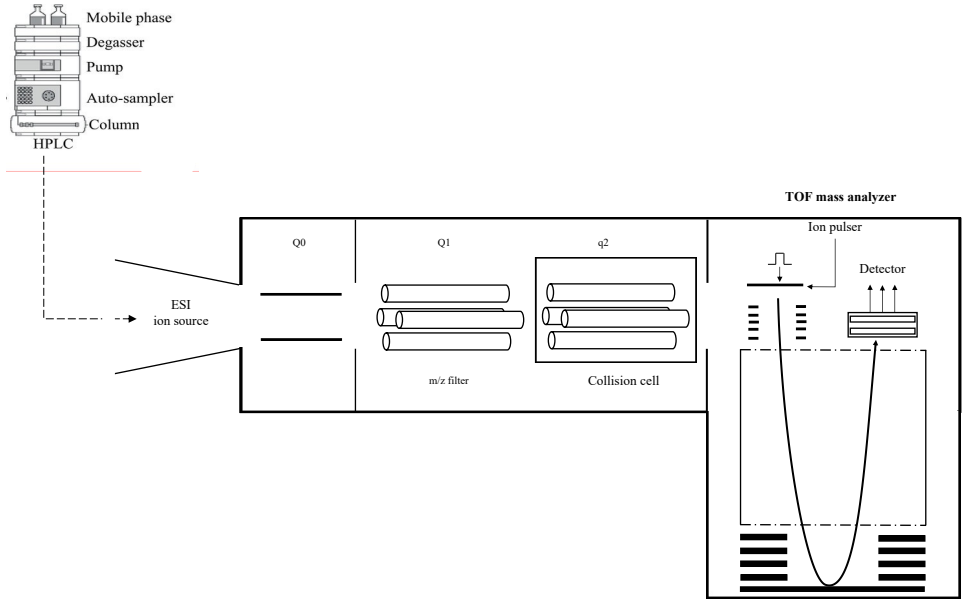

Figure 2.7: Schematic representation of LC-QTOF-MS instrument

The usual configuration of the Q-TOF instrument can be explained most simply as a QqQ with the third quadrupole replaced by a TOF mass analyzer. Additionally, a quadrupole (Q0) is added operating only in the RF only mode, as the q2. As TOF mass analyzer prefers a pulse of ions instead of a direct current like the quadrupole, it is placed after the quadrupole where the ions are filtered and then passed to the TOF. Adapted from [274].

In figure 2.8 it is displayed one an acquisition strategy of Q-TOF instruments called high-resolution MRM (HR-MRM) performed in a similar way to the typical MRM of QqQ instruments that allows a sensitive and fast quantification [271].

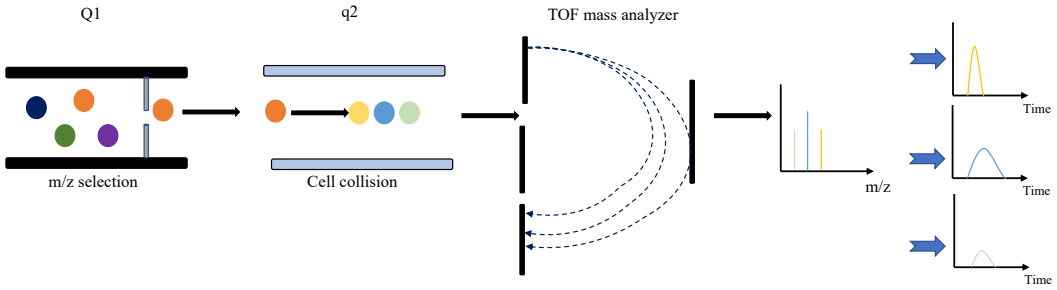

Figure 2.8: Schematic of the high-resolution MRM mode (HR-MRM) performed on a Q-TOF.

High-resolution MRM (HR-MRM) emerges as an alternative to the classical MRM to be performed in high-resolution instruments like the Q-TOF. In this analysis mode, the precursor ion is seleted in Q1, it will pass to the collision cell and then to the TOF mass analyzer. All possible transitions of that precursor are monitored instead of a single fragment on the conventional MRM. The resulting spectra of the entire mass range collected are recorded in a full scan high-resolution MS/MS. After the acquisition, the fragmented ions are can be extracted, generating an extracted-ion chromatogram (XIC).

2.2 Analytical method validation

Method validation is a procedure in which the performance parameters of analytical methods are evaluated to confirm that the methods are adequate for its intended purpose of providing reliable and accurate results [275–277].

Many areas such as quality control of food, environmental, pharmaceutical industry, forensic analysis, and clinical researches, make the validation a critical step to guarantee that the future results of the analysis are as close as possible to the real values and can be reproducible in other laboratories [234, 277–279].

Despite the known importance of method validation and being often considered an important requirement in chemical analysis, many professionals do not know how and why these procedures should be performed [278].

Among the established classical validation parameters are included selectivity, linearity, limits of detection and quantification (analytical thresholds), precision, accuracy, and robustness [275, 276, 278, 279], but also can be considered carry-over, matrix effects, [280] and recovery [278, 279]. However, these performance parameters depend on the type of analytical method to be developed [279].

Several guidelines from various regulatory agencies such as the EMA, the International Organization for Standardization (ISO), the FDA, the United States Pharmacopoeia (USP), and the International Union of Pure and Applied Chemistry (IUPAC) have been developed to facilitate regulation in the validation processes. The International Conference on Harmonization (ICH) was developed to harmonize various international guidelines, currently being one of the guides for validation processes [281, 282].

2.2.1 Selectivity and specificity

The way in which the method can unequivocally determine the analyte under study from a complex mixture in the presence of components is called selectivity [275, 283, 284].

While the terms selectivity and specificity are often mistakenly used as equivalents, they should not be used interchangeably [275]. Specificity assesses the ability of the analytical method to respond exclusively to the analyte of interest without interferences [275, 285].

Often in method validation, selectivity is usually the first to be evaluated. Since if an analytical method shows interferences, the other performance parameters are less reliable [278].

In chromatographic methods, selectivity refers to relative retention, which varies according to separation conditions, such as mobile phase, stationary phase, or temperature [236, 278]. The selectivity it is evaluated to ensure that the peak of the analyte response (manifested in the characteristic retention time) comes exclusively from the analyte and not from other compounds [286].

2.2.2 Linearity and working range

Linearity demonstrates the ability of the method to provide a response (analyte signals) directly proportional to the concentration of an analyte in the sample within a working range [234, 287].

Proper analytical calibration is necessary for reliable quantification. This process involves a series of steps that include the preparation of the calibration standard; the calibration methodology

(external standard or internal standard); the measurement of the instrument's response for each of them, and the construction of the calibration curve [284, 288, 289].

The construction of the calibration curve, also called the analytical curve, represents the relationship between the signal as a function of the analyte concentration. Therefore, in chromatographic analysis, it is constructed based on the peak areas of standard solutions with a known amount of the analyte under study [278, 279, 290]. The guidelines of the ICH specify a minimum of five levels of concentration to assess the range of linearity [234, 275, 284].

Once the calibration is defined and the checks are carried out based on the model parameters, quantification of the analyte being studied can be performed [286, 287].

The linear range can be expressed as the interval contained in the working range, where the signal is directly proportional to the concentration of the analyte [275].

The working range of an analytical procedure describes the interval between the upper and lower concentration of an analyte for which adequate precision, accuracy, and linearity have been demonstrated [234, 275, 279, 283]. The lower limit of the working range corresponds to the limit of quantitation (LOQ), while the upper end corresponds to concentrations in which there are significant anomalies in the sensitivity of the analytic method [291, 292]. Linear range and working range are derived from linearity studies [234].

2.2.3 Precision study

According to ICH, precision is a term used to describe the closeness of agreement between values obtained by repeated measurements under specific conditions of the same or similar samples [275, 278, 283, 293]. Precision relates to the random error or the degree of dispersion among individual test results when the method is applied repeatedly. It is typically expressed as standard deviation and the percentage of the coefficient of variation (CV), also known as the relative standard deviation (RSD) of the replicate measurements [234, 275, 278, 279, 283].

Precision can be estimated through analysis of quality control samples under conditions of repeatability, intermediate precision, and reproducibility [234, 278, 285, 293].

Repeatability, also called intraday test precision, expresses the closeness of the results obtained from a series of measurements on the same sample over the shortest time interval possible and under similar conditions (e.g with the same instrument, the same analyst, equipment) in the same laboratory [234, 293].

Unlike repeatability, intermediate precision is evaluated over a longer period using the same method but defining variations within the laboratory, such as different analysts, different days, different equipment, etc. [284, 285].

Under reproducibility conditions, precision assessment has to be carried out under different conditions, e.g., using different equipments, different days, other analysts, different reagent lots, etc. [283].

2.2.4 Accuracy

Accuracy is the closeness of an individual experimental value obtained by replicate measurements to a reference accepted as true value [275, 279, 283, 291].

It is a determining validation parameter of an analytical method because it allows estimating the total error that affects the method [275, 278]. Total error describes the simultaneous contribution of random and systematic error components that may affect a test result [275, 286]. Accuracy may

be evaluated in terms of absolute bias (direct difference between estimated value and corresponding reference) or relative bias (absolute bias divided by corresponding reference value) [283, 287].

Accuracy can be determined in four ways. By analyzing reference materials (samples of known concentration), by comparing the test results of a validated procedure existing, recovery test, or using the technique of standard addition [275, 278, 283, 286].

2.2.5 Analytical thresholds

The limit of detection (LOD) is defined as the lowest amount of analyte reliably detected in a mixture above the reference noise (commonly three times the noise level), but not necessarily quantified [234, 275, 283]. In qualitative terms, LOD is the lowest concentration that can be distinguished from the blank [285].

In turn, the limit of quantification (LOQ) refers to the lowest analyte concentration that can be quantified with an appropriate level of precision and accuracy and above the reference noise [234, 275].

LOD and LOQ are frequently assessed in analytical procedures in which the samples contain low concentrations of the analyte of interest [234]. Both limits can be calculated by different methods: by replicating the blank (the most recommended), based on the parameters of the curve, based on precision studies, by the signal to noise S/N approach and finally based on the standard deviation of fit [284, 287].

2.2.6 Carry-over

The carry-over is a term that denotes one type of systematic error, used to define the increase in the concentration of a sample derived from the residues of the last run that could be retained in the column, detector, or other parts of the instrument [294, 295].

In chromatography analysis, sample carry-over is an important encountered problem, especially at lower concentrations [296, 297].

2.2.7 Recovery

Recovery is defined as the ability of the method to respond to the total amount of the analyte present in the sample [279]. In different validation guidelines, the term recovery is mostly used as a parameter concerning extraction efficiency as a step of the sample preparation [278].

Recovery can be expressed as the percentage of the to the analyte response for the true concentration of the pure standard before the extraction procedure compared to the response (peak area) obtained from an amount of the analyte after sample workup added to and extracted from the matrix [284, 298].

2.2.8 Matrix effects

The terms interference and matrix effects are usually used as interchangeable concepts, but they are different concepts. The effect of a specific component on the result of the measurement is called interference. Whereas, matrix effects refer to changes from the combined effect of all the components present in the sample, except that the analyte under study can affect its identification and quantification [280].

Analyses performed by chromatography coupled to MS or MS/MS are susceptible to matrix effects, especially when using ESI as the ion source. These effects are often overlooked and can be confused with the appearance of new peaks or the loss of peaks in the chromatograms [212, 280, 299, 300].

Matrix effects could affect the certainty of the method, hence influence the identification and quantification of the analyte. So the evaluation of this parameter is essential [212, 280]. The two main protocols used to evaluate the degree of matrix effects on a method are postcolumn infusion and postextraction addition [299, 300].

2.3 Objectives

Metabolomics studies have been growing progressively in neuroscience as a high-performance tool in the search for predictive biomarkers of alterations in metabolic function, which are often used for disease diagnosis and disease progression monitoring. Furthermore, biomarkers can help to improve knowledge about brain functioning under normal or pathological conditions.

The dysfunction of several neurotransmitter systems has been linked to neurological disorders (i.e., Alzheimer's and Parkinson's diseases). Hence, neurotransmitters and their metabolites have been studied and used as biomarkers of these disorders.

In the specific case of AD, as part of synaptic dysfunction hypotheses, the dysfunction of the following systems has been postulated: cholinergic, glutamatergic, dopaminergic, serotonergic, and GABAergic. Evaluating the metabolism of all these neurotransmitters would be the ideal scenario. Although, given the lock-down and other measures caused by the pandemic of COVID-19, the access to the laboratory was restricted. Because of that, the project needed to be focused on a few of them.

The cholinergic and glutamatergic systems were chosen to be studied because of their importance in the currently available pharmacological therapies for AD symptoms.

Consequently, in this work, the objectives proposed were: i) the development, optimization, and validation of an LC-MS/MS targeted metabolomic method for the measurement of five metabolites, corresponding to the cholinergic (Cho and ACh) and glutamatergic metabolism (Gln, Glu, and GABA); and ii) the implementation of the developed quantification protocol for the measurement of the target compounds in CSF samples to assess differences between AD patients from two different groups, the Aβ+ and Aβ -.

Chapter 3

Materials and methods

3. Materials and methods

3.1 Materials

The materials used for the development and optimization of the method were:

- Multipipette Plus (Eppendorf®);
- Micropipettes Research Plus (Eppendorf®);
- Microcentrifuge tubes 1.5 mL (Eppendorf®);
- Centrifuge tubes 15 mL (VWR®);
- Microvials 300 µL (Fisherbrand).

3.2 Equipments

The equipment used in this work are listed below:

- Analytical balance CP 224S (Sartorius);
- Thermomixer comfort (Eppendorf®);
- Concentrator Plus (Eppendorf®);
- Vortex, model MS3 basic (IKA®).
- Components of the liquid chromatography coupled to a mass spectrometer system:
  - Liquid Chromatography System NanoLC 425 (Eksigent) with a column SeQuant®ZIC®-cHILIC (Merck) 3.0 µm, 150 x 0.3 mm,
  - Data acquisition was performed with a Triple TOF™ 6600 System (Sciex) using an ESI DuoSpray™ Source (Sciex) equipped with an emitter of 25 µm of internal diameter;
  - The mass spectrometer was operated by Analyst TF 1.8.1 (Sciex).
  - The LC-MS/MS data were processed using PeakView™ (Sciex) and Multiquant™ (Sciex) software.

3.2.1 Standards and reagents

The analytes and internal standards (ISs)used for the analytical method development, optimization and validation are presented in table 3.1. Additional information about these analytes is detailed in the Appendix A.1.

Table 3.1: List of analytes and internal standards used in the investigation.

Compound	MW (g/mol)	Brand
L-glutamic acid (Glu)	147.13	Sigma-Aldrich
γ-aminobutyric acid (GABA)	103.12	Sigma-Aldrich
L-glutamine (Gln)	146.14	Dr. Ehrenstorfer
Acetylcholine chloride (ACh)	181.66	Sigma-Aldrich
Choline chloride (Cho)	139.62	Sigma-Aldrich
L-glutamic acid (2,3,3,4,4-d5, 98%) (Glu-d5)	152.16	Cambridge Isotope Laboratories
4-aminobutyric acid (2,23,3,4,4-d6, 97%) (GABA-d6)	109.16	Sigma-Aldrich
L-Glutamine (2,3,3,4,4-d5, 97%) (Gln-d5)	151.18	Cambridge Isotope Laboratories
Acetylcholine chloride (N,N,N-trimethyl-d9) (ACh-d9)	190.72	Sigma-Aldrich
Choline chloride (trimethyl-d9, 98%) (Cho-d9)	148.68	Sigma-Aldrich

All solvents used, acetonitrile (ACN), methanol (MeOH), and water LC/MS grade, were purchased from HiPerSolv CHROMANORM®, VWR. Only formic acid (FA) LC/MS grade was obtained from Fisher Chemical.

3.2.2 Standard solutions

Standard stock solutions were prepared by dissolving approximately 20 mg of individually pure substance in a solvent. Since Glu, Gln and GABA have low solubility in methanol, they were prepared in water-methanol mixed solution (80:20, ν/ν), heated and agitated in a thermomixer to 50 °C at 750 rpm for fifteen minutes to obtain a homogeneous solution. The respective IS were prepared in the same way.

ACh, Cho, and their respective IS stock solutions were prepared in MeOH LC grade and homogenized by vortex mixing. All stock solutions were stored as aliquots of 1.5 ml and 0.5 ml at -20°C.

Four mix solutions, comprising the analytes and internal standards of each metabolism, were prepared. In accordance, mix standard solutions were prepared for the glutaminergic metabolism (Gln, Glu, and GABA) and respective internal standards (Gln-d5, Glu-d5, and GABA-d6), and for cholinergic metabolism (Cho and ACh) and respective internal standards (Cho-d9 and ACh-d9). All the mixed solutions were prepared with around 50 µM of each analyte diluting the stock solutions in a solution of ACN-FA (80:0.1, ν/ν).

Calibration standards from the mixture of the mix solutions where freshly prepared on the day of analysis, distributed in a wide range of concentrations of 0.01; 0.03; 0.05; 0.07; 0.1; 0.3; 0.5; 0.8; 1 and 4 µM of the analyte. The injection volume into the chromatographic system was 10 µL, corresponding to 100 to 40000 fmol of the compounds in the colum.

Quality controls (QCs) solutions were prepared at three concentration levels: low, medium, and high (0.05; 0.1 and 0.8 µM) from dilution of mixed solution.

3.3 Samples population

This study included forty AD patients aged between 46 and 80 years. CSF samples were collected at the Centro Hospitalar e Universitário de Coimbra (Coimbra, Portugal), with the code HUC-43-09 and, more recently, using CE-029/2019.

From the 40 CSF samples analyzed, 20 corresponded to patients with Aβ+ (52.5 % female and 47.5 % male) and 20 with Aβ normal or Aβ- (50% female and 50% male).

3.3.1 Sample preparation

All samples were prepared under the same analytical procedure following an extraction/precipitation protocol and subsequently resuspension. From the collected CSF samples, 200 µL were used, and four volumes of methanol (800 µl) were added. After homogenizing by vortex mixing, they were kept for one hour at -80 °C. Then, they were centrifuged (20,000×g for 20 minutes at 4 °C) to create a protein-free supernatant. The supernatant was collected in a microcentrifuge tube and evaporated to dryness in a concentrator, and then it was stored at -20 °C until use.

On the day of analysis, samples were reconstituted using 400 µl of a ACN-FA (80:0.1, ν/ν) solution and 50 µl of mixed compounds of internal standards. They were then sonicated (1 second on 1-second off cycles, for a total of 4 minutes) and taken to centrifugation (20,000×g for 5 minutes at 4 °C). The injection volume into the chromatographic system was 10 µL.

3.4 Instrumental conditions

This section describes some optimized parameters in order to develop an efficient and sensitive LC-MS/MS method.

3.4.1 Mass spectrometry

The MS analysis was performed with a triple TOF 6600, coupled with an ESI DuoSpray source operating in positive and negative ionization mode. To establish the best performing conditions for each compound, direct injections of the individual target metabolites standard solutions and their labeled standards into the mass spectrometer were performed at a flow rate of 5 µL/min using a syringe pump. The concentrations of the solutions were 100 µM for Glu, Glu-d5, GABA, GABA-d6, Cho and Cho-d9, and 10 µM for Gln, Gln-d5, ACh and ACh-d9, in an ACN : FA mixture (80:0.1 ν/ν).

For all compounds, the analysis was carried out in positive ionization mode. The fine-tuned ion source-dependent parameters were as follows: ion spray voltage floating (ISVF) was 5500 volts (V), source temperature 100 °C, curtain gas (CUR) 25 psi and ion source gas (GS1 and GS2) were set at 20 and 15 psi respectively.

Furthermore, compound-specific parameters, namely, declustering potentials (DP), collision energy (CE), and collision energy spread (CES) were set up as illustrated in table 3.3.

The QTOF-MS was operated in full scan MS/MS mode at high resolution across the 10–1500 m/z range, using 100 ms accumulation time per spectrum. Post-acquisition, fragmented ions were extracted generating a HR-MRM spectra.

All data were acquired using Analyst TF software 1.8.1 and the fragmentation spectra of each compound were analyzed by PeakView™.

Table 3.3: Optimized acquisition method parameters to each compound: declustering potential (DP); collision energy (CE), and collision energy spread.

Compound	Precursor ion (m/z)	Product ion	DP (eV)	CE (eV)	CES (eV)
Glutamate	148.06	84.05	70	20	10
		130.05		12	
		102.06		14	
Glutamine	147.08	130.05	70	12	10
		84.05		21	
		101.07		13	
GABA	104.07	87.05	70	13	10
		69.03		18	
		45.03		23	
		43.02		20	
Aceylcholine	146.12	87.05	80	18	10
		43.02		34	
		60.08		14	
Choline	104.11	60.08	100	22	10
		58.07		35	
		45.04		24	
		44.05		36	
Glutamate-d5	153.09	88.07	80	20	10
		89.08		18	
		87.06		21	
		107.09		14	
		135.08		11	
Glutamine-d5	152.11	135.08	85	12	10
		88.07		21	
		89.08		21	
		87.06		18	
GABA-d6	110.81	93.08	70	13	5
		92.11		12	
		49.06		24	
		46.04		20	
Aceylcholine-d9	155.18	87.05	65	18	10
		69.14		16	
		45.04		14	
Choline-d9	113.17	69.14	90	12	10
		66.12		20	
		45.04		16	
		49.08		19	

3.4.2 Liquid chromatography

For chromatographic optimization, three different chromatographic columns were tested: C18 (YMC-Triart) 3.0 µm, 150 x 0.3 mm; ChromXP amino (Eksigent) 3.0 µm, 150 x 0.3 mm; SeQuant®ZIC®-cHILIC (Merck) 3.0 µm, 150 x 0.3 mm. The best chromatographic separation and peak shape were reached with the cHILIC column, which was expected, given that the analytes under study are highly polar hydrophilic.

A mobile phase gradient program was developed to allow an efficient chromatographic separation of the analyte, the mobile phase consisted of a solvent B containing ACN in 0.1% FA, ν/ν and a solvent A, containing 10 mM and ammonium formate (NH_4HCO_2) in 0.1% FA, ν/ν.

The flow rate was fixed in 5 µL/min with a gradient elution starting from 80% of eluent B and 20% of eluent A as shown in table 3.4.

The volume injected of each calibration standard was 10 µL and between each chromatographic run, a blank sample was injected.

Table 3.4: Gradient elution optimized for the chromatographic analysis.

Time gradient (min)	Mobile phase (v/v)	
	Solvent B (%)	Solvent A (%)
0	80	20
7	50	50
9	50	50
10	80	20
15	80	20

3.5 Analytical method validation

After the optimization of the analytical method, its validation is needed to be carried out in order to prove the ability of the method to be applied in the established range complying with certain performance parameters, such as linearity, accuracy, and precision. To achieve this goal, the use of statistical tests is essential to summarize the data and make objective judgments. The LC-MS/MS method was validated for the compounds in solvent with respect to linearity, precision, accuracy, the limit of detection, and the limit of quantification . The statistical test and their acceptance criteria are described in detail in this section. All calculations made in the method validation procedure were performed in Microsoft Excel software.

3.5.1 Linearity

The evaluation of the linearity is essential to prove the ability of the developed method to offer results that are directly proportional to the concentration of the analyte [234, 287, 301].

The assessment of the linearity is not only carried out by means of a graphical representation of the measured instrument signals as a function of the analyte concentration, but also appropriate statistical procedures should be used, the linear regression model is the most frequent in this evaluation [289, 293, 301–304]. The objective of a regression is to create a model capable of estimating the relationship between x (independent variable) and y (dependent variable). In the case of the linear regression model this relationship is established by a best-fitting line mathematically expressed by equation (3.1), being b (slope) and a (intercept) the parameters estimated [301, 302].

$$y = bx + a \tag{3.1}$$

The model parameters (a intercept and b slope) are estimated by the ordinary least squares (OLS), the most commonly methodology used in the simplest regression model. As the fit line must pass through the centroid of the points, there are differences between the experimental values of y and the predicted values calculated from the model equation, these random errors of prediction are technically called residuals. OLS by the least-squares method minimizes the sum of squares

(SS) of these differences to determine the parameters that best describe the variables, calculated using equation (3.2) [302, 304–306].

$$SS = (y - \tilde{y})^2 \tag{3.2}$$

where y are the experimental values and $\tilde{y}$ corresponds to model predicted values.

The coefficient of correlation (r) resultant from the regression analysis is used to measure the linear correlation between the two variables, and this value should be positive or negative in the range $-1 \leq r \leq +1$ [278, 306, 307]. The r values can be calculated by equation (3.3), where $\dot{x}$ and $\dot{y}$ are the the mean of the values of x and y, respectively.

$$r = \frac{\sum \{(x_i - \dot{x})\,(y_i - \dot{y})\}}{\sqrt{\left[\sum (x_i - \dot{x})^2\right]\left[\sum (y_i - \dot{y})^2\right]}} \tag{3.3}$$

The value of the called coefficient of determination (R^2) ranges from zero to one. It is generally used to determine how well the model can describe experimental results [278, 303]. Values of $R^2 \geq 0.995$ considered evidence that the data fit the regression line. [234, 307, 308]. Nevertheless, several investigators considered r *or* R^2 a poor indicator in the linearity evaluation, hence other statistical tests should also be used, such as the residual analysis, Mandel test, and Rikilt's test [278, 285, 303].

The estimation of the standard deviation of the random errors in y ($S_{y/x}$) from the regression model is an important parameter to calculate in the linearity study. Since random errors also influence the values obtained for the slope and the intercept, their standard deviations S_b and S_a, respectively, should not be forgotten [288, 306]. These parameters were calculated by equations (3.4), for linear model, equation (3.5) and (3.6).

$$S_{y/xM_1} = \sqrt{\frac{(y - \tilde{y})^2}{n - 2}} \tag{3.4}$$

$$S_b = \frac{S_{y/x}}{\sqrt{\sum (x_i - \dot{x})^2}} \tag{3.5}$$

$$S_a = S_{y/x}\sqrt{\frac{\sum x_i^2}{n \sum (x_i - \dot{x})^2}} \tag{3.6}$$

where n is the number of calibration points and n-2 the degrees of freedom from the linear regression [306].

The linearity of the method was assessed from four calibration curves analyzed in a concentration range of 0.01 - 4.0 µM. To achieve this, the coefficient of determination, the standard deviation, the intercept and the slope from the linear regression model were evaluated, and the Mandel test was also performed.

3.5.1.1 Mandel test

The Mandel's fitting test is used to assess the linearity, verifying if the data set better fits the linear or quadratic regression by comparing the residual errors of both models [304, 308].

From the calibration curve was calculated a test value (TV) from equation (4.7), which is expressed as the difference of the sum of squares of the residuals, using a first model (M_1, linear) and the second model (M_2, quadratic), divided by their degrees of freedom [306, 307]. In the linear regression the degrees of freedom is *n-2* and for the quadratic regression is *n-3* [306]. This in turn, it is divided by the variance of a purely random estimate [307].

$$TV = \frac{\Delta\nu\sigma^2_{fit}}{\sigma^2_{pe}} = \frac{\Delta SS/\Delta\nu}{\sigma^2_{pe}} \tag{3.7}$$

The TV obtained follows a F-distribution, so, can be compared with a tabulated value $F_{crit} = F^u_{\alpha(\Delta\nu,n-3)}$ where α represent the significance level of 0.01 (99% level of confidence) and $\Delta\nu$ the difference between the degrees of freedom of the linear and quadratic regression, using the hypotheses shown in equation (3.8) [308].

$$\begin{cases} H_0 : S^2_{y/_{xM1}} \leq S^2_{y/_{xM2}} \\ H_1 : S^2_{y/_{xM1}} > S^2_{y/_{xM2}} \end{cases} \tag{3.8}$$

If the null hypothesis is verified, it means the differences between the variances from the linear and quadratic model are not statistically significant; therefore, the linear model is appropriate for the calibration curve. Otherwise, if it is rejected, it means that the calibration curve has a quadratic behavior and the linear model is not the most suitable [304, 307, 308].

3.5.2 Working range

During the method validation it is necessary to confirm if the developed method can be applied in the working range used [234]. In this study, the working range was derived from the linearity evaluation, with the respective confirmation that the method provide adequate linearity, precision and accuracy in the specified range [303].

When the methodology involves evaluating the performance of a calibration curve, the working range can be evaluated by means of a test of homogeneity of variances. The reason for evaluating the variances is that some assumptions about the errors (residuals) in y are considered during the regression analysis, namely: i) the errors are uncorrelated with the values of concentrations (x) ii) randomly distributed for the model, and iii) the magnitude is constant across all the different concentrations i.e., the variance should be approximately equal (homoscedastic) [289, 303, 304, 306, 307, 309].

Verification of these assumptions must be performed in any linear regression analysis, since it is necessary to have the right model for the data under analysis to ensure a reliable quantification [284, 303, 305, 310]. This verification can be carried out by means of a visual inspection of a residual plot and a homoscedasticity test by the F test [303, 305, 308, 310].

The homoscedasticity test was carried out at the lowest (0.05 µM) and one of the highest (0.8 µM) calibrators through 10 independent replicates. The variances of these standards were tested to examine whether there are significant differences between them, by applying equation (3.9).

$$TV = \frac{S^2_2}{S^2_1} \tag{3.9}$$

Being S^2_1 and S^2_2 the variances obtained for the lowest and the highest calibrator tested, respectively.

The variances were calculated as presented in equation (3.10), where i is the ith data of n total data; j is the number of replicates of each calibrator and (n_i- 1) is the degree of freedom.

$$S_i^2 = \frac{\sum_{j=1}^{n} (y_i - \tilde{y}_i)^2}{n_i - 1} \tag{3.10}$$

Then, the TV can be compared with a tabulated value of a F- distribution $F_\alpha^b(\nu_2, v_1)$ for a confidence level at 99%, using the following hypotheses (equation (3.11)) [305].

$$\begin{cases} H_0 : S_1^2 \approx S_2^2 \\ H_1 : S_1^2 \neq S_2^2 \end{cases} \tag{3.11}$$

If the null hypothesis is verified, it means there are no significant differences between the variances from the lowest and highest calibrator, and the residuals are randomly distributed across the working range [305]. In the case of rejecting the null hypothesis or verify any violation of the assumptions described above, it may be required to apply a weighting linear regression model to find the straight line for calibration [303, 307], or decrease the considered concentration range until reaching the homoscedasticity [303].

3.5.2.1 Weighted least-squares linear regression

Once heteroscedasticity has been evidenced, the use of weighted least squares (WLS) is the most effective because this model calculates a weight to each variance value at each calibration point to harmonize the difference of variances [278, 303, 306].

Taking into account the above-mentioned information, the most appropriate weighting factor would be inversely proportional to the corresponding variance at each point, as presented in the equation (3.12). Therefore, for those points with lower variance would be assigned higher weights [305].

$$w_i = \frac{1}{S_i^2} \tag{3.12}$$

However, this is not practical at all, so empirical weights based on the variables ($x$concentration and y detector response) are usually studied, such as $1/x$, $1/x^2$, $1/\sqrt{x}$, $1/y$, $1/y^2$ and $1/\sqrt{y}$ [305, 310]. The decision about which weighting factor to choose should be made according to the percentage relative error (%RE) [305]. Thus, the one which originated the lowest value of the sum of %RE (Σ %RE), plus gave rise to a random distribution in a graph of %RE versus concentration, is considered as the best weighting factor [278, 305]. On the other hand, Gu (2014) [309] recommended the use of the weighting factor of $1/x^2$ for bioanalytical LC-MS / MS assays.

The %RE is a sensitive indicator of the effectiveness of the adjustment. It can be obtained by comparing the concentration obtained from the regression (C_{exp}) and the nominal standard concentration (C_{nom}), equation (3.13) [303, 305].

$$\%RE = \frac{C_{exp} - C_{nom}}{C_{nom}} \times 100 \tag{3.13}$$

The acceptance criterion was set up on ±15 % RE, or in the case of LOQ was 20% [310].

The parameters a, b from the linear regression must now be calculated considering the w_i established, this can be achieved using equation (3.14) and (3.15) [303, 305].

$$b_w = \frac{\sum w_i \times \sum w_i x_i y_i - \sum w_i x_i \times \sum w_i y_i}{\sum w_i \times \sum w_i x_i^2 - \left(\sum w_i x_i\right)^2} \tag{3.14}$$

$$a_w = \frac{\sum w_i x_i^2 \times \sum w_i y_i - \sum w_i x_i \times \sum w_i x_i y_i}{\sum w_i \times \sum w_i x_i^2 - \left(\sum w_i x_i\right)^2} \tag{3.15}$$

where x_i and y_i represents the data pair i from n total data, and w_i represents the chosen weighting factor.

The r-value must also be calculated using the chosen weighting factor by equation (3.16) [303, 305].

$$r = \frac{\sum w_i \times \sum w_i x_i y_i - \sum w_i x_i \times \sum w_i y_i}{\sqrt{\sum w_i \times \sum w_i x_i^2 - \left(\sum w_i x_i\right)^2} \times \sqrt{\sum w_i \times \sum w_i y_i^2 - \left(\sum w_i y_i\right)^2}} \tag{3.16}$$

Also, the standard error of the response can be recalculated using equation (3.17).

$$S_{y/x} = \sqrt{\frac{\sum w_i \times (y - \tilde{y})^2}{n - 2}} \tag{3.17}$$

3.5.3 Precision and accuracy studies

Evaluation of both, precision and accuracy of the analytical methods, were measured for QC samples [307]. Since both parameters vary throughout the working range, their evaluation must be performed at least three levels of concentrations [303, 307]. Taking this into account, the three different QCs were prepared at three different concentration levels of 0.05, 0.1 and 0.8 μM, corresponding to concentration levels low, medium, and high, respectively.

As it was already mentioned previously in the Section 2.2.3, precision assessment can be performed at three levels: repeatability, intermediate precision, and reproducibility [234, 278, 285]. However, in this study, the precision was assessed with respect to repeatability and intermediate precision, since reproducibility is assessed when the method is applied in different laboratories [291, 310].

Repeatability and intermediate precision can be expressed as the % RSD; the accepted criteria for both parameters are values that fall within 15% RSD for all concentrations except at lower limit of quantification level (LLOQ), which must be ±20% [281, 284, 303, 310]. The % RSD can be calculated following the equation (3.18).

$$\%RSD = \frac{s}{\dot{x}} \times 100 \tag{3.18}$$

where S is the standard deviation and $\dot{x}$ the mean of the values obtained [306].

Also both parameters can be determined using single-factor analysis of variance (ANOVA) calculation [291, 310]. Intermediate precision is calculated as the square root of the sum of the squares of the variances within groups and between groups, divided by the mean of the measured concentrations. While repeatability can be determined as the square root of the sum of the squares of the within-group variance, also divided by the mean of the measured concentration [291].

To estimate the accuracy of the method QCs samples were used to evaluate the precision. The accuracy was obtained by the comparison of the experimental concentrations and the nominal con-

centrations, expressed in terms of % RE [307]. Accuracy can be calculated through equation (3.13), the same acceptance criteria mentioned above in precision studies should be applied [303, 307].

3.5.4 Analytical thresholds

More than one approach to calculating analytical limits has been reported by several validation guidelines [278, 284, 291, 293, 310]. The most commonly used approaches are detailed below:

i) Based on the standard deviation of the intercept of the calibration curve, the determination of the LOD and LOQ was carried out using equations (4.19) and (4.20), respectively [293, 311].

$$LOD = \frac{y_{LD} - a}{b} \tag{3.19}$$

$$LOQ = \frac{y_{LQ} - a}{b} \tag{3.20}$$

where y_{LD} and y_{LQ} are the limits of detection and quantification of the instrument signal, respectively. These values were calculated from equations (3.21) and (3.22), using the line intercept value (a), its respective deviation (S_a) and applying the t-student test at the 95% confidence level for (n-p) degrees of freedom.

$$y_{LD} = a + 2 \times t^{u}_{0.05}(n-p) \times S_a \tag{3.21}$$

$$y_{LQ} = a + 6 \times t^{u}_{0.05}(n-p) \times S_a \tag{3.22}$$

ii) Based on the residual standard deviation of a regression line, the y_{LD} and y_{LQ} values were obtained applying equations (3.23) and (3.24) [311].

$$y_{LD} = 2 \times t^{u}_{0.05}(n-p) \times S_{y/x} \tag{3.23}$$

$$y_{LQ} = 3 \times 2 \times t^{u}_{0.05}(n-p) \times S_{y/x} \tag{3.24}$$

iii) Based on the precision approach, the LOD and LOQ can be taken as the lowest concentration at which the acceptance criteria of 15% RSD are met, and 20% for LOQ [312].

iv) Based on the S/N approach, the limits are calculated by comparing the signals produced by one analyte with those produced in the blank samples around the retention time of the analyte. Being established as LOD the lowest analyte concentration which produces a signal equal to 3 times greater than that measured in the blank sample (3:1), and for LOQ equal to or greater than 10 times (10:1) of the signal measured in the blank sample [284, 293, 301, 313, 314].

Chapter 4

Results and discussion

4. Results and discussion

4.1 Method development

In this project, the development and optimization of an LC-MS/MS method for the measurement of Gln, Glu, GABA, Cho and ACh analytes were carried out.

This section describes the results obtained in the optimization stage, focused on the mass spectrometry parameters. The optimization was carried out to obtain the best conditions for each analyte.

4.1.1 Compound optimization and fragmentation pattern

One important step during the optimization stage was the determination of several conditions of each individual analyte as well their labeled standard mentioned in the Section 3.4.1. Furthermore, in this study, values of DP and CE were tested to establish the optimal conditions for each compound, to produce stable and highly sensitive fragmentation spectra (MS/MS) with a lower noise baseline.

The DP was ramped from 0 to 300 V, to set the proper voltage to prevent ions from agglutinating in the inlet orifice of the mass spectrometer, and at the same time avoid that very high DP voltages could be applied, which can affect the ionization efficiency [315].

In figure 4.1 is shown the intensity profile corresponding to the protonated molecular ions of Glu, Gln, GABA, ACh and Cho versus a gradual increase in the DP applied to each of them. The DP values in which the signal intensities of the compounds did not vary significantly were ranged between 30 and 110 V. The DP ramp record for the labeled standards is presented in Appendix A.1.

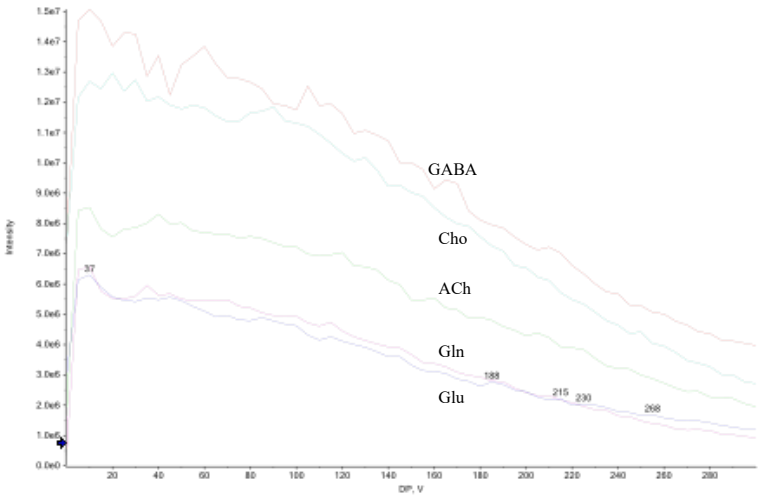

Figure 4.1: Declustering potential (DP) ramping from 0-300 V for glutamate, glutamine, GABA, ACho and Cho.

MS/MS fragmentation for each compound was performed under CE ramping in a range of 5 to 45 V, in order to find the optimal CE to improve the fragmentation of the precursor ions. Then, taking into account the CE values of each fragment, was chosen a single value for all fragments. For

Gln and Glu, the optimal value of CE was 15 V; while for GABA, Cho and ACh higher collision energies were necessary, being 26 V for GABA and Cho, and 25 for ACh, as shown in figure 4.2. For the internal standards the CE ramping is illustrated in Appendix figure A.2. The MS/MS spectra and possible fragmentation pathways were acquired and analyzed for each compound after optimization of these parameters.

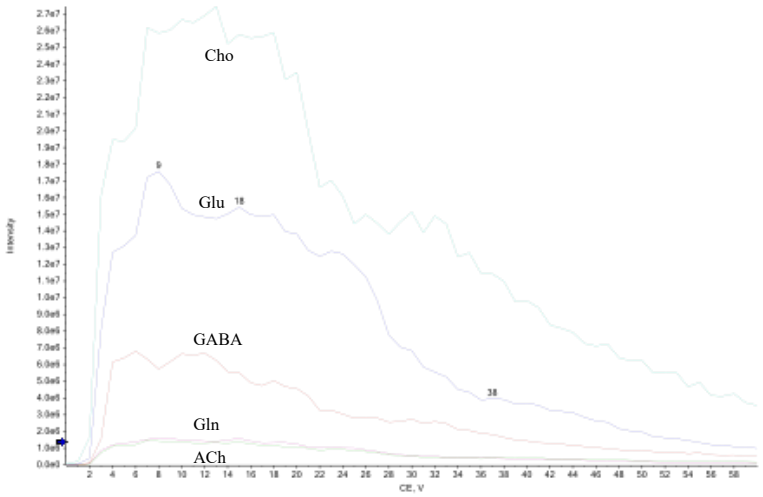

Figure 4.2: Collision energy (CE) ramping for glutamate, glutamine, GABA, ACho and Cho, in a range of 5 to 45 V.

It is possible to notice in the fragmentation spectrum (figure 4.3) the precursor ion m/z 148.06 $[M+H]^+$ corresponds to the protonated Glu. The observed fragment m/z 130.05 is formed by the loss of water $[M+H-H_2O]^+$. Then, the loss of H_2O+CO gives rise to the fragment with higher intensity, the fragment of m/z 84.05. The fragment m/z 102.06 is formed by a loss of H_2O+CO from $[M+H]^+$, this also can lead to the fragment m/z 84.05 through the loss of water [316].

Figure 4.3: MS/MS spectrum for Glu precursor ion m/z 148.06 $[M+H]^+$. The fragments were acquired by ESI in positive ionization mode with a collision energy of 15 V. Adapted from: Zhang, et al., 2019.

Regarding to the fragmentation spectrum of the IS (figure 4.4), Glu-d5, its precursor ion corresponds to the peak with m/z 153.09 $[M+H]^+$. The most intense fragments m/z 88.07, 89.08,

87.97, 107.09 and 135.98 were chosen to be monitored.

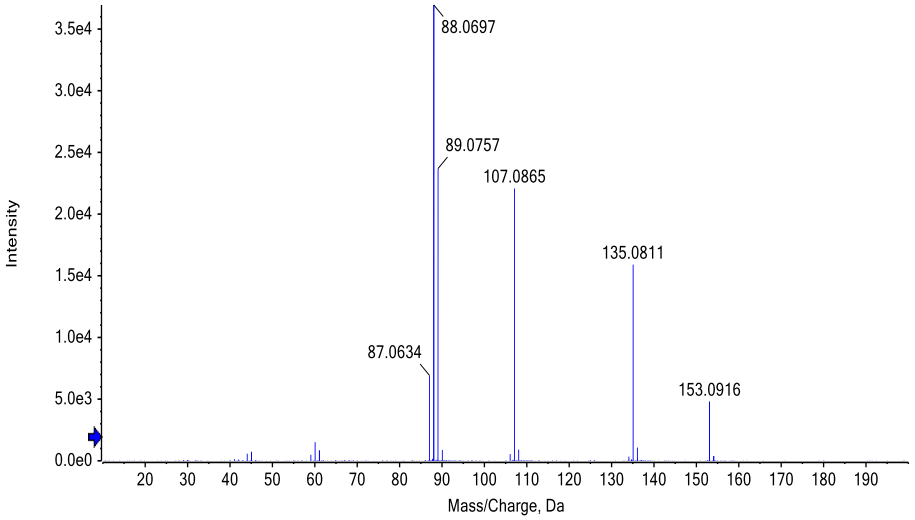

Figure 4.4: MS/MS spectrum for Glu-d5 precursor ion m/z 153.09 $[M+H]^+$. The fragments were acquired by ESI in positive ionization mode with a collision energy of 16 V.

The fragmentation spectrum of Gln is showN in figure 4.5, the m/z 147.07 corresponds to the protonated molecule $[M+H]^+$.

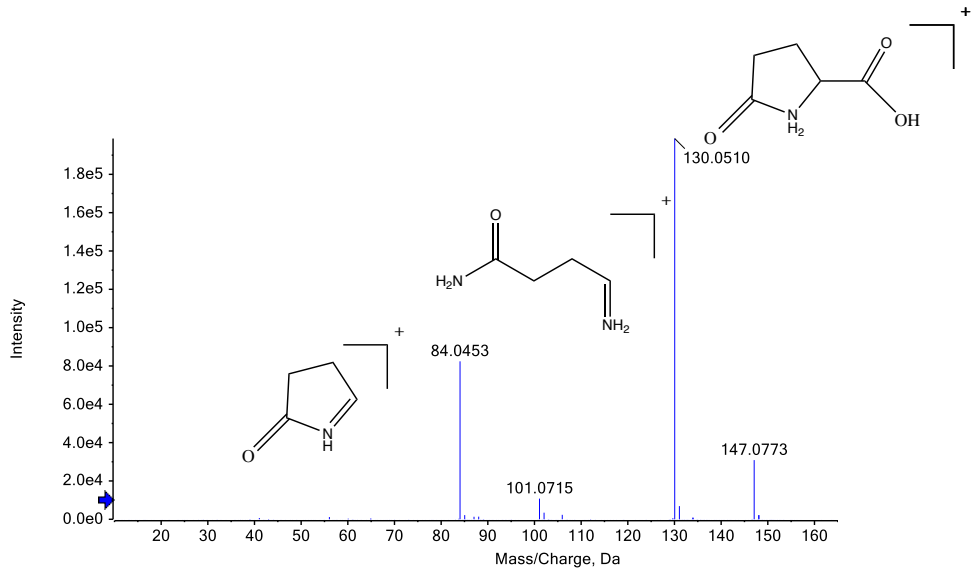

Figure 4.5: MS/MS spectrum for Gln precursor ion m/z 147.07 $[M+H]^+$. The fragments were acquired by ESI in positive ionization mode with a collision energy of 15 V. Adapted from: Zhang, et al., 2019.

The three fragment ions were monitored, the fragment m/z 130.05 is the peak with higher intensity formed by the loss of ammonia $[M+H-NH_3]^+$. The subsequent loss of H_2O+CO brings on the second higher peak, the fragment of m/z 84.05. Finally the fragment m/z 101.07 was formed by a loss of NH_3+CO from $[M+H-NH_3]^+$ [316]. The fragmentation pathways of the fragment ions in Glu and Gln spectra were postulated by Zhang, et al., 2019 [316].

The fragmentation spectrum obtained from the IS Gln-d5 presented in figure 4.6, the m/z

152.11 corresponds to the the protonated molecule $[M+H]^+$. As in the other spectra already mentioned, the highest intensity peaks were chosen to monitor the analyte, these were, m/z 88.07, 87.07, 107.09 and 135.08.

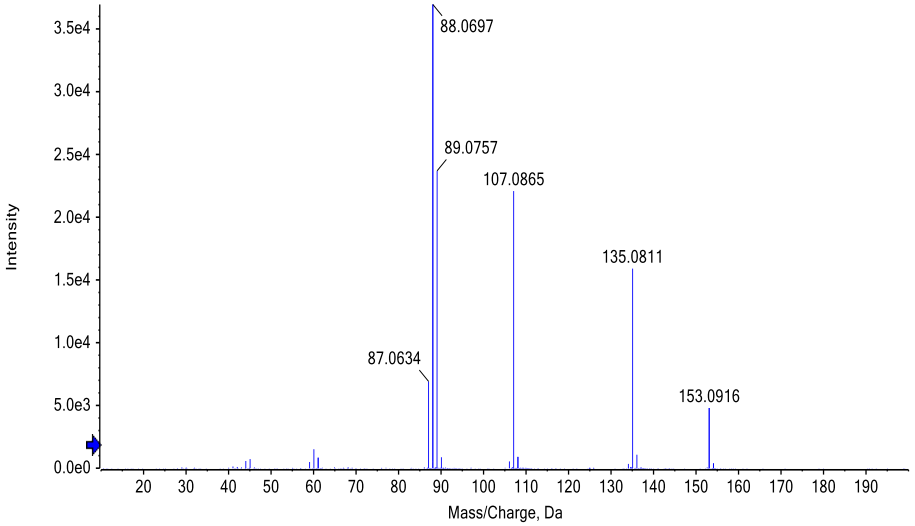

Figure 4.6: MS/MS spectrum for Gln-d5 precursor ion m/z 152.11 $[M+H]^+$. The fragments were acquired by ESI in positive ionization mode with a collision energy of 13 V.

In the fragmentation spectrum of GABA figure 4.7, the peak at m/z 104.07 $[M+H]^+$corresponds to the entire molecule.

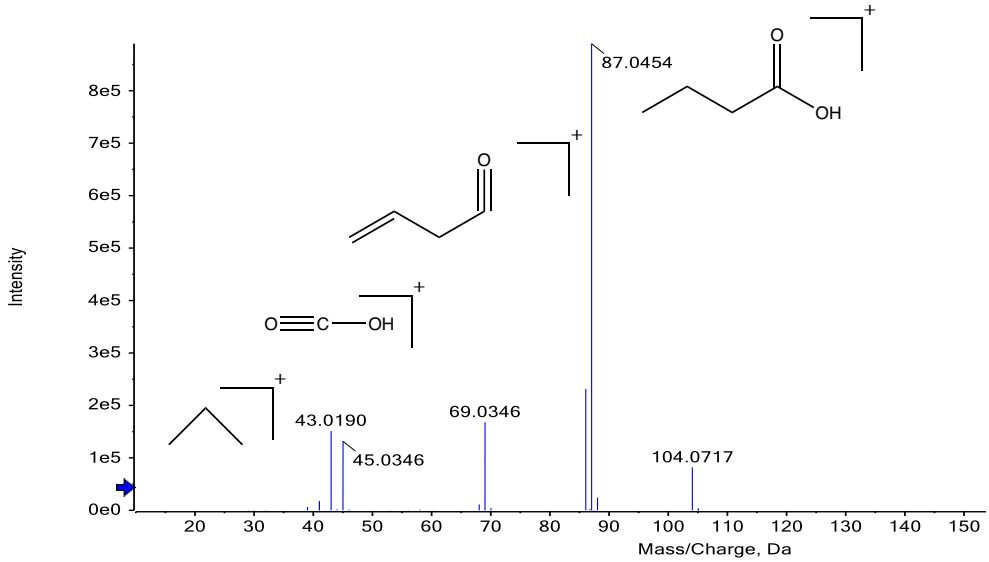

Figure 4.7: MS/MS spectrum for GABA precursor ion m/z 104.07 $[M+H]^+$. The fragments were acquired by ESI in positive ionization mode with a collision energy of 26 V.ChemDraw Professional (16.0).

During the fragmentation, the peaks m/z 87.05, 69.03, 43.02 and 45.04 were observed. The most intense peak corresponds to the fragment m/z 87.05, formed by the loss of ammonia $[M+H-NH_3]^+$, and its subsequent loss of H_2O gives rise to the peak at m/z 69.03.

In the spectrum obtained for the IS GABA-d6 (figure 4.8), it is possible to identify the entire

molecule at the peak m/z 110.11 $[M+H]^+$. The fragments with m/z 93.08, 92.10, 49.06 and 46.04 were chosen for the posterior analysis.

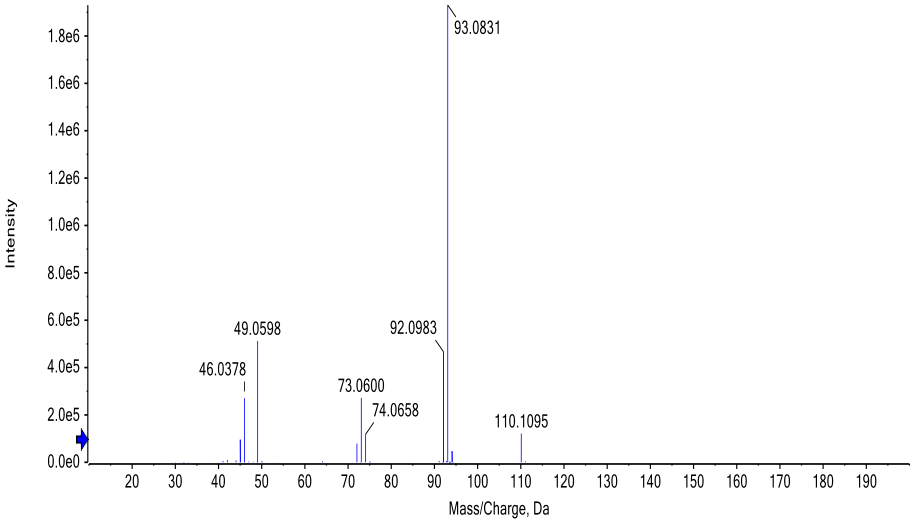

Figure 4.8: MS/MS spectrum for GABA-d6 precursor ion m/z 110.11 $[M+H]^+$. The fragments were acquired by ESI in positive ionization mode and with a collision energy of 16 V.

The MS/MS product ion scan of ACh (figure 4.9) shows the entire molecule with m/z 146.11 $[M+H]^+$. For this analyte, the fragments generated were m/z 87.05, 60 and 43.02.

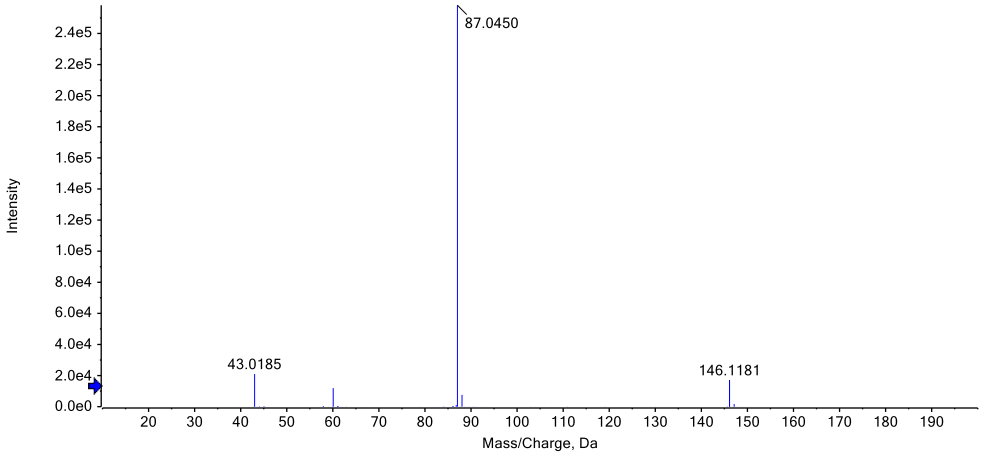

Figure 4.9: MS/MS spectrum acquired for ACh precursor ion m/z 146.12 $[M+H]^+$. The fragments were acquired by ESI in positive ionization mode and with a collision energy of 25 V.

In the MS/MS spectrum for ACh-d9 (figure 4.10) it is shown the m/z 155.18, which corresponds to the the protonated molecule $[M+H]^+$. As expected, a fragmentation spectrum similar to that of ACh was generated; thus the peaks observed were m/z 87.05, 69.14 and 43.02.

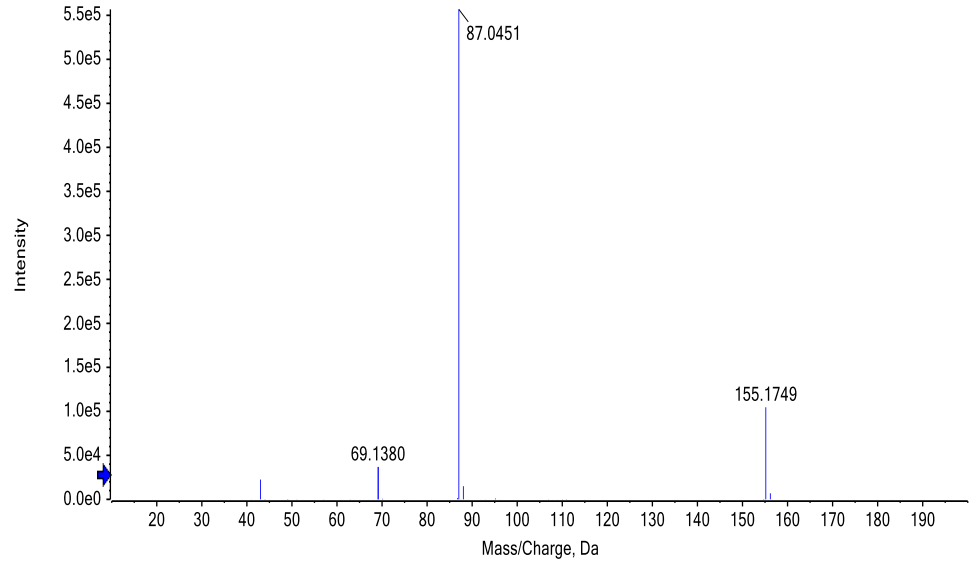

Figure 4.10: MS/MS spectrum acquired for ACh-d9 precursor ion m/z 155.18 $[M+H]^+$. The fragments were acquired by ESI in positive ionization mode and with a collision energy of 16 V.

Regarding to the fragmentation spectrum of Cho (figure 4.11), the entire molecule m/z 104.11 $[M+H]^+$ was observed. The fragments monitored were m/z 60.08, 58.07 and 45.04.

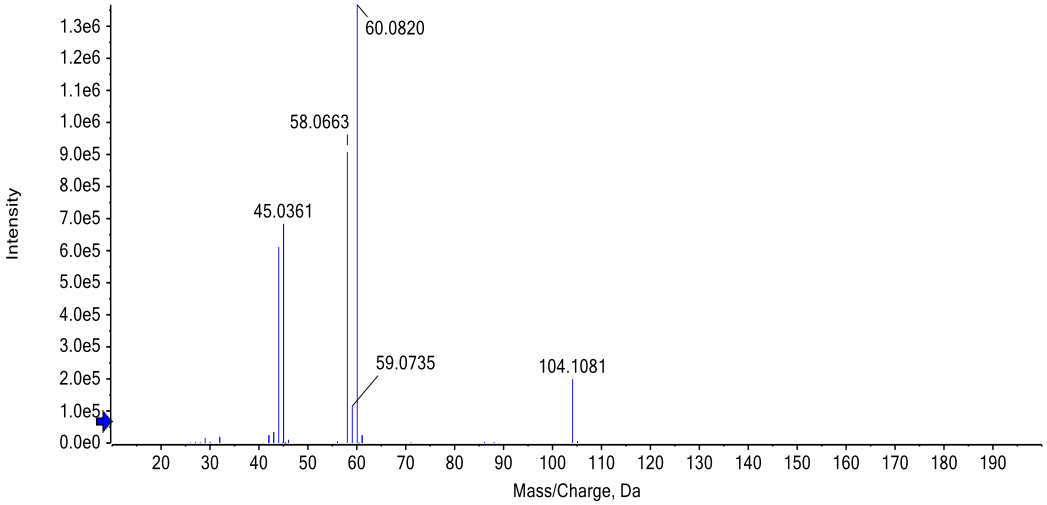

Figure 4.11: MS/MS spectrum acquired for Cho precursor ion m/z 104.11 $[M+H]^+$. The fragments were acquired by ESI in positive ionization mode and with a collision energy of 26 V.

Finally, in figure 4.12 the MS/MS spectrum for Cho-d9 m/z 113.23 is illustrated. The fragments m/z 69.14, 66.12, 49.08 and 45.04 were monitored for this internal standard.

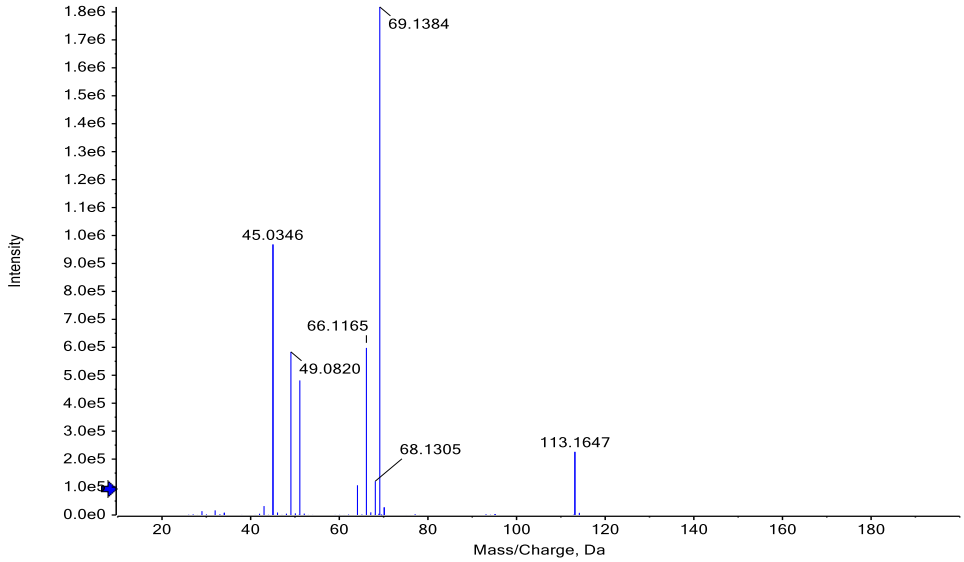

Figure 4.12: MS/MS spectrum acquired for Cho-d9 precursor ion m/z 113.23 $[M+H]^+$. The fragments were acquired by ESI in positive ionization mode and with a collision energy of 27 V.

4.1.2 Compound identification and verification

In order to confirm that the peak response is generated by the target compound, for MS/MS methods it is necessary to have ion transitions for quantification and qualification with the analyte retention time coinciding with the IS chosen [317].

In the first instance, the development, optimization, and validation of the method for the analysis of five analytes, corresponding to the cholinergic (Cho and ACh) and glutamate metabolism (Gln, Glu, and GABA) were proposed. However, after the optimization step, the compounds were studied in mixed solutions, and both analytes of cholinergic metabolism, ACh and Cho, presented a non-linear behavior of the signal response produced with respect to the concentration, generating intense peaks from low concentrations and maintaining approximate values throughout the concentration range, as it can be seen in the Appendix A.2, figure A.3. Because of this, it was decided to focus on the analytes of glutamatergic metabolism in the next steps.

For the selection of the quantification ion for each analyte, the following criteria were considered: it must present a high-intensity peak, best peak shapes, and have a suitable level of linearity and precision [223].

In figure 4.13, representative LC-MS/MS chromatograms for each selected Glu fragments are shown. The three fragments have a similar peak shape and retention time, but there are differences between the intensities of the signal produced by each fragment, being fragment 84.05 the most intense. LC-MS/MS chromatograms for Gln, GABA, and labeled standards are presented in the Appendix A.

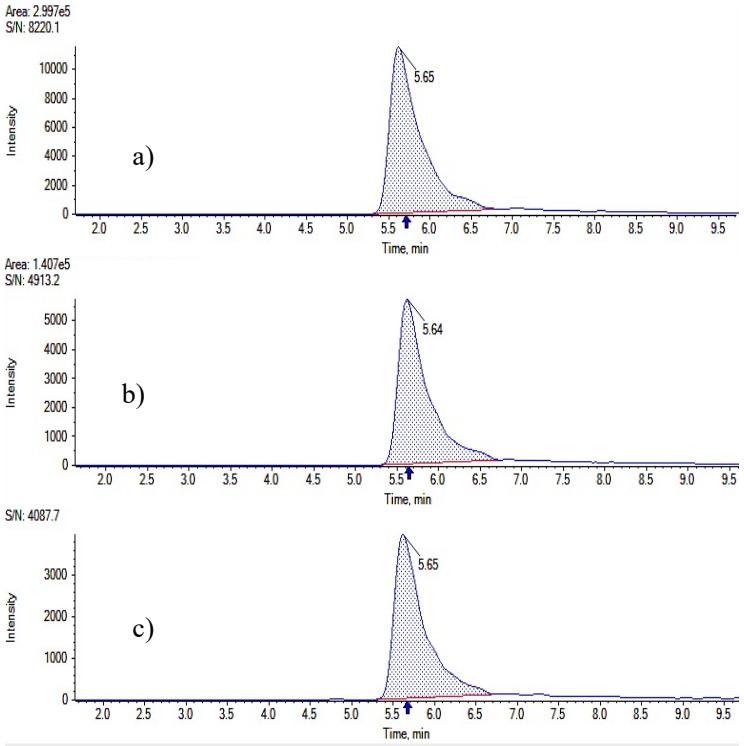

Figure 4.13: Representative LC-MS/MS chromatograms of the fragments monitored for glutamate, a) m/z 84 b) m/z 130 and c) m/z 102.

Taking into account the criteria established above,, the ions used in quantification were m/z 84.05 for Glu and Gln, and m/z 69.03 for GABA, table 4.1.

Table 4.1: Transitions used for quantification and identification, and mean values of retention time of each analyte.

Compound	Transition (m/z)		Retention time (min)
	Quantification	Qualify	
Glu	148.07 → 84.05	148.07 → 130.05 148.07 → 102.06	5.66(0.040)
Gln	147.07 → 84.05	147.07 → 130.05 147.07 → 101.07	5.96(0.013)
GABA	104.07 → 69.03	104.07 → 87.05 104.07 → 43.02	5.01(0.093)

During the analysis of biological matrices such as plasma, urine, CSF, and tissue, variations in the signal of the samples can occur, either due to losses during the sample preparation, loss of injection volume, or matrix effect.

The addition of the IS to every sample analyzed at a fixed concentration is typical for bioanalytical methods performed in LC-MS. Since the chosen IS must have physicochemical properties similar to the analyte of interest, its use allows for corrections as the analyte/IS response ratio would reflect the concentration of the analyte despite the aforementioned situations. Therefore, the use of an appropriate IS can improve the precision and accuracy in a quantification [318].

The following table illustrates the fragment used in the quantification analysis of each analyte and the mean retention time table 4.2.

Table 4.2: Internal standard transitions monitored for the quantification of their respective analytes and mean value of retention time of each labeled standard.

Compound	Quantification transition (m/z)	Retention time (min)
Glu-d5	153.09 → 107.09	5.68(0.041)
Gln-d5	152.18 → 135.08	5.97(0.021)
GABA-d6	110.81 → 93.08	5.00(0.079)

4.2 Method validation

Validation of the analytes corresponding to the glutamate metabolism was carried out, in order to guarantee the quality and reliability of the analytical results. For this purpose, statistical methods were used as an essential part, to summarize data and make objective judgments about the differences between data sets. The performance parameters evaluated were: linearity, working range, analytical limits (LOD and LOQ), precision and accuracy.

4.2.1 Linearity

After a preliminary linearity study, ranging from 0.01 to 4 pmol/µL, in which the statistical criteria for a linear behavior were not fulfilled, a shorter linearity range was assessed, ranging from 0.05 to 1 pmol/µL. An example of the preliminary test carried out is shown in Appendix A.3.2.

Linearity was evaluated from calibration curves (n=4) in the mentioned range. The calibration graph of the quantitation fragment of Glu is illustrated in figure 4.14.

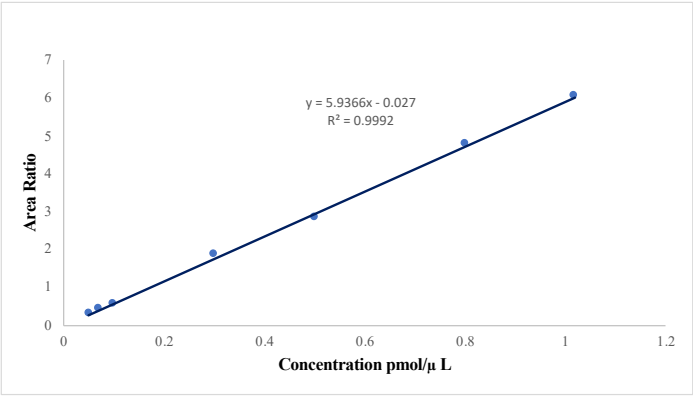

Figure 4.14: Calibration curve of the quantification transition 148.06→84.05 of glutamate in the range of 0.05 to 1.018 pmol/µL .

Since IS were added in the calibrants for each of the corresponding analytes, the response relationship between the analyte and the IS was used. To begin evaluating the linearity, the homoscedasticity of the data was assumed; thus a simple linear regression model was used to try to explain the relationship between the peak area and the known concentrations of the standards.

Based on the criterion of $R^2 \geq 0.995$, all three analyzed molecules were found to be linear throughout the working range for each day (table 4.3). Furthermore, during the evaluation of the

residuals from the linear regression, all the values were less than the twice of the the standard error of the regression and randomly distributed around the x-axis (figure 4.15).

Table 4.3: Parameters obtained in the linearity study by means of the simple linear regression model for each analyte in solvent.

Compound	Transition	Working range (pmol/µL)	Calibration curve	R^2	$S_{y/x}$
Glu	148.07 → 84.05	0.050 − 1.018	$y = 5.937x - 0.027$	0.999	0.070
Gln	147.07 → 84.05	0.049 − 1.003	$y = 1.911x + 0.021$	0.999	0.0027
GABA	104.07 → 69.03	0.050 − 1.024	$y = 0.551x - 0.010$	0.999	0.0032

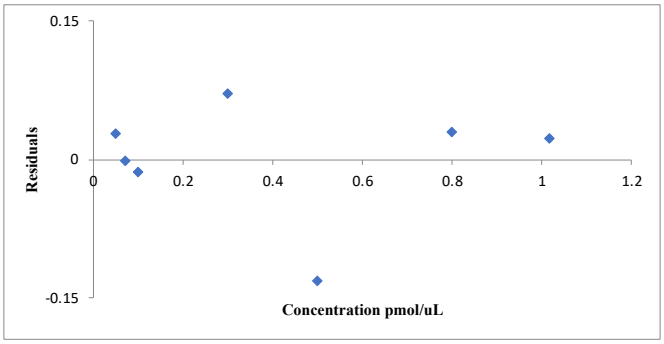

Figure 4.15: Plot of the residuals versus concentration from the simple linear regression of m/z 84.05 of glutamate.

Using a t statistic and a p-value, the significance of the regression coefficients was demonstrated. The slope value was highly significant (different from zero), as expected in a calibration experiment. On the other hand, the assumption that the intersect passes through zero was confirmed, so the intersept is not statistically different from zero ($t^b_{0.05(5)} = 2.57$). By means of an F-test of the overall significance, the fit of the chosen model was compared with a regression model without predictors, taking as a null hypothesis that both models present the same fit. This was confirmed by the p-value of the F-test, which was lower than the level of significance used (0.01).

The regression model showed a high significant predictive capacity for the three analytes, since the values of TV calculated were less than the critical values F_{crit}. The results obtained are presented in the Appendix A.3.1.

4.2.1.1 Mandel test

The linearity of the calibration process was also investigated by the Mandel's fitting test. This test makes it possible to decide which model is the most appropriate to calibrate the instrumental response, by verifying if the data set better fits first degree or quadratic polynomials by comparing the residual errors of both models [308].

The F test was used as a means of verifying the adequacy of the values. The calculated TV for each analyte was less than the critical value (F_{crit}) at the 99% confidence level (table 4.4). This means that the variance between both simple and quadratic model is not significantly different. The quadratic model does not better explain the relationship between the variables, so in this case, the linear model is the most appropriate for the calibration curves.

In addition, the p values were higher than the significance level used (0.01), which allows to

confirm the aforementioned . Therefore, the linearity of all three analytes was found to be linear on each day.

Table 4.4: Results of the Mandel test obtained by comparing a linear & quadratic regression model.

Compound	Transition	Test value (TV)	F_{crit} (N-1;N-3; 99%)	P_{value}
Glu	148.06/84.05	0.46		0.686
Gln	147.07/84.05	0.02	21.20	0.890
GABA	104.07/69.03	0.49		0.521

4.2.2 Working range

To evaluate the working range, visual evaluations were carried out from a plot of residues generated in the regression model versus concentration. An example of the plots obtained is presented in figure 4.16 for Glu fragment ion at m/z 84.05. This plot shows residuals not homogeneously distributed nor centered at zero as expected. It can also be inferred that the observed dispersion increased as a function of concentration; that is, residues were highest in the standard with the highest concentration, thus suggesting that the assumption of homoscedasticity is not fulfilled.

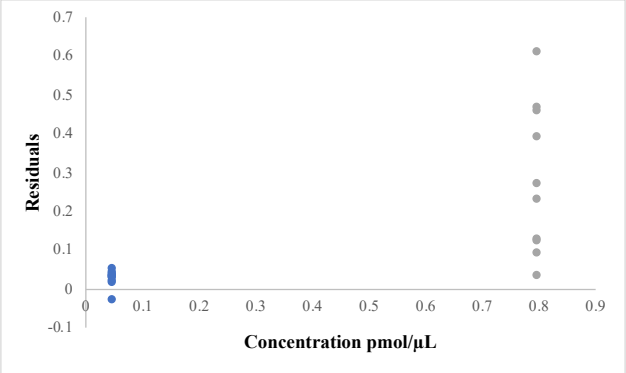

Figure 4.16: Plot of the residuals versus concentration used in the homoscedasticity study of the transition 148.06→84.05 of glutamate.

To confirm these results, an F test was performed to assess the homogeneity of the variances. First, the presence of outliers was discarded using the Grubbs test. Later on, it was possible to compare the variances from the lowest and one of the highest calibrators, in ten independent replicates.

The TV obtained for each of the compounds was much higher than the corresponding critical value ($F^{b}_{0.01(9,9)} = 6.54$) at 95% level of confidence; therefore, the assumption that the variations were similar across the entire working range was rejected. In table 4.5, the results obtained for the quantification fragments of each compound are presented.

Table 4.5: Results of homogeneity test.

Compound	Transition	Test value (TV)	F_{crit} (N-1;N-1; 95%)	P_{value}
Glu	148.06/84.05	230.14		0.000
Gln	147.07/84.05	22.25	6.54	0.000
GABA	104.07/69.03	123.57		0.000

4.2.2.1 Weighted least-squares linear regression

Once the assumption of homoscedasticity of the data was rejected, the approach used to harmonize the variances was a weighted regression. To choose the best weighting factor, empirical weights were evaluated, that is $1/x$, $1/x^2$, $1/y$ and $1/y^2$, considering as a criterion for its choice the one that originated the lowest value of the sum of relative errors % RE and a R^2 ≧0.995.

For glutamate, it was possible to verify that models 3 and 2, with the weight factor $1/x$ and $1/x^2$, respectively, gave the lowest sum of relative error (table 4.6).

Table 4.6: Nominal concentrations and their respective sum of absolute relative errors, calculated using unweighted and weighted models with empirical weights $1/x$, $1/x^2$, $1/y$ and $1/y^2$ for glutamate's transition 148.06→84.05.

Nominal concentration (pmol/µL)	Model 1 $1/x^0$ (OLS)	Model 2 $1/x$ (WLS)	Model 3 $1/x^2$ (WLS)	Model 4 $1/y$ (WLS)	Model 5 $1/y^2$ (WLS)
0.05	36.84	30.82	20.25	34.50	24.84
0.07	17.73	13.00	11.34	14.17	13.39
0.1	40.68	41.48	44.31	39.93	41.67
0.3	5.58	4.69	7.09	4.87	9.44
0.5	5.22	9.04	12.56	9.56	14.38
0.8	13.85	13.22	16.19	13.27	19.38
1.018	8.87	10.71	9.33	9.89	9.84
Σ |%RE|	128.78	122.96	121.06	126.19	132.96
Mean R^2	0.997	0.999	0.996	0.999	0.995

When analyzing the criterion based on R^2 , it was possible to determine that all the proposed models meet the established criterion (≧0.995), being models 2 ($1/x$.) and 4 ($1/y$) the ones that presented the highest value. Consequently, the best weighting factor determined for glutamate's transition 148.06→84.05 was the $1/x^2$. In the figure 4.17, it can be distinguished that the errors obtained with model 3 ($1/x^2$) are distributed in a narrower and more harmonic band than in the simple linear model.

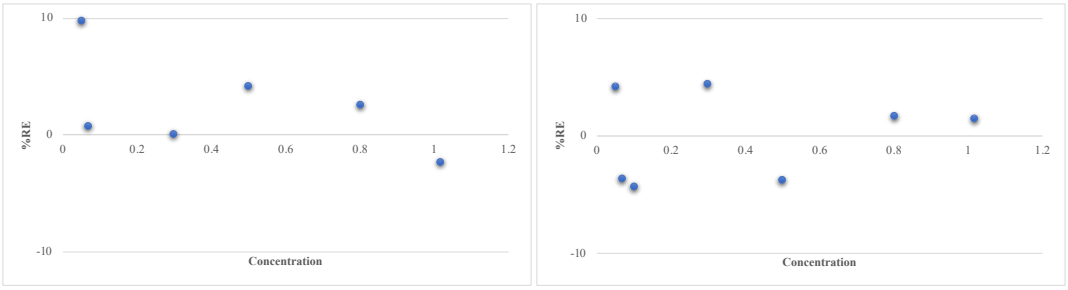

Figure 4.17: Plot of the percentage of relative error (% RE) versus the concentration corresponding to glutamate at m/z 84.05 obtained for model 1 unweighted (left) and the chosen model $1/x^2$ (right).

Regarding the remaining analytes, the same evaluation was carried out to choose the best weighting factor. Thus, for glutamine (Appendix A.3.4), evaluating the %RE data, the models that gave the lowest value were model 3 ($1/x^2$) and model 5 ($1/y^2$) with 104.52 and 105.78, respectively. All models met the criterion of R^2 ≧0.995, taking all this into account, the model 3 ($1/X^2$) was chosen.

Finally, for GABA, the best weighting factor was model 2 ($1/x$), since it was the one that presented the lowest % RE value, as with the other compounds, all models obtained values of R^2 higher than those used as acceptance criteria (Appendix A.3.3).

4.2.3 Precision and accuracy

The precision of the method was assessed, namely intermediate precision (on three different days) and repeatability (on the same day) conditions. The study was carried out using QCs at three levels of concentration: high, medium and low, $n = 6$ for repeatability, and n=10 for intermediate precision. The obtained values for both approaches were expressed as % RSD, calculated using equation (3.18).

The results obtained for each analyte at the intermediate level of precision and repeatability are shown in the table 4.7. As an acceptance criterion, it was set at ±15% of the nominal value and ±20% for the LOQ.

All three analytes, for both intermediate precision and repeatability, met this criterion. So, it can be concluded that the analytical method developed is highly precise in terms of intermediate precision and repeatability for Glu, Gln and GABA.

Then, to verify the influence of the day factor on the results obtained, the single-factor Anova statistical tool was applied. By analyzing the results obtained, it is verified, in all the three analytes, the experimental value does not exceed the critical value ($F^u_{0.05(2,7)} = 4.30$), indicating that the day factor does not influence the results obtained, there is thus agreement between the results obtained on the different days.

Table 4.7: Results obtained for the precision analysis at the level of repeatability and intermediate precision.

Compound	Nominal concentration (pmol/µM)	Intermediate precision %RSD	Repeatability %RSD
Glu	0.05	4.3	3.7
	0.10	11.2	4.8
	0.80	4.04	4.1
Gln	0.05	7.3	4.3
	0.10	6.9	5.9
	0.79	7.09	2.4
GABA	0.05	12.7	5.1
	0.10	10	3.2
	0.81	5.5	2.4

Regarding the accuracy analysis, this was expressed in terms of mean relative error % RE, calculated using equation (3.13). Critical acceptance, as in the precision study was established at ±15% of the nominal value and ±20% for the LOQ.

The results are shown in the table 4.8; from these data,it is possible to conclude that all the three analytes fulfilled the critical acceptance; thus, it is demonstrated the accuracy of the method to these two analytes. Therefore, the method is highly precise and accurate for the analytes studied.

Table 4.8: Results obtained for the accuracy analysis at three concentration levels and with six daily replicates per QC.

Compound	Nominal concentration (pmol/µM)	Mean observed concentration (pmol/µL)	Accuracy%RE
Glu	0.05	0.06	11
	0.10	0.10	-3.0
	0.80	0.87	-8.6
Gln	0.05	0.04	12
	0.10	0.11	8.4
	0.79	0.91	14
GABA	0.05	0.06	16
	0.10	0.12	15
	0.81	0.88	8.8

4.2.4 Analytical thresholds

As already mentioned in the section 3.5.4, the analytical limits can be calculated from different approaches, in this study was used the approaches based on the residual standard deviation of a regression line and repeatability studies. Since the intercept has no statistical significance, it was not used in calculating this estimate.

After choosing the best calibration model for each of the molecules, the residual standard deviation of the regression line was recalculated (equation 3.17). The results of LOD and LOQ are presented in Tables 4.9.

Table 4.9: The limits of detection (LOD) and quantification (LOQ) defined through the two estimation modes (repeatability studies and the standard deviation of the fit).

	Repeatability		$S_{y/x}$	
Compound	LOD (pmol/µL)	LOQ (pmol/µL)	LOD (pmol/µL)	LOQ (pmol/µL)
Glu	0.006	0.020	0.100	0.290
Gln	0.009	0.030	0.090	0.260
GABA	0.007	0.002	0.024	0.071

Based on the limits obtained through the repeatability approach, the lowest analyte concentration detected for Glu was 0.006 pmol/µL, while the LOQ was 0.02 pmol/µL. Through the another approach, the limits obtained were higher (LOD= 0.100 pmol/µL and LOQ= 0.290 pmol/µL).

For Gln, like Glu, based on the thresholds calculated using the repeatability approach, the lower limits of both, LOD and LOQ, were obtained (0.009 and 0.03 pmol/µM).

In the case of GABA, the lowest levels obtained were reached using the same approach based on repeatability. The LOD and LOQ were defined in 0.007 and 0.002 pmol/µL, respectively.

It was confirmed that in the three compounds the LOQs were lower than the concentration of the first pattern of the calibration curve.

4.2.5 CSF analysis

CSF spiked samples with 100 µL of the mixed analyte solution and 10 µL of IS solution were used to determine whether a correct detection and identification of the compounds in the matrix occurs, or otherwise the matrix effects inhibit the signal response.

The figure 4.18 illustrates the chromatogram obtained for the glutamate quantification fragment. When comparing the CSF "blank" sample with the spiked samples, no differences were obtained in the signal response, that is, the molecule was not correctly detected. It was verified that no apparent changes happen with the labeled standard (Glu-d5, m/z 107.08) as well. It can be assumed that there was signal suppression for this analyte due to possible matrix effects, so, it was not possible to measure Glu in real samples.

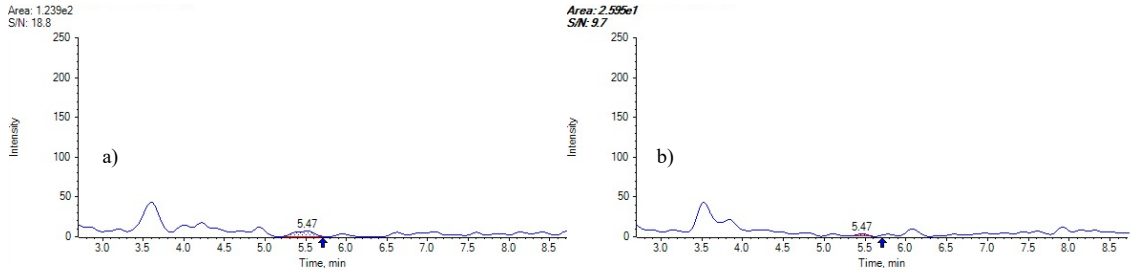

Figure 4.18: Chromatogram of glutamate for quantification of the transition 148.06→84.05 in a) "blank" CSF sample with no analytes spiking and b) CSF sample spiked with 3000 fmol of Glu from a mixed solution.

In addition, analyzing the areas of the different transitions, it was found that the area of the quantification ion (84.05, color blue) and the ion with an m/z 130.05 (color magenta), was not the one expected according to the ratios obtained by the patterns of the curve figure 4.19. The same happened with fragment m/z 102.06 (in orange), being its intensity in the CSF blank and spiked samples much higher than that observed in the calibration standards. Taking this into account, it could be inferred that the effects of the matrix affected the ability to measure the compound in the CSF, so the presence of this analyte in this matrix was not confirmed, with which the measurement of glutamate in the biological samples was not performed.

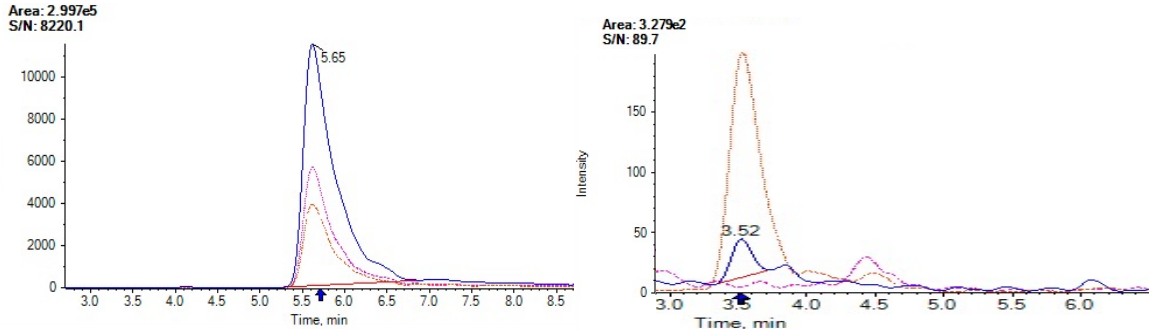

Figure 4.19: Comparison in the area ratios of the monitored transitions for glutamate in standard solutions (left), and in spiked samples (right). In orange the fragment at m/z 102.06, magenta for m/z 130.05, and blue for m/z 84.05.

In the case of Gln, its detection was verified in the spiked samples, as shown in figure 4.20. Emphasizing that the retention time was very similar between both samples, coinciding with the

values observed in the solvent studied 5.96(0.013).

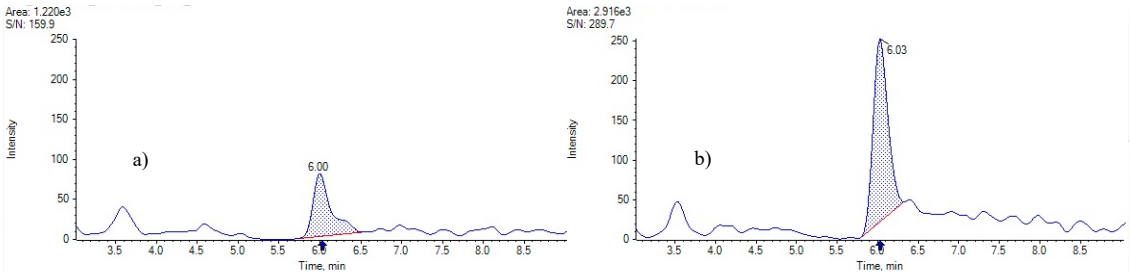

Figure 4.20: Chromatogram of glutamine for quantification of the transition 147.07→84.05 n a) "blank" CSF sample with no analytes spiking and b) CSF sample spiked with 2960 fmol of Gln from a mixed solution.

In the same way, for GABA, the detection of this compound was verified in the spiked sample, but its retention time slightly varied compared to expected from the test performed by the calibration curves 5.01(0.093) figure 4.21. Once the detection of glutamine and GABA in CSF were demonstrated, the measurements of these analytes were carried out in the biological samples.

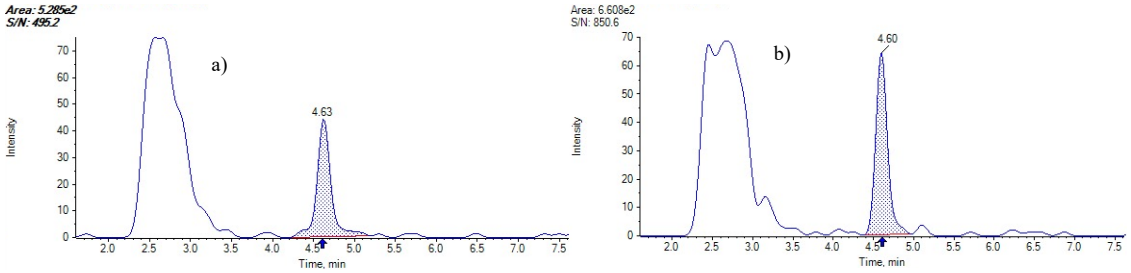

Figure 4.21: Chromatogram of GABA for quantification of the transition 104.07→69.03 in a) "blank" CSF sample with no analytes spiking and b) CSF sample spiked with 3000 fmol of GABA from a mixed solution containing Glu, Gln, GABA plus labeled standards.

4.3 Method application in CSF samples

Once the validation process was carried out, the method was applied to analyze the study samples. The study included forty CSF samples from AD patients with Aβ+ and Aβ- studies. Supplementary information of these samples is presented in appendices A.4, in which are detailed the age and sex of each patient. The content measured for each analyte is also shown in the appendix A.4.

Since transition ions are considered a physical property of an analyte of interest [319], the transition ion ratios (less intense ion / more intense ion) was assessment in order to improve the confidence in the measurement of the target metabolites.

Thus, the mean of the ion ratio of each compound from the calibration solutions (Appendix A.4 table A.7), was compared with the means of ion ratios of the samples. According to the European Commission Decision (2002/657/EC) for analytical methods the ion relative tolerance is sets at ±20% to ±50% depending on the relative ion intensities [317, 320]. Also the variability of the ion ratio was assessed, expressed as % RSD, the ±20% of deviation is defined in different guidelines [317, 319, 321].

Additionally, difference of the retention time was calculated, using the average of the retention times of the samples compared to those of the labeled standard. For this evaluation, the tolerance limit is set at ±2.5% [320, 322].

The results of monitoring ion ratios and the difference of the retention time are reported in 4.10. The analysis of the ion ratios, also can be observed in figure 4.22, where it is shown all three fragments monitored in the CSF samples and in the solvent for Gln and GABA.

Table 4.10: Analysis of the ion ratios of the areas (AR) and mean values of retention time of glutamine and GABA in CSF samples.

Parameters	Gln			GABA		
	AR 130/84	AR 101/84	RT	AR 69/87	AR 43/87	RT
Mean	0.969	21.3	6.02	0.40	7.24	4.55
%RE	-29.9	173	0.76	-16.5	134	0.56
% RSD	4.01	21.1	0.31	15.4	31.4	0.57

In the case of glutamine, although the m/z 101.07 did not meet the parameters previously established for the analysis of ion's ratio, the m/z 130.05 was in agreement with these parameters, so this ion was used for the confirmation of the analyte. Regarding the differences in retention times, both ions were within the tolerance of 2.5% established.

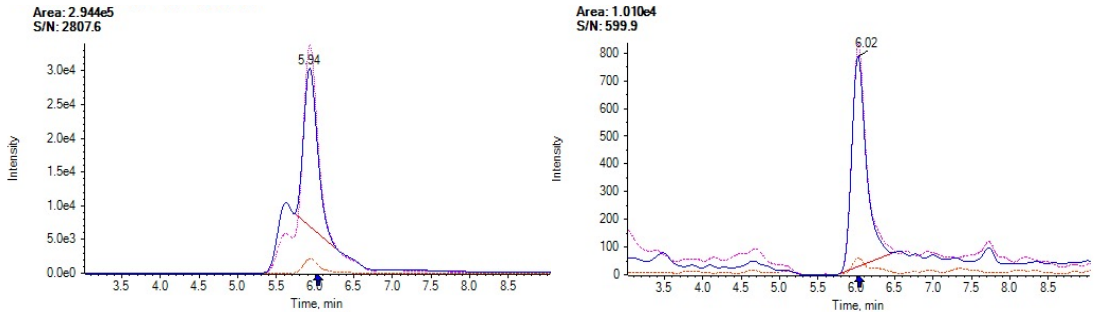

(a) Gln

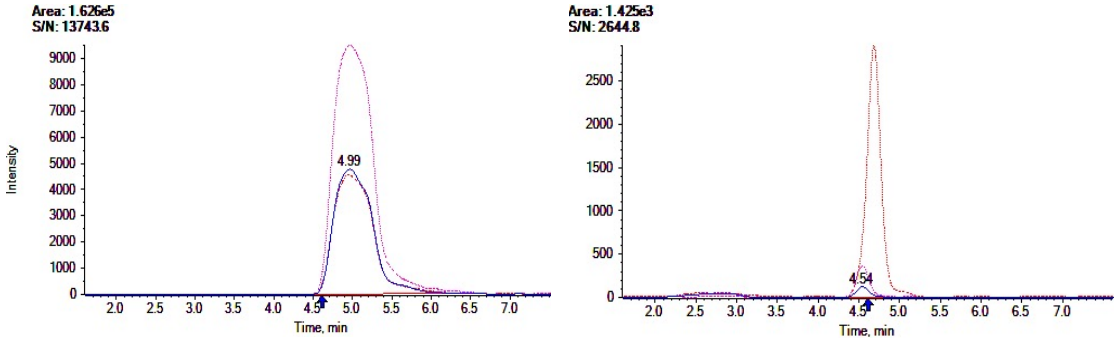

(b) GABA

Figure 4.22: Chromatogram of the monitored transitions for glutamine and GABA in the curve (left) and in the CSF samples (right).

Gln (a) the transition at m/z 101.07 in orange, magenta for m/z 84.05, and blue for m/z 130.05. GABA (b) m/z 43.02 in orange, magenta for m/z 87.05 and blue for m/z 69.03.

With regards to GABA, as was expected the relationship between m/z 87.05 m/z 69.03 gave greater reliability in the confirmation of the compound in the CSF samples. For the ion m/z 43.02, great variability in the area ratio and difference compared to the standards was obtained, so this transition was discarded for the confirmation of GABA. Like Gln, the retention time was very similar to that of the internal standard used.

The results of the measurements obtained for these compounds were graphically represented in box plots, using R statistical software and ggplot2 package. Through this tool it was possible to visually compare the ranges and the distribution of the areas of the groups in the study. Moreover, to verify if there is a significant difference in the median of measurements in the Aβ+ and Aβ- groups, a non-parametric Wilcoxon-Mann-Whitney for independent samples was performed. In this test, no significant difference between the two groups was established as a null hypothesis for p-values greater than 0.05.

The figure 4.23 shows measurements of glutamine, comparing in the first square the measurements between Aβ+ and Aβ- from all patients, as in the second and third frame this comparison between groups is performed in female and male patients, respectively.

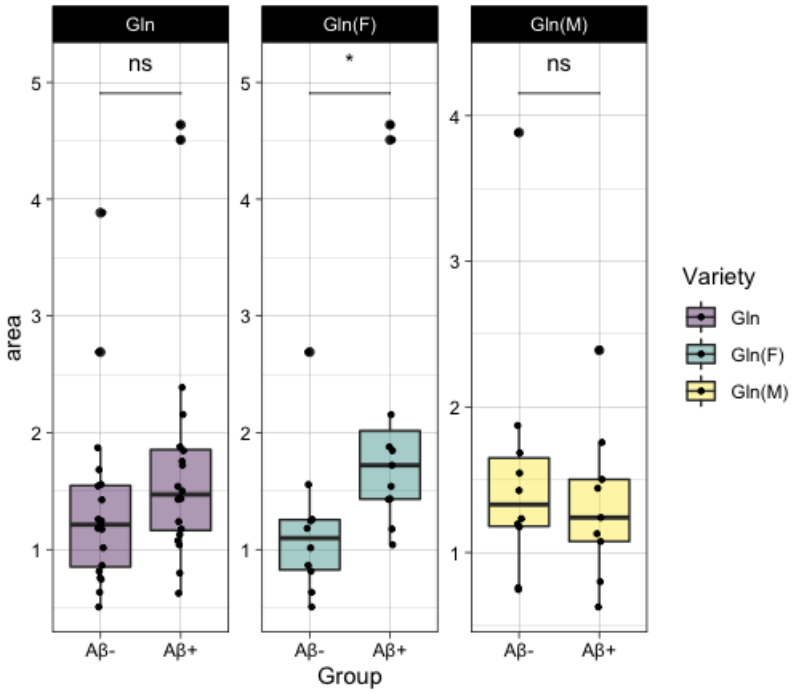

Figure 4.23: Box plot of the data acquired for the glutamine measurements in CSF samples from patients with AD, comparing Aβ+ and Aβ- groups and focused on gender.

In an overall analysis, higher values were observed in the quantities of glutamine in the patients with Aβ+ compared with those of the Aβ- group (see Appendix 4.2, table A.8). However, the medians of glutamine in both groups do not differ significantly, with a fold change of 1.21, p-value = 0.108.

About the data focused on gender, in females, a significant increase of the quantities of glutamine in the Aβ+ patients was determined, fold change of 1.57 *(*p-value = 0.013).

In the case of males, no significant differences were found between both groups, reporting values of fold change of 0.87, p-value = 0.720 (Appendix A.4.2, table A.9).

With respect to GABA, in figure 4.24 it is shown the box plot comparing the data obtained from Aβ+ and Aβ- groups in the first square. Similar values of medians and variability were found in the Aβ+ and Aβ- patients. Thus, no significant statistical differences were found, fold change of 0.87, p-value = 0.056 (Appendix A.4.3, table A.10).

When analyzing the data of the AD patients focused in the gender, in females (second frame), greater content of GABA was observed for the Aβ- group comparing with Aβ+, however, no significant differences were found between the two groups, fold change of 0.73 p-value = 0.051.

For males, similar values between Aβ+ and Aβ- groups were observed, thus, no significant differences were found between the two groups, fold change 0.98, p-value = 0.497 (Appendix 4.3, table A.11).

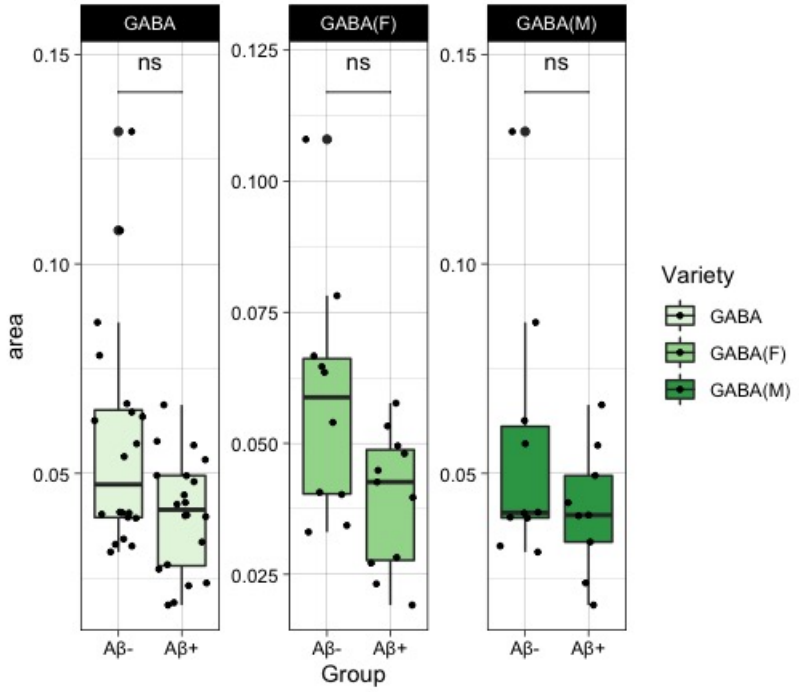

Figure 4.24: Box plot of the data acquired for the measurement of GABA in CSF samples from patients with AD, comparing Aβ+ and Aβ- groups and focused on gender.

Additionally, since GABA is a metabolite of glutamate, and glutamine acts as both a precursor and a metabolite in the called glutamate-glutamine (GABA) cycle [323, 324], the measurements in the CSF samples obtained were also analyzed as GABA/Gln ratios, in order to determine if there are differences in this relationship between the Aβ+ and Aβ- groups. These results are presented in figure 4.25.

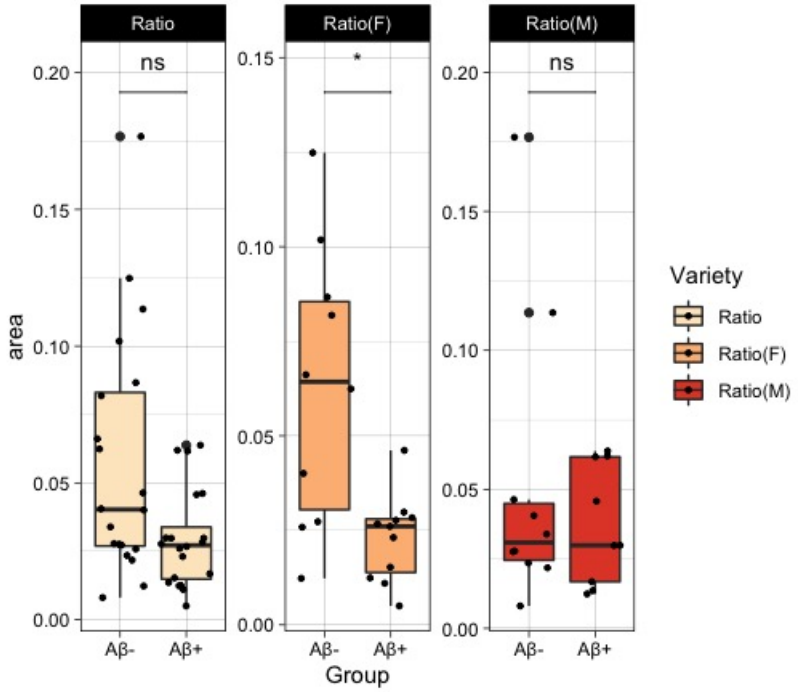

Figure 4.25: Box plot of the ratios of GABA and glutamine measurements, comparing Aβ+ and Aβ- groups and focused on gender.

Analyzing these ratios, was observed similar values of median in both groups (Aβ+ and Aβ-), with greater variability in the Aβ+ patients (Appendix A.4.2, table A.12). However, no significant differences was found, p-value 0.070.

Focused in the gender, in female patients the median of group Aβ- was much higher than that obtained for group Aβ+, using a Wilcoxon test was obtained a p-value of 0.038, which indicates that there is a significant difference between the ratio of the GABA/Gln measurements in the Aβ+ and Aβ- groups (Appendix A.4.2, table A.13). Regarding the ratio in males, very similar values were obtained for both groups, with no statistically significant difference between groups (p-value = 0.968).

In addition, the data was also assessed based on age (figure 4.26). The data were pooled taking as the cut-off point the age of 60 years; this threshold is used to differentiate patients with AD with early onset and late onset (Seccion 1.1.1. Alzheimer's disease aetiology). Therefore, two groups were formed: patients with AD under 60 years of age and over 60 years.

In the group of patients over 60 years old, a slight increase was observed in the levels of Gln, in AD patients with Aβ+ compared with those with Aβ-. However, when the medians of both groups were analyzed, it was found not to be significantly difference between them, fold change of 1.31 (p-value = 0.189). Regarding to the patients under 60 years, the Gln levels observed were very close between both groups (Aβ+ and Aβ-), showing no significant changes (fold change of 0.99, p-value = 0.918) (Appendix A.4.2, table A.14).

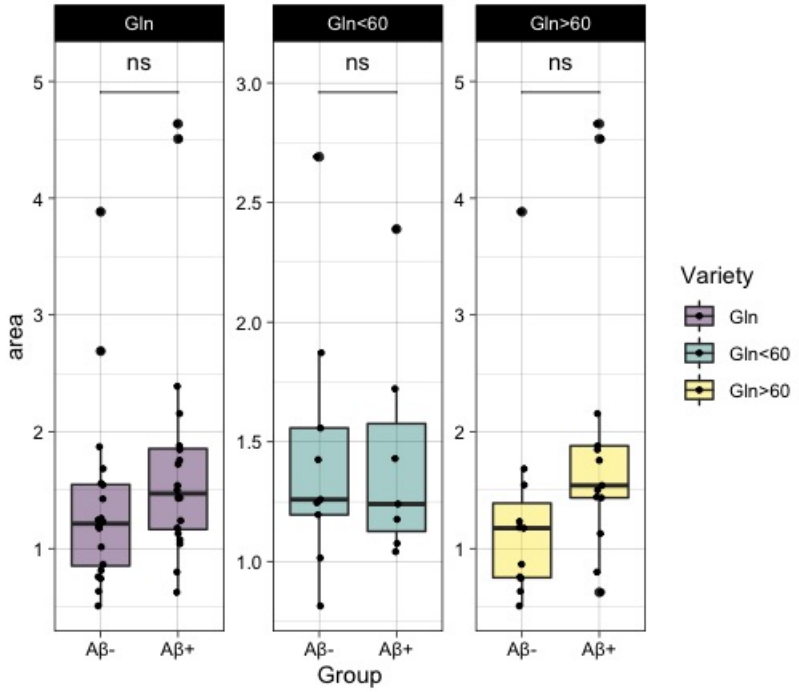

Figure 4.26: Box plot of the data acquired for the measurement of glutamine in CSF samples from patients with AD, comparing Aβ+ and Aβ- groups and focused on age.

In line with the analysis performed in the glutamine focused in the age of the AD patients, the content of GABA was grouped by age, namely patients with 60 years old or older and younger that 60 years old figure 4.27.

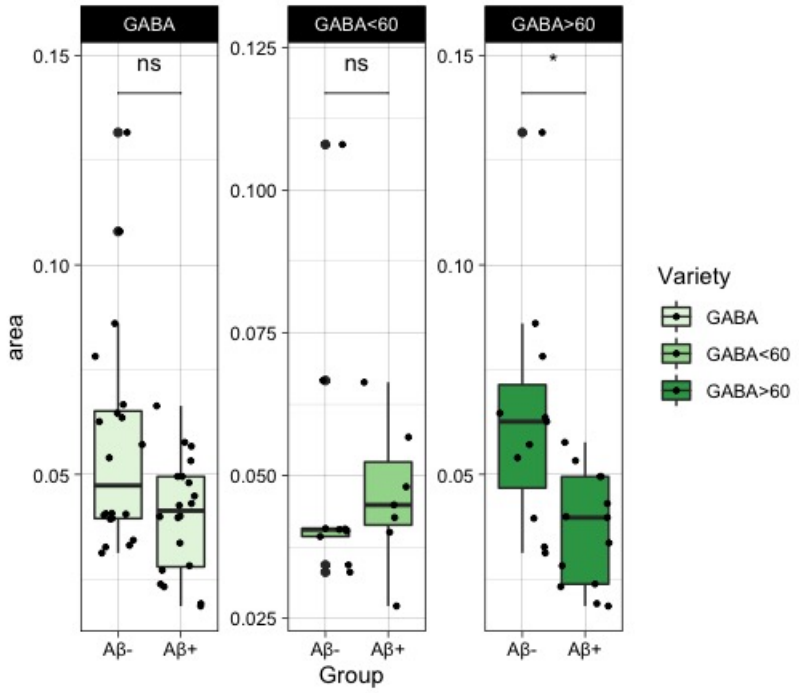

Figure 4.27: Box plot of the data acquired for the measurement of GABA in CSF samples from patients with AD, comparing Aβ+ and Aβ- groups and focused on age.

The CSF GABA levels observed in patients younger than 60 years were slightly lower than those found in patients older than 60 years (Appendix 4.3, table A.15). Analyzing the measures between the groups Aβ- and Aβ+, statistically significant differences in the medians were found in the patients with 60 age and older, reporting fold change of 0.63, p-value = 0.006. While no significant differences were reported in the patients under 60 years old, fold change 1.11, p-value = 0.536.

When observing the measurements of the GABA/glutamine ratio, a slight difference was found between the Aβ+ and Aβ- patients (figure 4.28), however, this difference was no significant p-value = 0.105 (Appendix A.4.2, table A.16).

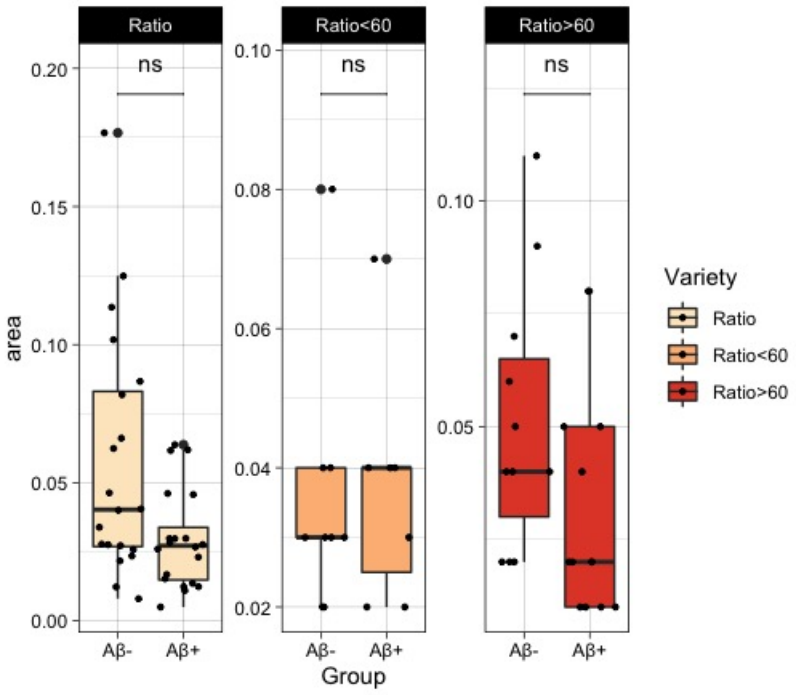

Figure 4.28: Box plot of the ratios of GABA and glutamine measurements, comparing Aβ+ and Aβ- groups and focused on age.

In patients older than 60 years, it was observed that the production of GABA is reduced while glutamine increased in the group of patients with Aβ+, nevertheless, no statistically significant differences between Aβ+ and Aβ- groups were detected, p-value = 0.164. In patients younger than 60 years, the medians of the measurements were very similar between the groups, no significant differences was found, p-value = 0.741.

In this study, both groups are comprised of AD patients. Since to date, no data have been obtained from other studies that analyze these neurotransmitters between the two groups (Aβ+ and Aβ-), some results obtained in other studies for these neurotransmitters comparing patients with AD and healthy control subjects are described below.

In agreement with the non significant differences levels of glutamine between Aβ+ and Aβ- obtained in this work, in a meta-analysis performed by Manyevitchm et al., 2018, a non-significant increase in CSF glutamine levels were reported between AD patients and healthy control subjects [81]. While Madeira et al, 2018 found a significant increased CSF levels of glutamine in patients with probable AD compared with healthy control [325]. In contrast, descreased CSF levels in AD

patients were reported in the study of Hashimoto et al., 2016 [326]. While no significant changes between AD patients and neurological controls were reported in the recent study of Tommaso et al., 2021 [327].

A statistically significant difference between the levels of glutamine in CSF between Aβ+ and Aβ- female patients was identified in our study, indicating higher levels of this analyte in the females with Aβ+. In male patients, this significant differences were not identified. In contrast, no gender differences in glutamine levels were found in the study performed by Madeira et al, 2018 [325].

The same analysis for GABA, no significant differences between Aβ+ and Aβ- patients were identified in our work. In contrast, in the study performed by Manyevitchm et al., 2018, CSF GABA levels were found to be significantly decreased in AD patients compared to healthy control subjects [81].

However, in the analysis for ages, a statistically significant difference was identified in the levels of GABA in the AD patients with 60 or older, showing increased CSF levels of this analyte in the Aβ- group compared with the Aβ+. This could indicate that above 60, GABA reflects the deposition of Aβ in the brain. However, more studies are needed to clarify these results.

Chapter 5

Conclusions

5. Conclusions

In the present work, the main objective was the development of an LC-MS/MS method, capable of performing the measurement of target metabolites (choline, acetylcholine, glutamate, glutamine and GABA) that characterizes the cholinergic and glutaminergic systems in CSF samples.

To achieve this purpose, the direct injection of individual analytes into the MS and LC-MS/MS system was carried out as part of a method optimization stage. In this way, it was possible to estimate the optimal conditions for each analyte in terms of chromatographic separation and an adequate fragmentation in the MS, setting up the experiment in an HR-MRM mode. However, when it was attempted to analyze all the analytes in a mix solution, a non-linear response was observed of the analytes corresponding to the cholinergic system.

Therefore, in the next stages of the project, only the analytes of glutamate metabolism were studied.

Moreover, a validation procedure was executed, and the following performance parameters were assessed in solvent samples: linearity, working range, precision, accuracy, and analytical threshold.

In terms of linearity, the developed method proved to be capable of offering results directly proportional to the concentration of the analytes in intervals of 0.05-1 pmol/µL for each compound. Linearity assessment was also performed, not just based on the coefficient of determination (R^2) but also evaluating the residuals generated from the linear regression model. Likewise, a Mandel test confirmed the linearity of the method, indicating that a simple first degree polynomial model can be used to fit the data.

Once the heteroscedasticity of the residuals was found in the data of all molecules, a weighted regression model was used to harmonize the variances. In this sense, weighting factors that best fit the data of each molecule were chosen $1/x^2$ for both Glu and Gln; and $1/x$ for GABA.

The analytical method showed high precision under intermediate precision and repeatability conditions, expressed by the low relative standard deviation (%RSD) values for all studied molecules. Furthermore, the method demonstrated accuracy in measurements determinated for each of the molecules. The limit of quantification in this method was: 0.02, 0.03, and 0.002 pmol/µL for glutamate, glutamine, and GABA, respectively.

After the validation procedure, it was tested if the compounds were detected correctly in the matrix, CSF. Glutamine and GABA were detected and identified in CSF, in the case of glutamate, matrix effects affected the ability of the method to measure it, so it was not possible to perform the measurement of this compound. It is essential in future works to study possible improvements to the method in order to reduce the matrix effects, with the purpose of improving its ability to identify this molecule in CSF.

Finally, the analytical method was applied to CSF samples. Two study groups were used in this project, samples from AD patients with positive or negative amyloid studies (Aβ+ and Aβ-). With the help of statistics, it was possible to establish differences in the CSF levels measured between the Aβ+ and Aβ- groups. Analyzing both groups, these differences were non-significant in glutamine measurements (1.21-fold change, p-value = 0.109), while, interestingly, we found a significant increase levels of this analyte in the females with Aβ+, fold change of 1.57 (p-value = 0.013). In addition, no age significant differences in glutamine levels were found in this study.

For GABA, non-significant differences were identified between the Aβ+ and Aβ- patients. Nevertheless, in patients with 60 or older, a significant increased in the CSF GABA levels of the Aβ-

group compared with the Aβ+ was found, reporting a fold change of 0.63, p-value = 0.006. On the other hand, in the gender analysis, no differences were identified in GABA levels in this study.

Regarding to the significant increase in the ratio measurements of GABA/glutamine found in the Aβ- group of females, it is likely that glutamine production increased while GABA increased in Aβ- female patients, as a reflection of a hypothetical increased glutamate levels. However, to suggest this it is necessary to have glutamate measurements and a full study of various metabolic pathways should be performed. More studies are needed to clarify whether glutamine and GABA differ or not in patients belonging to Aβ+ and Aβ- groups, furthermore, the study of how gender and age influence the alteration of CSF levels of these neurotransmitters should be amplified.

Given neurotransmitter dysfunction has been linked to AD, its detection has become an important factor in the diagnosis and control of the disease, as well as in the development of treatments. This study represents a relevant contribution in their follow-up, by demonstrating to be able to identify and perform a measurement of glutamine and GABA.

Bibliography

[1] Polis B, Samson AO. Chapter 1. A new perspective on Alzheimer's disease as a brain expression of a complex metabolic disorder. In: Wisniewski T, editor. Alzheimer's Disease. Codon Publications; 2019. p. 1–22. Available from: https://doi.org/10.15586/alzheimersdisease.2019.ch1.

[2] Machado APR, Carvalho IO, da Rocha SHM. Neuroinflamation in Alzheimer's disease. R Bras Mil Ci. 2020;6(14):30–38.

[3] Yilmaz U. Alzheimer-Demenz. Der Radiologe. 2015;55:386–388. Available from: https://doi.org/10.1007/s00117-014-2796-2.

[4] Iraji A, Khoshneviszadeh M, Firuzi O, Khoshneviszadeh M, Edraki N. Novel small molecule therapeutic agents for Alzheimer disease: Focusing on BACE1 and multi-target directed ligands. Bioorg Chem. 2020;97:103649. Available from: https://doi.org/10.1016/j.bioorg.2020.103649.

[5] Ghosh I, Sankhe R, Mudgal J, Arora D, Nampoothiri M. Spermidine, an autophagy inducer, as a therapeutic strategy in neurological disorders. Neuropeptides. 2020;83:102083. Available from: https://doi.org/10.1016/j.npep.2020.102083.

[6] Darin J, Isaac M, McCleery J, Tabet N. Aspirin, steroidal and non-steroidal anti-inflammatory drugs for the treatment of Alzheimer's disease. Cochrane Database of Syst Rev. 2012;(2). Available from: https://doi.org//10.1002/14651858.CD006378.pub2.

[7] Oboudiyat C, Glazer H, Seifan A, Greer C, Isaacson R. Alzheimer's disease. Semin Neurolo. 2013 Nov;33(4):313–329. Available from: https://doi.org/10.1055/s-0033-1359319.

[8] Mantzavinos V, Alexiou A. Biomarkers for Alzheimer's disease diagnosis. Curr Alzheimer Res. 2017;14:1149–1154. Available from: https://doi.org/10.2174/1567205014666170203125942.

[9] Holtzman DM, Morris JC, Goate AM. Alzheimer's disease: the challenge of the second century. Sci Transl Med. 2011;3(77). Available from: https://doi.org/10.1126/scitranslmed.3002369.

[10] Livingston G, Sommerlad A, Orgeta V, Costafreda SG, Huntley J, Ames D, et al. Dementia prevention, intervention, and care. The Lancet. 2017 Dec;390(10113):2673–2734. Available from: https://doi.org/10.1016/S0140-6736(17)31363-6.

[11] Mangialasche F, Solomon A, Winblad B, Mecocci P, Kivipelto M. Alzheimer's disease: clinical trials and drug development. The Lancet Neurology. 2010;9(7):702 – 716. Available from: https://doi.org/10.1016/S1474-4422(10)70119-8.

[12] Georges J. Dementia in Europe Yearbook 2019. Estimating the prevalence of dementia in Europe. Alzheimer Europe. 2019;Available from: https://www.alzheimer-europe.org/content/download/195515/1457520/file/FINAL%2005707%20Alzheimer%20Europe%20yearbook%202019.pdf.

[13] Lane C, Hardy J, Schott J. Alzheimer's disease. Eur J Neurol. 2017 Jan;1(25):59–70. Available from: https://doi.org/doi:10.1111/ene.13439.

[14] Tiwari S, Atluri V, Kaushik A, Yndart A, Nair M. Alzheimer' disease: pathogenesis, diagnostics, and therapeutics. Int J Nanomed. 2019;14:5541 – 5554. Available from: https://doi.org/10.2147/IJN.S200490.

[15] Khan TK. Chapter 1- Introduction to Alzheimer's disease biomarkers. In: Khan TK, editor. Biomarkers in Alzheimer's Disease. Academic Press; 2016. p. 3 – 23. Available from: https://doi.org/10.1016/B978-0-12-804832-0.00001-8.

[16] Ranjan VD, Qiu L, Tan EK, Zeng L, Zhang Y. Modelling Alzheimer's disease: Insights from in vivo to in vitro three-dimensional culture platforms. J Tissue Eng Regener Med. 2018;12(9):1944–1958. Available from: https://doi.org/10.1002/term.2728.

[17] Parul K, Thakur A, Goswami K, Ahuja K. Pathophysiology and management of alzheimer's disease: an overview. Journal of Analytical & Pharmaceutical Research. 2018 04;7(2). Available from: https://doi.org/10.15406/japlr.2018.07.00230.

[18] Sajjad R, Arif R, Shah AA, Manzoor I, Mustafa G. Pathogenesis of Alzheimer's Disease: Role of Amyloid-beta and Hyperphosphorylated Tau Protein. Indian Journal of Pharmaceutical Sciences. 2018;80:581–591. Available from: https://doi.org/10.4172/pharmaceutical-sciences.1000397.

[19] Marr RA. The Amyloid beta Precursor Protein and Cognitive Function in Alzheimer's Disease. In: Lazarov O, Tesco G, editors. Genes, Environment and Alzheimer's Disease. San Diego: Academic Press; 2016. p. 97 –133. Available from: https://doi.org/10.1016/B978-0-12-802851-3.00004-8.

[20] Kovac A, Somikova Z, Zilka N, Novak M. Liquid chromatography-tandem mass spectrometry method for determination of panel of neurotransmitters in cerebrospinal fluid from the rat model for tauopathy. Talanta. 2014;119:284 – 290. Available from: http://www.sciencedirect.com/science/article/pii/S0039914013008266.

[21] Sangubotla R, Kim J. Recent trends in analytical approaches for detecting neurotransmitters in Alzheimer's disease. TrAC Trends in Analytical Chemistry. 2018;105:240 – 250. Available from: https://doi.org/10.1016/j.trac.2018.05.014.

[22] Masliah E, Salmon DP. When Cognitive Decline Becomes Pathology: From Normal Aging to Alzheimer's Disease. In: Lazarov O, Tesco G, editors. Genes, Environment and Alzheimer's Disease. San Diego: Academic Press; 2016. p. 29 – 50. Available from: https://doi.org/10.1016/B978-0-12-802851-3.00002-4.

[23] Janeiro MH, Ardanaz CG, Sola-Sevilla N, Dong J, Cortés-Erice M, Solas M, et al. Biomarkers in Alzheimer's disease. Advances in Laboratory Medicine / Avances en Medicina de Laboratorio. 2021;2(1):27–37. Available from: https://doi.org/10.1515/almed-2020-0090.

[24] Khoury R, Ghossoub E. Diagnostic biomarkers of Alzheimer's disease: A state-of-the-art review. Biomarkers in Neuropsychiatry. 2019;1:100005. Available from: https://doi.org/10.1016/j.bionps.2019.100005.

[25] Khan TK. Chapter 2- Clinical diagnosis of Alzheimer's disease. In: Khan TK, editor. Biomarkers in Alzheimer's Disease. Academic Press; 2016. p. 27 – 48. Available from: https://doi.org/10.1016/B978-0-12-804832-0.00002-X.

[26] Dickie DA, Quinn TJ, Dawson J. In: Rea PM, editor. The Whole Picture: From Isolated to Global MRI Measures of Neurovascular and Neurodegenerative Disease. Cham: Springer International Publishing; 2019. p. 25–53. Available from: https://doi.org/10.1007/978-3-030-31904-5_3.

[27] Kirkland AE, Sarlo GL, Holton KF. The role of magnesium in neurological disorders. Nutrients. 2018;10(6). Available from: https://doi.org/10.3390/nu10060730.

[28] Karch CM, Goate AM. Alzheimer's disease risk genes and mechanisms of disease pathogenesis. Biol Psychiatry. 2015;77(1):43 – 51. The New Psychiatric Genetics: Toward Next Generation Diagnosis and Treatment. Available from: https://doi.org/10.1016/j.biopsych.2014.05.006.

[29] Butterfield DA, Pocernich CB. The glutamatergic system and Alzheimer's disease. CNS Drugs. 2003;17(9):641–652. Available from: https://doi.org/10.2165/00023210-200317090-00004.

[30] Bartolotti N, Lazarov O. Lifestyle and Alzheimer's disease: The role of environmental factors in disease development. In: Lazarov O, Tesco G, editors. Genes, Environment and Alzheimer's Disease. San Diego: Academic Press; 2016. p. 197 – 237. Available from: https://doi.org/10.1016/B978-0-12-802851-3.00007-3.

[31] Macedo AC, Balouch S, Tabet N. Is sleep disruption a risk factor for Alzheimer's disease? J Alzheimers Dis. 2017;58(4):993 –1002. Available from: https://doi.org/10.3233/JAD-161287.

[32] Perkovic MN, Strac DS, Tudor L, Konjevod M, Erjavec GN, Pivac N. Catechol-o-methyltransferase, cognition and Alzheimer's disease. Curr Alzheimer Res. 2005;15(5):408–419. Available from: https://doi.org/10.2174/1567205015666171212094229.

[33] Van-Erum J, Van-Dam D, De-Deyn PP. Alzheimer's disease: neurotransmitters of the sleep-wake cycle. Neuroscience & Biobehavioral Reviews. 2019;105:72 – 80. Available from: https://doi.org/10.1016/j.neubiorev.2019.07.019.

[34] Bero AW, Tsai LH. Alzheimer's Disease and the Sleep-Wake Cycle. In: Lazarov O, Tesco G, editors. Genes, Environment and Alzheimer's Disease. San Diego: Academic Press; 2016. p. 295 – 317. Available from: http://www.sciencedirect.com/science/article/pii/B9780128028513000103.

[35] Venkataraman A, Kalk N, Sewell G, Ritchie CW, Lingford-Hughes A. Alcohol and Alzheimer's Disease-Does Alcohol Dependence Contribute to Beta-Amyloid Deposition, Neuroinflammation and Neurodegeneration in Alzheimer's Disease? Alcohol and Alcoholism. 2016 12;52(2):151–158. Available from: https://doi.org/10.1093/alcalc/agw092.

[36] Matloff WJ, Zhao L, Ning K, Conti DV, Toga AW. Interaction effect of alcohol consumption and Alzheimer disease polygenic risk score on the brain cortical thickness of cognitively normal subjects. Alcohol. 2020;85:1 – 12. Available from: https://doi.org/10.1016/j.alcohol.2019.11.002.

[37] Haziq K, Geok Chin T, Siti Fatimah I, Mohd Farooq S, Isa Naina M, Rashidi M Pakri M, et al. Alcohol use disorder, neurodegeneration, Alzheimer's and Parkinson's disease: Interplay between oxidative stress, neuroimmune response and excitotoxicity. Front Cell Neurosci. 2020;14. Available from: https://doi.org/10.3389/fncel.2020.00282.

[38] Reitz C, Rogaeva E, Beecham GW. Late-onset vs nonmendelian early-onset Alzheimer disease. Neurology Genetics. 2020;6(5). Available from: https://doi.org/10.1212/NXG.0000000000000512.

[39] Bekris L, Yu C, Bird T, Tsuang D. Genetics of Alzheimer disease. J Geriatr Psychiatry Neurol. 2010;23(4):213–227. Available from: https://doi.org/10.1177/0891988710383571.

[40] Wu L, Rosa-Neto P, Hsiung GYR, Sadovnick AD, Masellis M, Black SE, et al. Early-onset familial Alzheimer's disease (EOFAD). Can J Neurol Sci. 2012;39(4):436–445. Available from: https://doi.org/10.1017/S0317167100013949.

[41] Khan TK. Chapter 4 - Genetic biomarkers in Alzheimer's disease. In: Khan TK, editor. Biomarkers in Alzheimer's Disease. Academic Press; 2016. p. 103 – 135. Available from: https://doi.org/10.1016/B978-0-12-804832-0.00004-3.

[42] Havoutis GH. Analysis of diagnostic, preventive, and disease-modifying therapeutic measures of Alzheime's disease. Nova Southeastern University. 2017;Available from: https://nsuworks.nova.edu/cnso_stucap/334.

[43] George-Hyslop S. Genetic factors in the genesis of Alzheimer's disease. Ann N Y Acad Sci. 2000;924(1):1–7. Available from: https://doi.org/10.1111/j.1749-6632.2000.tb05552.x.

[44] Wilkins JM, Trushina E. Application of metabolomics in Alzheimer's disease. Frontiers in neurology. 2018;8(719). Available from: https://doi.org/10.3389/fneur.2017.00719.

[45] Yan MH, Wang X, Zhu X. Mitochondrial defects and oxidative stress in Alzheimer's disease and Parkinson disease. Free Radical Biol Med. 2013;62:90 – 101. Neurodegeneration. Available from: https://doi.org/10.1016/j.freeradbiomed.2012.11.014.

[46] Shea YF, Chu LW, Chan AOK, Ha J, Li Y, Song YQ. A systematic review of familial Alzheimer's disease: Differences in presentation of clinical features among three mutated genes and potential ethnic differences. J Formos Med Assoc. 2016;115(2):67–75. Available from: https://doi.org/10.1016/j.jfma.2015.08.004.

[47] Zhang L, Chen C, Mak M, Lu J, Wu Z, Chen Q, et al. Advance of sporadic Alzheimer's disease animal models. Med Res Rev. 2019 07;40. Available from: https://doi.org/10.1002/med.21624.

[48] Ballard C, Gauthier S, Corbett A, Brayne C, Aarsland D, Jones E. Alzheimer's disease. The Lancet. 2011;377(9770):1019 – 1031. Available from: https://doi.org/10.1016/S0140-6736(10)61349-9.

[49] Chakrabarti S, Khemka VK, Banerjee A, Chatterjee G, Ganguly A, Biswas A. Metabolic Risk Factors of Sporadic Alzheimer's Disease: Implications in the Pathology, Pathogenesis and Treatment. Aging and disease. 2015 Aug;6(4):286–299. Available from: https://doi.org/10.14336/AD.2014.002.

[50] Naj AC, Carney RM, Hahn SE, Slifer MA, Haines JL, Pericak-Vance MA. Genetics of Alzheimer Disease. In: Rimoin D, Pyeritz R, Korf B, editors. Emery and Rimoin's Principles and Practice of Medical Genetics. Oxford: Academic Press; 2013. p. 1–20. Available from: https://doi.org/10.1016/B978-0-12-383834-6.00116-6.

[51] Bateman RJ, West T, Yarasheski K, Patterson BW, Lucey B, Cirrito JR, et al. Stable Isotope Labeling Kinetics in CNS Translational Medicine: Introduction to SILK Technology. In: Nomikos GG, Feltner DE, editors. Translational Medicine in CNS Drug Development. vol. 29 of Handbook of Behavioral Neuroscience. Elsevier; 2019. p. 173 – 190. Available from: https://doi.org/10.1016/B978-0-12-803161-2.00011-4.

[52] McKeon-O'Malley C, Tanzi R. Etiology, genetics, and pathogenesis of Alzheimer's disease. In: Hof PR, Mobbs CV, editors. Functional Neurobiology of Aging. San Diego: Academic Press; 2001. p. 333 – 348. Available from: https://doi.org/10.1016/B978-012351830-9/50024-X.

[53] Ashford JW. Treatment of Alzheimer's Disease: Trazodone, Sleep, Serotonin, Norepinephrine, and Future Direction. J Alzheimers Dis. 2019;p. 923–930. Available from: https://doi.org/10.3233/JAD-181106.

[54] Tanzi RE. The genetics of Alzheimer disease. Cold Spring Harbor perspectives in medicine. 2012;2(10). Available from: https://doi.org/10.1101/cshperspect.a006296.

[55] Skaper S, Facci L, Zusso M, Giusti P. Synaptic plasticity dementia and Alzheimer's disease. CNS Neurol Disord Drug Targets. 2017;16(3):220–233. Available from: https://doi.org/10.2174/1871527316666170113120853.

[56] Thal DR, Fandrich M. Protein aggregation in Alzheimer's disease: Amyloid beta and tau and their potential roles in the pathogenesis of AD. Acta Neuropathol. 2015;129:163–165. Available from: https://doi.org/10.1007/s00401-015-1387-2.

[57] Farooqui AA. Chapter 1 - Classification and molecular aspects of neurotraumatic diseases: Similarities and differences with neurodegenerative and neuropsychiatric diseases. In: Farooqui AA, editor. Ischemic and Traumatic Brain and Spinal Cord Injuries. Academic Press; 2018. p. 1 – 40. Available from: https://doi.org/10.1016/B978-0-12-813596-9.00001-8.

[58] Farooqui AA. Biomarkers for Alzheimer's Disease. In: Farooqui AA, editor. Neurochemical Aspects of Alzheimer's Disease. Academic Press; 2017. p. 247 – 277. Available from: https://doi.org/10.1016/B978-0-12-809937-7.00007-0.

[59] Briggs R, Kennelly S, ONeill D. Drug treatments in Alzheimer disease. Clin Med. 2016;16(3):247–253. Available from: https://doi.org/10.7861/clinmedicine.16-3-247.

[60] Obulesu M. Introduction: Alzheimer's disease pathology and therapeutics. In: Obulesu M, editor. Alzheimer's Disease Theranostics. Academic Press; 2019. p. 1 – 6. Available from: https://doi.org/10.1016/B978-0-12-816412-9.00001-X.

[61] O'Brien RJ, Wong PC. Amyloid precursor protein processing and Alzheimer's disease. Annual review of neuroscience. 2011;34:185–204. Available from: https://doi.org/10.1146/annurev-neuro-061010-113613.

[62] Lozupone M, Solfrizzi V, D'Urso F, Gioia ID, Sardone R, Dibello V, et al. Anti-amyloid-protein agents for the treatment of Alzheimer's disease: an update on emerging drugs. Expert Opin Emerging Drugs. 2020;25(3):319–335. PMID: 32772738. Available from: https://doi.org/10.1080/14728214.2020.1808621.

[63] Giedraitis V, Sundelof J, Irizarry MC, Garevik N, Hyman BT, Wahlund LO, et al. The normal equilibrium between CSF and plasma amyloid β levels is disrupted in Alzheimer's disease. Neurosci Lett. 2007;427(3):127 – 131. Available from: https://doi.org/10.1016/j.neulet.2007.09.023.

[64] De Falco A, Cukierman DS, Hauser-Davis RA, Rey NA. Doença de Alzheimer: Hipóteses etiológicas e perspectivas de tratamento. Quim Nova. 2016 Jan;39:63–80. Available from: http://dx.doi.org/10.5935/0100-4042.20150152iso.

[65] Puzzo D, Privitera L, Leznik E, Fà M, Staniszewski A, Palmeri A, et al. Picomolar amyloid-B positively modulates synaptic plasticity and memory in hippocampus. J Neurosci. 2008;28(53):14537–14545. Available from: https://doi.org/10.1523/JNEUROSCI.2692-08.2008.

[66] Khan TK. Chapter 5 - Alzheimer's disease Cerebrospinal Fluid (CSF) biomarkers. In: Khan TK, editor. Biomarkers in Alzheimer's Disease. Academic Press; 2016. p. 139 – 180. Available from: https://doi.org/10.1016/B978-0-12-804832-0.00005-5.

[67] Fagan AM. What does it mean to be 'amyloid-positive'? Brain. 2015;138:514–516. Available from: https://doi.org/10.1093/brain/awu387.

[68] Aghajanov M, Chavushyan V, Matinyan S, Danielyan M, Yenkoyan K. Alzheimer's disease-like pathology-triggered oxidative stress, alterations in monoamines levels, and structural damage of locus coeruleus neurons are partially recovered by a mix of proteoglycans of embryonic genesis. Neurochem Int. 2019;131:104531. Available from: https://doi.org/10.1016/j.neuint.2019.104531.

[69] Albensi BC. Chapter 2 - Dysfunction of mitochondria: Implications for Alzheimer's disease. In: Fernyhough P, Calcutt NA, editors. Mitochondrial Dysfunction in Neurodegeneration and Peripheral Neuropathies. vol. 145 of International Review of Neurobiology. Academic Press; 2019. p. 13 – 27. Available from: https://doi.org/10.1016/bs.irn.2019.03.001.

[70] Salazar AM, Leisgang AM, Ortiz AA, Murtishaw AS, Kinney JW. Alterations of GABA B receptors in the APP/PS1 mouse model of Alzheimer's disease. Neurobiol Aging. 2021;97:129 – 143. Available from: https://doi.org/10.1016/j.neurobiolaging.2020.10.013.

[71] Strac DS, Muck-Seler D, Pivac N. Neurotransmitter measures in the cerebrospinal fluid of patients with Alzheimer's Disease: A review. Psychiatria Danubina. 2015;27(1):14–24. Available from: https://hrcak.srce.hr/155883.

[72] Maitre M, Klein C, Patte-Mensah C, Mensah-Nyagan AG. Tryptophan metabolites modify brain A beta peptide degradation: A role in Alzheimer's disease? Progress in Neurobiology. 2020;190:101800. Available from: https://doi.org/10.1016/j.pneurobio.2020.101800.

[73] Guo T, Noble W, Hanger DP. Roles of tau protein in health and disease. Acta Neuropathol. 2017;133:665–704. Available from: https://doi.org/10.1007/s00401-017-1707-9.

[74] Simić G, Babić Leko M, Wray S, Harrington C, Delalle I, Jovanov-Milosević N, et al. Tau Protein Hyperphosphorylation and Aggregation in Alzheimer's Disease and Other Tauopathies, and Possible Neuroprotective Strategies. Biomolecules. 2016;6(1). Available from: https://doi.org/10.3390/biom6010006.

[75] Takeda S. Tau propagation as a diagnostic and therapeutic target for dementia: potentials and unanswered questions. Front Neurosci. 2019;13:1274. Available from: https://doi.org/10.3389/fnins.2019.01274.

[76] Mietelska-Porowska A, Wasik U, Goras M, Filipek A, Niewiadomska G. Tau protein modifications and interactions: their role in function and dysfunction. International journal of molecular sciences. 2014;15(3):4671–4713. Available from: https://doi.org/10.3390/ijms15034671.

[77] Colović MB, Krstić DZ, Lazarević-Pasti TD, AM AMB, MVasić V. Acetylcholinesterase inhibitors: pharmacology and toxicology. Curr Neuropharmaco. 2013;11(3):313–335. Available from: https://doi.org/10.2174/1570159X11311030006.

[78] Zaagsma J, Meurs H. Acetylcholine. In: Laurent GJ, Shapiro SD, editors. Encyclopedia of respiratory medicine. Oxford: Academic Press; 2006. p. 1 – 5. Available from: https://doi.org/10.1016/B0-12-370879-6/00002-8.

[79] Terry AV, Buccafusco JJ. The cholinergic hypothesis of age and Alzheimer's disease-related cognitive deficits: Recent challenges and their Implications for novel drug development. Journal of Pharmacology and Experimental Therapeutics. 2003;306(3):821–827. Available from: https://jpet.aspetjournals.org/content/306/3/821.

[80] Francis PT. The interplay of neurotransmitters in Alzheimer's disease. CNS Spectr. 2005;11:6–9. Available from: https://doi.org/10.1017/s1092852900014164.

[81] Manyevitch R, Protas M, Scarpiello S, Deliso M, Bass B, Nanajian A, et al. Evaluation of Metabolic and Synaptic Dysfunction Hypotheses of Alzheimer's Disease (AD): A Meta-Analysis of CSF Markers. Curr Alzheimer Res. 2018;15(2):164–181.

[82] Ferreira-Vieira T, Guimaraes IM, Silva F, Ribeiro F. Alzheimer's disease: Targeting the cholinergic system. Curr Neuropharmacol. 2016;14(1):101–115. Available from: https://doi.org/10.2174/1570159x13666150716165726 9.

[83] Snowden AA Stuart G anda Ebshiana, Hye A, Pletnikova O, O'Brien R, Yang A, Troncoso J, et al. Neurotransmitter imbalance in the brain and Alzheimer's disease pathology. J Alzheimers Dis. 2019;72(1):35–43. Available from: https://doi.org/10.3233/JAD-190577.

[84] Uutela P, Reinila R, Piepponen P, Ketola RA, Kostiainen R. Analysis of acetylcholine and choline in microdialysis samples by liquid chromatography/tandem mass spectrometry. Rapid Commun Mass Spectrom. 2005;19(20):2950–2956. Available from: https://doi.org/10.1002/rcm.2160.

[85] Wei M, Liu Y, Pi ZF, Yue K, Li S, Hu M, et al. Correction: Investigation of plasma metabolomics and neurotransmitter dysfunction in the process of Alzheimer's disease rat induced by amyloid beta 25-35. RSC Adv. 2021 02;11:7416–7416. Available from: https://doi.org/10.1039/D1RA90081A.

[86] Zhou Y, Danbolt NC. Glutamate as a neurotransmitter in the healthy brain. J Neural Transm. 2014;121(8):799–817. Available from: https://doi.org/10.1007/s00702-014-1180-8.

[87] Francis PT. Glutamatergic systems in Alzheimer's disease. Int J Geriatr Psychiatry. 2003;18(S1):S15–S21. Available from: https://doi.org/10.1002/gps.934.

[88] Pomara N, Singh R, Deptula D, Chou JC, Schwartz MB, LeWitt PA. Glutamate and other CSF amino acids in Alzheimer's disease. The American Journal of Psychiatry. 1992;149(2):251–254. Available from: https://doi.org/10.1176/ajp.149.2.251.

[89] Schon KR, Ratnaike T, van den Ameele J, Horvath R, Chinnery PF. Mitochondrial diseases: A diagnostic revolution. Trends Genet. 2020;36(9):702 – 717. Available from: https://doi.org/10.1016/j.tig.2020.06.009.

[90] Kann O, Kovács R. Mitochondria and neuronal activity. American Journal of Physiology-Cell Physiology. 2007;292(2):C641–C657. PMID: 17092996. Available from: https://doi.org/10.1152/ajpcell.00222.2006.

[91] Weidling I, Swerdlow RH. Mitochondrial dysfunction and stress responses in Alzheimer's disease. Biology. 2019;8(2). Available from: https://doi.org/10.3390/biology8020039.

[92] Swerdlow RH, Khan SM. The Alzheimer's disease mitochondrial cascade hypothesis: An update. Experimental Neurology. 2009;218(2):308 – 315. Mitochondria and Neurodegeneration. Available from: https://doi.org/10.1016/j.expneurol.2009.01.011.

[93] Lin MT, Beal MF. Mitochondrial dysfunction and oxidative stress in neurodegenerative diseases. Nature. 2006;443(7113):787–795. Available from: https://doi.org/10.1038/nature05292.

[94] Swerdlow RH, Khan SM. A mitochondrial cascade hypothesis for sporadic Alzheimer's disease. Med Hypotheses. 2004;63(1):8 –20. Available from: https://doi.org/10.1016/j.mehy.2003.12.045.

[95] Almannai M, El-Hattab AW, Ali M, Soler-Alfonso C, Scaglia F. Clinical trials in mitochondrial disorders, an update. Mol Genet Metab. 2020;Available from: https://doi.org/10.1016/j.ymgme.2020.10.002.

[96] Wajner M, Vargas CR, Amaral AU. Disruption of mitochondrial functions and oxidative stress contribute to neurologic dysfunction in organic acidurias. Arch Biochem Biophys. 2020;p. 108646. Available from: https://doi.org/10.1016/j.abb.2020.108646.

[97] Swerdlow RH. Pathogenesis of Alzheimer's disease. Clinical interventions in aging. 2007;2(3):347–359. Available from: https://europepmc.org/articles/PMC2685260.

[98] Zverová M. Clinical aspects of Alzheimer's disease. Clin Biochem. 2019;72:3 – 6. Available from: https://doi.org/10.1016/j.clinbiochem.2019.04.015.

[99] Ly TN, Park S. High performance detection of Alzheimer's disease biomarkers based on localized surface plasmon resonance. J Ind Eng Che. 2020;91:182–190. Available from: https://doi.org/10.1016/j.jiec.2020.07.051.

[100] Blennow K, Zetterberg H. The past and the future of Alzheimer's disease fluid biomarkers. J Alzheimers Dis. 2018 03;62:1125–1140. Available from: https://doi.org/10.3233/JAD-170773.

[101] Shen L, Xia S, Zhang H, Yao F, Liu X, Zhao Y, et al. Precision medicine: Role of biomarkers in early prediction and diagnosis of Alzheimer's disease. In: Nalbantoglu S, Amri H, editors. Molecular Medicine. Rijeka: IntechOpen; 2019. Available from: https://doi.org/10.5772/intechopen.82035.

[102] Matsuda H, Imabayashi E. Molecular neuroimaging in Alzheimer's disease. Neuroimaging Clinics of North America. 2012;22(1):57–65. Imaging in Alzheimer's Disease and Other Dementias. Available from: https://doi.org/10.1016/j.nic.2011.11.005.

[103] Suppiah S, Didier MA, Vinjamuri S. The Who, When, Why, and How of PET amyloid imaging in management of Alzheimer's disease-review of literature and interesting images. Diagnostics (Basel). 2019 Jun;9(2):65. Available from: https://doi.org/10.3390/diagnostics9020065.

[104] Pini L, Pievani M, Bocchetta M, Altomare D, Bosco P, Cavedo E, et al. Brain atrophy in Alzheimer's disease and aging. Ageing Res Rev. 2016;30:25 – 48. Brain Imaging and Aging. Available from: https://doi.org/10.1016/j.arr.2016.01.002.

[105] de Wilde A, van der Flier WM, Pelkmans W, Bouwman F, Verwer J, Groot C, et al. Association of amyloid positron emission tomography with changes in diagnosis and patient treatment in an unselected memory clinic cohort: The ABIDE project. JAMA Neurology. 2018 09;75(9):1062–1070. Available from: https://doi.org/10.1001/jamaneurol.2018.1346.

[106] Ishii K. Amyloid positron emission tomography in the therapeutic strategies for Alzheimer's disease. Brain and Nerve. 2017 07;69:809–818. Available from: https://doi.org/10.11477/mf.1416200824.

[107] Kolanko MA, Win Z, lavia Loreto, Patel N, Carswell C, andRichard J Perry AG, et al. Amyloid PET imaging in clinical practice. Practical Neurology. 2020;20(6):451–462. Available from: https://doi.org/10.1136/practneurol-2019-002468.

[108] Johnson KA, Minoshima S, Bohnen NI, Donohoe KJ, Foster NL, Herscovitch P, et al. Appropriate use criteria for amyloid PET: A report of the amyloid imaging task force, the society

of nuclear medicine and molecular imaging, and the Alzheimer's association. Alzheimer's & Dementia. 2013;9(1):E1–E16. Available from: https://alz-journals.onlinelibrary.wiley.com/doi/abs/10.1016/j.jalz.2013.01.002.

[109] Jr JCR, R BJ, Vladimir K. Cerebral amyloid PET imaging in Alzheimer's disease. Acta Neuropathol. 2013;126(5). Available from: https://doi.org/10.1007/s00401-013-1185-7.

[110] Mosconi L, McHugh PF. FDG- and amyloid-PET in Alzheimer's disease: is the whole greater than the sum of the parts? Q J Nucl Med Mol Imaging. 2011;55(3):250–264. Available from: https://www.ncbi.nlm.nih.gov/pmc/articles/PMC3290913/.

[111] Landau SM, Horng A, Fero A, Jagust WJ. Alzheimer's disease neuroimaging initiative. Amyloid negativity in patients with clinically diagnosed Alzheimer disease and MCI. Neurology. 2016;86(15):1377–1385. Available from: https://doi.org/10.1212/WNL.0000000000002576.

[112] Marcus C, Mena E, Subramaniam R. Brain PET in the Diagnosis of Alzheimer's Disease. Clinical nuclear medicine. 2014 10;39:e413–e426.

[113] Pitt J. Chapter 49 - Biomarkers of Alzheimer's disease. In: Gupta RC, editor. Biomarkers in Toxicology. second edition ed. Academic Press; 2019. p. 885–894. Available from: https://doi.org/10.1016/B978-0-12-814655-2.00049-9.

[114] Shi J, Sabbagh MN, Vellas B. Alzheimer's disease beyond amyloid: strategies for future therapeutic interventions. BMJ. 2020;371. Available from: https://doi.org/10.1136/bmj.m3684.

[115] Stutzmann G. The pathogenesis of Alzheimer's disease is it a lifelong "calciumopathy"? Neuroscientist. 2007;13(5):546–559. Available from: https://doi.org/10.1177/1073858407299730.

[116] Cavalli E, Battaglia G, Basile MS, Bruno V, Petralia MC, Lombardo SD, et al. Exploratory analysis of iPSCS-derived neuronal cells as predictors of diagnosis and treatment of Alzheimer disease. Brain Sci. 2020;10(3). Available from: https://doi.org/10.3390/brainsci10030166.

[117] Hampel H, Mesulam MM, Cuello AC, Farlow MR, Giacobini E, Grossberg GT, et al. The cholinergic system in the pathophysiology and treatment of Alzheimer's disease. Brain. 2018 05;141(7):1917–1933. Available from: https://doi.org/10.1093/brain/awy132.

[118] Johnson JW, Kotermanski SE. Mechanism of action of memantine. Curr Opin Pharmacol. 2006;6(1):61 – 67. Neurosciences. Available from: https://doi.org/10.1016/j.coph.2005.09.007.

[119] Olajide O, Gbadamosi I, Yawson E, Arogundade T, Asogwa N, Adeniyi P. Hippocampal degeneration involves glutamate excitoxicity during the pathogenesis of Alzheimer's disease. Biol Psychiatry. 2020;87(9, Supplement):S294 – S295. 75th Annual Scientific Convention and Meeting. Available from: https://doi.org/10.1016/j.biopsych.2020.02.759.

[120] Cooper JR. Neurotransmitters. In: Smelser NJ, Baltes PB, editors. International encyclopedia of the social & behavioral sciences. Oxford: Pergamon; 2001. p. 10612 – 10619. Available from: https://doi.org/10.1016/B0-08-043076-7/03447-1.

[121] Matys J, Gieroba B, Jóźwiak K. Recent developments of bioanalytical methods in determination of neurotransmitters in vivo. J Pharm Biomed Anal. 2020;180:113079. Available from: https://doi.org/10.1016/j.jpba.2019.113079.

[122] Deutch AY. Chapter 6 - Neurotransmitters. In: Squire LR, Berg D, Bloom FE, du Lac S, Ghosh A, Spitzer NC, editors. Fundamental neuroscience. fourth edition ed. San Diego: Academic Press; 2013. p. 117–138. Available from: https://doi.org/10.1016/B978-0-12-385870-2.00006-8.

[123] Purves D, Augustine G, Fitzpatrick D, Fitzpatrick D, Katz LC, LaMantia AS, et al. Neuroscience. Second edition ed. Sinauer Associates; 2001. Available from: https://www.ncbi.nlm.nih.gov/books/NBK11035/.

[124] Blanco ME, Mayo OB, Bandiera T, Tonelli DDP, Armirotti A. LC-MS/MS analysis of twelve neurotransmitters and amino acids in mouse cerebrospinal fluid. J Neurosci Methods. 2020;341:108760. Available from: https://doi.org/10.1016/j.jneumeth.2020.108760.

[125] Klein MO, Battagello DS, Cardoso AR, Hauser DN, Bittencourt JC, Correa RG. Dopamine: Functions, signaling, and association with neurological diseases. Cell Mol Neurobiol. 2019;39:31–59. Available from: https://doi.org/10.1007/s10571-018-0632-3.

[126] Balakrishnan A, Padigaru M, Morde A. Chapter 19 - Cognitive health and nutrition: a millennial correlation. In: Ghosh D, editor. Nutraceuticals in Brain Health and Beyond. Academic Press; 2021. p. 281–292. Available from: https://doi.org/10.1016/B978-0-12-820593-8.00019-7.

[127] Schwartz JH. Neurotransmitters. In: S RV, editor. Encyclopedia of the human brain. New York: Academic Press; 2002. p. 601 – 611. Available from: https://doi.org/10.1016/B0-12-227210-2/00251-X.

[128] Ceccarini J, Liu H, Van Laere K, Morris ED, Sander CY. Methods for quantifying neurotransmitter dynamics in the living brain with PET imaging. Front Physiol. 2020;11:792. Available from: https://doi.org/10.3389/fphys.2020.00792.

[129] Audhya T, Adams JB, Johansen L. Correlation of serotonin levels in CSF, platelets, plasma, and urine. Biochimica et Biophysica Acta (BBA) - General Subjects. 2012;1820(10):1496 – 1501. Available from: https://doi.org/10.1016/j.bbagen.2012.05.012.

[130] Nordberg A, Rinne J, Kadir A, Langstrom B. The use of PET in Alzheimer disease. Nat Rev Neurol. 2010;6:78–87. Available from: https://doi.org/10.1038/nrneurol.2009.217.

[131] Roy U, Stute L, Hofling C, Hartlage-Rubsamen M, Matysik J, Roner S, et al. Sex - and age - specific modulation of brain GABA levels in a mouse model of Alzheimer's disease. Neurobiol Aging. 2018;62:168 – 179. Available from: https://doi.org/10.1016/j.neurobiolaging.2017.10.015.

[132] Kumar K, Kumar A, Keegan R, Deshmukh R. Recent advances in the neurobiology and neuropharmacology of Alzheimer's disease. Biomed Pharmacother. 2017 12;98. Available from: https://doi.org/10.1016/j.biopha.2017.12.053.

[133] Pan X, Kaminga AC, Wen SW, Wu X, Acheampong K, Liu A. Dopamine and dopamine receptors in Alzheimer's disease: A systematic review and network meta-analysis. Front Aging Neurosci. 2019;11:175. Available from: https://doi.org/10.3389/fnagi.2019.00175.

[134] Lombardero L, Llorente-Ovejero A, Manuel I, Rodríguez-Puertas R. Chapter 28 - Neurotransmitter receptors in Alzheimer's disease: from glutamatergic to cholinergic receptors. In: Martin CR, Preedy VR, editors. Genetics, Neurology, Behavior, and Diet in Dementia. Academic Press; 2020. p. 441 – 456. Available from: https://doi.org/10.1016/B978-0-12-815868-5.00028-1.

[135] Pruss A. Neurotransmission. In: Olson A, editor. Drugs and the Neuroscience of Behavior: An Introduction to Psychopharmacology. second edition ed. SAGE Publications, Inc; 2018. p. 59–100.

[136] Juárez OH, Calderón GD, Hernández GE, Barragán MG. The role of dopamine and its dysfunction as a consequence of oxidative stress. Oxid Med Cell Longev. 2016;2016(9730467). Available from: https://doi.org/10.1155/2016/9730467.

[137] D'Amelio M, Nistico R. Unlocking the secrets of dopamine in Alzheimer's Disease. Pharmacol Res. 2018;128(399). Available from: https://doi.org/10.1016/j.phrs.2017.06.018.

[138] Días ASA, Pinto JCA, Magalhãess M, Mendes VM, Manadas B. Analytical methods to monitor dopamine metabolism in plasma: Moving forward with improved diagnosis and treatment of neurological disorders. J Pharm Biomed Anal. 2020;187:113323. Available from: https://doi.org/10.1016/j.jpba.2020.113323.

[139] Bahena-Trujillo R, Flores G, no JAAM. Dopamina: síntesis, liberación y receptores en el sistema nervioso central. Rev Biomed. 2000;201211:39–60. Available from: http://www.uady.mx/~biomedic/rb001116.pdf.

[140] Mackie P, Lebowitz J, Saadatpour L, Nickoloff E, Gaskill P, Khoshbouei H. The dopamine transporter: An unrecognized nexus for dysfunctional peripheral immunity and signaling in Parkinson's Disease. Brain, Behavior, and Immunity. 2018;70:21 – 35. Available from: https://doi.org/10.1016/j.bbi.2018.03.020.

[141] Cumming P. The life history of dopamine. In: imaging Dopamine. first edition ed. Cambridge: Cambridge University Press; 2009. p. 5–18. Available from: https://doi.org/10.1017/CBO9780511575853.003.

[142] Ortez C, Duarte ST, Ormazábal A, Serrano M, Pérez A, Pons R, et al. Cerebrospinal fluid synaptic proteins as useful biomarkers in tyrosine hydroxylase deficiency. Molecular genetics and metabolism. 2015;114(1):34–40. Available from: https://doi.org/10.1016/j.ymgme.2014.10.014.

[143] Taylor LA, Creese I. Dopamine. In: Ramachandran VS, editor. Encyclopedia of the Human Brain. New York: Academic Press; 2002. p. 115 – 122. Available from: https://doi.org/10.1016/B0-12-227210-2/00122-9.

[144] Gnegy ME. Chapter 14 - Catecholamines. In: Brady ST, Siegel GJ, Albers RW, Price DL, editors. Basic Neurochemistry. eighth edition ed. New York: Academic Press; 2012. p. 283 – 299. Available from: https://doi.org/10.1016/B978-0-12-374947-5.00014-6.

[145] Aggarwal S, Mortensen OV. Overview of monoamine transporters. Current Protocols in Pharmacology. 2017;79(1):12.16.1–12.16.17. Available from: https://doi.org/10.1002/cpph.32.

[146] Carvey PM. Dopamine. In: Kompoliti K, Metman LV, editors. Encyclopedia of Movement Disorders. Oxford: Academic Press; 2010. p. 316 – 321. Available from: https://doi.org/10.1016/B978-0-12-374105-9.00319-1.

[147] Bortolato M, Chen K, Shih JC. Monoamine oxidase inactivation: From pathophysiology to therapeutics. Adv Drug Deliv Rev. 2008;60(13):1527 – 1533. Mitochondrial Medicine and Mitochondrion-Based Therapeutics. Available from: https://doi.org/10.1016/j.addr.2008.06.002.

[148] Muñoz P, Huenchuguala S, Paris I, Segura-Aguilar J. Dopamine Oxidation and Autophagy. Parkinson's disease. 2012 08;2012:920953.

[149] Cumming P. Dopamine synthesis and metabolism rates. In: Imaging dopamine. first edition ed. Cambridge: Cambridge University Press; 2009. p. 85–98. Available from: https://doi.org/10.1017/CBO9780511575853.009.

[150] Perreault H, Lattová E. Mass Spectrometry. In: Moo-Young M, editor. Comprehensive Biotechnology. second edition ed. Burlington: Academic Press; 2011. p. 669 – 677. Available from: https://doi.org/10.1016/B978-0-08-088504-9.00077-5.

[151] Tóth BE, Vecsernyós M, Zelles T, Kádaár K, Nagy GM. Role of peripheral and brain-derived dopamine (DA) in immune regulation. Advances in Neuroimmune Biology. 2012;33:111–155. Available from: https://doi.org/10.3233/NIB-2012-012044.

[152] Peitzsch M, Mangelis A, Eisenhofer G, Huebner A. Age-specific pediatric reference intervals for plasma free normetanephrine, metanephrine, 3-methoxytyramine and 3-O-methyldopa: Particular importance for early infancy. Clin Chim Acta. 2019;494:100 – 105. Available from: https://doi.org/10.1016/j.cca.2019.03.1620.

[153] Antkiewicz-Michaluk L, Ossowska K, Romańska I, Michaluk J, Vetulani J. 3-Methoxytyramine, an extraneuronal dopamine metabolite plays a physiological role in the brain as an inhibitory regulator of catecholaminergic activity. Eur J Pharmacol. 2008;599(1):32 – 35. Available from: https://doi.org/10.1016/j.ejphar.2008.09.033.

[154] Eisenhofer G, Goldstein DS. Peripheral Dopamine Systems. In: Robertson D, Biaggioni I, Burnstock G, Low PA, editors. Primer on the Autonomic Nervous System (Second Edition). second edition ed. San Diego: Academic Press; 2004. p. 176 –177. Available from: https://doi.org/10.1016/B978-012589762-4/50046-3.

[155] Fuertes I, Barata C. Characterization of neurotransmitters and related metabolites in Daphnia magna juveniles deficient in serotonin and exposed to neuroactive chemicals that affect its behavior: A targeted LC-MS/MS method. Chemosphere. 2021;263:127814. Available from: https://doi.org/10.1016/j.chemosphere.2020.127814.

[156] Suominen T, Uutela P, andJonas Bergquist RAK, Hillered L, Finel M, Zhang H, et al. Determination of serotonin and dopamine metabolites in human brain microdialysis and

cerebrospinal fluid samples by UPLC-MS/MS. Discovery of intact glucuronide and sulfate conjugates. PLOS ONE. 2013;8(6). Available from: https://doi.org/10.1371/journal.pone.0068007.

[157] Batllori M, Molero LM, Ormazabal A, Casado M, Sierra C, García CA, et al. Analysis of human cerebrospinal fluid monoamines and their cofactors by HPLC. Nat Protoc. 2017 Nov;12(11):2359–2375. Available from: https://doi.org/10.1038/nprot.2017.103.

[158] Zhang C, Xia Y, Jiang W, Wang C, Han B, Hao J. Determination of non-neuronal acetylcholine in human peripheral blood mononuclear cells by use of hydrophilic interaction ultra-performance liquid chromatography-tandem mass spectrometry. J Chromatogr B. 2016;1022:265 – 273. Available from: https://doi.org/10.1016/j.jchromb.2016.04.024.

[159] Amenta F, Tayebati S. Pathways of acetylcholine synthesis, transport and release as targets for treatment of adult-onset cognitive dysfunction. Curr Med Chem. 2008;15(5):488–498. Available from: https://doi.org/10.2174/092986708783503203.

[160] Zhu Z, Zhang L, Cui Y, Li M, Ren R, Li G, et al. Functional compensation and mechanism of choline acetyltransferase in the treatment of cognitive deficits in aged dementia mice. Neuroscience. 2020;442:41 – 53. Available from: https://doi.org/10.1016/j.neuroscience.2020.05.016.

[161] Metabolism of acetylcholine: synthesis and turnover. In: Karczmar AG, editor. Exploring the Vertebrate Central Cholinergic Nervous System. Boston, MA: Springer US; 2007. p. 81–149. Available from: https://doi.org/10.1007/978-0-387-46526-5_3.

[162] Kose LP, Bingol Z, Kaya R, Goren AC, Akincioglu H, Durmaz L, et al. Anticholinergic and antioxidant activities of avocado (Folium perseae) leaves - phytochemical content by LC-MS/MS analysis. Int J Food Prop. 2020;23(1):878–893. Available from: https://doi.org/10.1080/10942912.2020.1761829.

[163] Bhagavan NV, Ha CE. Chapter 16 - Lipids I: Fatty Acids and Eicosanoids. In: Bhagavan NV, Ha CE, editors. Essentials of Medical Biochemistry. second edition ed. San Diego: Academic Press; 2015. p. 269 – 297. Available from: https://doi.org/10.1016/B978-0-12-416687-5.00016-6.

[164] Schousboe A, Scafidi S, Bak L, Waagepetersen H, McKenna M. Glutamate metabolism in the brain focusing on astrocytes. Adv Neurobiol. 2014;11:13–30. Available from: https://doi.org/10.1007/978-3-319-08894-5_2.

[165] Eckstein JA, Ammerman GM, Reveles JM, Ackermann BL. Analysis of glutamine, glutamate, pyroglutamate, and GABA in cerebrospinal fluid using ion pairing HPLC with positive electrospray LC/MS/MS. J Neurosci Methods. 2008;171(2):190 – 196. Available from: https://doi.org/10.1016/j.jneumeth.2008.02.019.

[166] Tapiero H, Mathé G, Couvreur P, Tew KD. II. Glutamine and glutamate. Biomed Pharmacother. 2002;56(9):446 – 457. Available from: https://doi.org/10.1016/S0753-3322(02)00285-8.

[167] Niu P, Dong X, Wang Y, Liu L. Enzymatic production of alpha-ketoglutaric acid from l-glutamic acid via l-glutamate oxidase. J Biotechnol. 2014;179:56 – 62. Available from: https://doi.org/10.1016/j.jbiotec.2014.03.021.

[168] Hinton T, Johnston GAR. GABA-enriched teas as neuro-nutraceuticals. Neurochem Int. 2020;141:104895. Available from: https://doi.org/10.1016/j.neuint.2020.104895.

[169] Spillane JA, White P, Goodhardt MJ, Flack RHA, Bowen DM, Davison AN. Selective vulnerability of neurones in organic dementia. Nature. 1977;266:558–559.

[170] Lowe SL, T FP, W PA, Palmer AM, Davison AN, Bowen DM. Gamma-aminobutyric acid concentration in brain tissue at two stages of AlzheimerÂŽs disease. Brain. 1988 08;111(4):785–799. Available from: https://doi.org/10.1093/brain/111.4.785.

[171] Ramos B, Baglietto-Vargas D, del Rio JC, Moreno-Gonzalez I, Santa-Maria C, Jimenez S, et al. Early neuropathology of somatostatin/NPY GABAergic cells in the hippocampus of a PS1xAPP transgenic model of Alzheimer's disease. Neurobiol Aging. 2006;27(11):1658–1672. Available from: https://www.sciencedirect.com/science/article/pii/S0197458005002903.

[172] Righetti PG, Boschetti E. Chapter 6 - Biomedical Involvements of Low-Abundance Proteins. In: Righetti PG, Boschetti E, editors. Low-Abundance Proteome Discovery. Boston: Elsevier; 2013. p. 197 – 231. Available from: https://doi.org/10.1016/B978-0-12-401734-4.00006-3.

[173] Galasko D, Xiao M, Xu D, Smirnov D, Salmon D, Dewit N, et al. Synaptic biomarkers in CSF aid in diagnosis, correlate with cognition and predict progression in MCI and Alzheimer's disease. Alzheimer's & Dementia: Translational Research & Clinical Interventions. 2019 Dec;5:871–882. Available from: https://doi.org/10.1016/j.trci.2019.11.002.

[174] Calvin C, Boer C, Raymont V, Gallacher J, Koychev I. Prediction of Alzheimer's disease biomarker status defined by the 'ATN framework' among cognitively healthy individuals: results from the EPAD longitudinal cohort study. Alzheimer's Research & Therapy. 2020 11;12. Available from: https://doi.org/10.1186/s13195-020-00711-5.

[175] Mendes VM, Coelho M, Manadas B. Untargeted Metabolomics Relative Quantification by SWATH Mass Spectrometry Applied to Cerebrospinal Fluid. In: Santamaria E, Fernandez-Irigoyen J, editors. Cerebrospinal Fluid (CSF) Proteomics. Methods in Molecular Biology. vol. 2044. first edition ed. Springer; 2019. p. 321–336. Available from: https://doi.org/10.1007/978-1-4939-9706-0_20.

[176] Selleck M, Senthil M, Wall N. Making Meaningful Clinical Use of Biomarkers. Biomark Insights. 2017;12:1–7. Available from: https://doi.org/10.1177/1177271917715236.

[177] Cummings J. In: Guest PC, editor. The Role of Biomarkers in Alzheimer's Disease Drug Development. Cham: Springer International Publishing; 2019. p. 29–61. Available from: https://doi.org/10.1007/978-3-030-05542-4_2.

[178] Blennow K, Zetterberg H. Biomarkers for Alzheimer's disease: current status and prospects for the future. J Intern Med. 2018;284(6):643–663. Available from: https://doi.org/10.1111/joim.12816.

[179] D'Abramo C, D'Adamio L, Giliberto L. Significance of Blood and Cerebrospinal Fluid Biomarkers for Alzheimer's Disease: Sensitivity, Specificity and Potential for Clinical Use. Journal of Personalized Medicine. 2020;10(3). Available from: https://doi.org/10.3390/jpm10030116.

[180] Gabelli C. Blood and cerebrospinal fluid biomarkers for Alzheimer's disease. Journal of Laboratory and Precision Medicine. 2020;5(15). Available from: http://dx.doi.org/10.21037/jlpm.2019.12.04.

[181] Gauthier S, Ng KP, Pascoal TA, Hua Z, Pedro RN. Targeting Alzheimer's Disease at the Right Time and the Right Place: Validation of a Personalized Approach to Diagnosis and Treatment. J Alzheimers Dis. 2018;64(1):23–31.

[182] Altuna-Azkargorta M, Mendioroz-Iriarte M. Blood biomarkers in Alzheimer's disease. Neurología. 2020;Available from: https://doi.org/10.1016/j.nrleng.2018.03.006.

[183] Abou-Hamden A, Drake JM. Chapter 30 - Hydrocephalus and Arachnoid Cysts. In: Swaiman KF, Ashwal S, Ferriero DM, Schor NF, Finkel RS, Gropman AL, et al., editors. Swaiman's Pediatric Neurology. sixth edition ed. Elsevier; 2017. p. 226 – 232. Available from: https://doi.org/10.1016/B978-0-323-37101-8.00030-8.

[184] Jones AW. Alcohol: acute and chronic use and postmortem findings. In: Payne-James J, Byard RW, editors. Encyclopedia of Forensic and Legal Medicine. second edition ed. Oxford: Elsevier; 2016. p. 84 – 107. Available from: https://doi.org/10.1016/B978-0-12-800034-2.00013-6.

[185] Han CY, Backous DD. Basic Principles of Cerebrospinal Fluid Metabolism and Intracranial Pressure Homeostasis. Otolaryngol Clin North Am. 2005;Available from: https://doi.org/10.1016/j.otc.2005.01.005.

[186] Brodbelt MA, Stoodley M. CSF pathways: a review. Br J Neurosurg. 2007;21(5):510–520. Available from: https://doi.org/10.1080/02688690701447420.

[187] Zetterberg H, Blennow K. Chapter 30 - Chronic traumatic encephalopathy: fluid biomarkers. In: Hainline B, Stern RA, editors. Sports Neurology. vol. 158 of Handbook of Clinical Neurology. Elsevier; 2018. p. 323 – 333. Available from: https://doi.org/10.1016/B978-0-444-63954-7.00030-6.

[188] Tumani H, Huss A, Bachhuber F. Chapter 2 - The cerebrospinal fluid and barriers - anatomic and physiologic considerations. In: Deisenhammer F, Teunissen CE, Tumani H, editors. Cerebrospinal Fluid in Neurologic Disorders. vol. 146 of Handbook of Clinical Neurology. Elsevier; 2018. p. 21–32. Available from: https://doi.org/10.1016/B978-0-12-804279-3.00002-2.

[189] Carrasco MM. Biomarcadores en la enfermedad de Alzheimer: definición, significación diagnóstica y utilidad clínica. In: S VE, editor. Psicogeriatría. vol. 1; 2009. p. 101–114.

[190] jing Li N, tao Liu W, Li W, qi Li S, hui Chen X, shun Bi K, et al. Plasma metabolic profiling of Alzheimer's disease by liquid chromatography/mass spectrometry. Clin Biochem. 2010;43(12):992 – 997. Available from: https://doi.org/10.1016/j.clinbiochem.2010.04.072.

[191] Olsson B, Lautner R, Andreasson U, Ohrfelt A, Portelius E, Bjerke M, et al. CSF and blood biomarkers for the diagnosis of Alzheimer's disease: a systematic review and meta-analysis. The Lancet Neurology. 2016;15(7):673 – 684. Available from: https://doi.org/10.1016/S1474-4422(16)00070-3.

[192] Hansson O, Seibyl J, Stomrud E, Zetterberg H, Trojanowski JQ, Bittner T, et al. CSF biomarkers of Alzheimer's disease concord with amyloid-B PET and predict clinical progression: A study of fully automated immunoassays in BioFINDER and ADNI cohorts. Alzheimer's & Dementia. 2018;14(11):1470–1481. Available from: https://www.sciencedirect.com/science/article/pii/S1552526018300293.

[193] Ossenkoppele R, Jansen WJ, Rabinovici GD, Knol DL, van der Flier WM, van Berckel BNM, et al. Prevalence of Amyloid PET Positivity in Dementia Syndromes A Meta-analysis. JAMA. 2015;313(19):1939–1949.

[194] Roberts RO, Aakre JA, Kremers WK, Vassilaki M, Knopman DS, Mielke MM, et al. Prevalence and Outcomes of Amyloid Positivity Among Persons Without Dementia in a Longitudinal, Population-Based Setting. JAMA Neurology. 2018 08;75(8):970–979. Available from: https://doi.org/10.1001/jamaneurol.2018.0629.

[195] Gaetani L, Blennow K, Calabresi P, Filippo M, Parnetti L, Zetterberg H. Neurofilament light chain as a biomarker in neurological disorders. Journal of Neurology, Neurosurgery & Psychiatry. 2019 04;90:jnnp–2018. Available from: https://doi.org/10.1136/jnnp-2018-320106.

[196] Jin M, Cao L, Dai Yp. Role of Neurofilament Light Chain as a Potential Biomarker for Alzheimer's Disease: A Correlative Meta-Analysis. Front Aging Neurosci. 2019;11:254. Available from: https://www.frontiersin.org/article/10.3389/fnagi.2019.00254.

[197] Park SA, Han SM, Kim CE. New fluid biomarkers tracking non-amyloid-β and non-tau pathology in Alzheimer's disease. Exp Mol Med. 2020;52:552–568. Available from: https://doi.org/10.1038/s12276-020-0418-9.

[198] Mendes VM, Coelho M, Tomé AR, Cunha RA, Manadas B. Validation of an LC-MS/MS Method for the Quantification of Caffeine and Theobromine Using Non-Matched Matrix Calibration Curve. Molecules. 2019;24(16). Available from: https://www.mdpi.com/1420-3049/24/16/2863.

[199] Cifuentes CV, López VC, Salazar SJ, Peña KP, Pérez L, J S, et al. An update of the classical and novel methods used for measuring fast neurotransmitters during normal and brain altered function. Current neuropharmacology. Curr Neuropharmacol. 2014;12(6):490–508. Available from: https://doi.org/10.2174/1570159X13666141223223657.

[200] Dominique S, Kumar P, Xing P, Mathault J, De Koninck P, Boisselier E, et al. A review of neurotransmitters sensing methods for neuro-engineering research. Applied sciences. 2019;2(4719):1–31. Available from: https://doi.org/10.3390/app9214719.

[201] Sethi S, Brietzke E. Omics-based biomarkers: application of metabolomics in neuropsychiatric disorders. Int J Neuropsychopharmacol. 2015 10;19(3). Pyv096. Available from: https://doi.org/10.1093/ijnp/pyv096.

[202] O'Gorman A, Brennan L. The role of metabolomics in determination of new dietary biomarkers. Proc Nutr Soc. 2017;76(3):295–302. Available from: https://doi.org/10.1017/S0029665116002974.

[203] Abdellah T, Carlos A, Marret S, Bekri S. Omics-based strategies in precision medicine: toward a paradigm shift in inborn errors of metabolism investigations. Int J Mol Sci. 2016;17:1555. Available from: https://doi.org/10.3390/ijms17091555.

[204] Babar MM, Afzaal H, Pothineni VR, us Sahar S Zaidi N, Ali Z, Zahid MA, et al. Chapter 14 - Omics approaches in industrial biotechnology and bioprocess engineering. In: Barh D, Azevedo V, editors. Omics Technologies and Bio-Engineering. Academic Press; 2018. p. 251–269. Available from: https://doi.org/10.1016/B978-0-12-815870-8.00014-0.

[205] Hasin Y, Seldin M, Lusis A. Multi-omics approaches to disease. Genome Biol. 2017;18(83). Available from: https://doi.org/10.1186/s13059-017-1215-1.

[206] Roberts LD, Souza AL, Gerszten RE, Clish CB. Targeted Metabolomics. Curr Protoc Mol Biol. 2012;p. 1–24. Available from: https://doi.org/10.1002/0471142727.mb3002s98.

[207] Sengupta A, Narad P. Chapter 5 - Metabolomics. In: Arivaradarajan P, Misra G, editors. Omics Approaches, Technologies And Applications. Springer Nature Singapore; 2018. p. 75–97. Available from: https://doi.org/10.1007/978-981-13-2925-8_5.

[208] Hook V, Kind T, Podvin S, Palazoglu M, Tran C, Toneff T, et al. Metabolomics analyses of 14 classical neurotransmitters by GC-TOF with LC-MS illustrates secretion of 9 cell-cell signaling molecules from sympathoadrenal chromaffin cells in the presence of lithium. ACS Chem Neurosci. 2019;10(3):1369–1379. Available from: https://doi.org/10.1021/acschemneuro.8b00432.

[209] Lei Z, Huhman D, Sumner L. Mass spectrometry strategies in metabolomics. The Journal of biological chemistry. 2011 06;286:25435–42. Available from: https://doi.org/10.1074/jbc.R111.238691.

[210] Almontashiri NAM, Zha L, Young K, Law T, Kellogg M, Bodamer O, et al. Clinical validation of targeted and untargeted metabolomics testing for genetic disorders: A 3 year comparative study. Sci Rep. 2020;10. Available from: https://doi.org/10.1038/s41598-020-66401-2.

[211] Klupczynska A, Misiura M, Miltyk W, Oscilowska I, Palka J, Kokot ZJ, et al. Development of an LC-MS targeted metabolomics methodology to study proline metabolism in mammalian cell cultures. Molecules. 2020;25(20):4639. Available from: https://doi.org/10.3390/molecules25204639.

[212] Zhou B, Xiao J, Tuli L, Ressom H. LC-MS-based metabolomics. Molecular bioSystems. 2012 02;8:470–81. Available from: https://doi.org/10.1039/c1mb05350g.

[213] Dunn WB. Mass Spectrometry in Systems Biology: An Introduction. In: Jameson D, Verma M, Westerhoff HV, editors. Methods in Systems Biology. vol. 500 of Methods in Enzymology. Academic Press; 2011. p. 15 – 35. Available from: https://doi.org/10.1016/B978-0-12-385118-5.00002-5.

[214] Iuliano A, Franzese M. Introduction to biostatistics. In: Ranganathan S, Gribskov M, Nakai K, SchÃ¶nbach C, editors. Encyclopedia of Bioinformatics and Computational Biology. Oxford: Academic Press; 2019. p. 648–671. Available from: https://doi.org/10.1016/B978-0-12-809633-8.20353-1.

[215] Barua A, Deb PK, Maheshwari R, Tekade RK. Chapter 10 - Statistical techniques in pharmaceutical product development. In: Tekade RK, editor. Dosage Form Design Parameters. Advances in Pharmaceutical Product Development and Research. Academic Press; 2018. p. 339–362. Available from: https://doi.org/10.1016/B978-0-12-814421-3.00010-5.

[216] Konieczna L, Roszkowska A, Stachowicz-Stencel T, Synakiewicz A, Baczek T. Bioanalysis of a panel of neurotransmitters and their metabolites in plasma samples obtained from pediatric patients with neuroblastoma and Wilms' tumor. J Chromatogr B. 2018;1074-1075:99 – 110. Available from: https://doi.org/10.1016/j.jchromb.2017.12.031.

[217] Liu D, An Z, Li P, Chen Y, Zhang R, Liu L, et al. A targeted neurotransmitter quantification and nontargeted metabolic profiling method for pharmacometabolomics analysis of olanzapine by using UPLC-HRMS. RSC Adv. 2020;Available from: https://doi.org/10.1039/d0ra02406f.

[218] Lu J, Hu W, Cao W, Xie S, Li Z, Tao Y, et al. Rapid and reproducible dibutylation derivatization coupled with ultra-high performance liquid chromatography-tandem mass spectrometry for the simultaneous determination of dopamine, norepinephrine and 5-hydroxytryptamine in rat brain microdialysates. Int Journal of Analytical Mass Spectrometry and Chromatography. 2018;6:21–36. Available from: https://doi.org/10.4236/ijamsc.2018.62002.

[219] Ji C, Li W, dan Ren X, El-Kattan AF, Kozak R, Fountain S, et al. Diethylation labeling combined with UPLC/MS/MS for simultaneous determination of a panel of monoamine neurotransmitters in rat prefrontal cortex microdialysates. Anal Chem. 2008;80:9195–9203. Available from: https://doi.org/10.1021/ac801339z.

[220] Prokai L, Frycák P, Stevens SJ, Nguyen V. Measurement of acetylcholine in rat brain microdialysates by LC - isotope dilution tandem MS. Chromatographia. 2008;16801-105. Available from: https://doi.org/10.1365/s10337-008-0697-0.

[221] Kirsch SH, Herrmann W, Rabagny Y, Obeid R. Quantification of acetylcholine, choline, betaine, and dimethylglycine in human plasma and urine using stable-isotope dilution ultra performance liquid chromatography-tandem mass spectrometry. J Chromatogr B. 2010;878(32):3338 – 3344. Available from: https://doi.org/10.1016/j.jchromb.2010.10.016.

[222] Hows MEP, Lacroix L, Heidbreder C, Organ AJ, Shah AJ. High-performance liquid chromatography/tandem mass spectrometric assay for the simultaneous measurement of dopamine, norepinephrine, 5-hydroxytryptamine and cocaine in biological samples. J Neurosci Methods. 2004;138(1):123 – 132. Available from: https://doi.org/10.1016/j.jneumeth.2004.03.021.

[223] Lamy E, Pilyser L, Paquet C, Bouaziz-Amar E, Grassin-Delyle S. High-sensitivity quantification of acetylcholine and choline in human cerebrospinal fluid with a validated LC-

MS/MS method. Talanta. 2020;p. 121881. Available from: http://www.sciencedirect.com/science/article/pii/S0039914020311723.

[224] Skoog DA, West DM, Holler FJ, Crouch SR. Introduction to analytical separations. In: Fundamentals of Analytical Chemistry. ninth edition ed. Cengage Learning; 2014. p. 847–886. Available from: https://doi.org/10.1007/s00216-013-7242-1.

[225] Coskun O. Separation techniques: Chromatography. North Clin Istanb. 2016;3(2):152–160. Available from: https://doi.org/10.14744/nci.2016.32757.

[226] Dong MW. HPLC instrumentation in pharmaceutical analysis: status, advances, and trends. In: Ahuja S, Dong MW, editors. Handbook of Pharmaceutical Analysis by HPLC. vol. 6 of Separation Science and Technology. Academic Press; 2005. p. 47 – 75. Available from: https://doi.org/10.1016/S0149-6395(05)80047-9.

[227] Yashin YI, Yashin AY. Chapter 10 - Liquid Chromatography. In: Pico Y, editor. Chemical Analysis of Food::Techniques and Applications. Boston: Academic Press; 2012. p. 285 – 310. Available from: https://doi.org/10.1016/B978-0-12-384862-8.00010-8.

[228] Skoog DA, Holler FJ, Crouch SR. Separation methods. In: Kiselica S, editor. Principles of instrumental analysis. sixth edition ed. David Harris; 2007. p. 761–828.

[229] Lenehan CE. Chromatography: basic principles. In: Siegel JA, Saukko PJ, Houck MM, editors. Encyclopedia of Forensic Sciences. second edition ed. Elsevier/ Academic Press; 2013. p. 573–578. Available from: https://doi.org/10.1016/B978-0-12-382165-2.00244-0.

[230] Pragst F. High performance liquid chromatography in forensic toxicological analysis. In: Bogusz MJ, editor. Forensic Science, Handbook of Analytical Separations. vol. 6. Elsevier Science;; 2008. p. 447–489,.

[231] Blum F. High performance liquid chromatography. Br J Hosp Med. 2014;75(Sup2):C18–C21. PMID: 24521830. Available from: https://doi.org/10.12968/hmed.2014.75.Sup2.C18.

[232] Thurman EM, Ferrer I, Fernández-Alba A. LC-MS. I: Basic principles and technical aspects of LC-MS for pesticide analysis. In: Chromatographic-Mass Spectrometric Food Analysis for Trace Determination of Pesticide Residues. vol. 43 of Comprehensive Analytical Chemistry. Elsevier; 2005. p. 369 – 401. Available from: https://doi.org/10.1016/S0166-526X(05)80028-5.

[233] Engelhardt H. Bonded Stationary Phases. In: Corradini D, editor. Handbook of HPLC. Chromatographic Science Series. vol. 101. second edition ed. CRC Press; 2011. p. 47–75.

[234] Shabir GA, Lough WJ, Arain SA, Bradshaw TK. Evaluation and Application of Best Practice in Analytical Method Validation. Journal of Liquid Chromatography & Related Technologies. 2007;30(3):311–333. Available from: https://doi.org/10.1080/10826070601084753.

[235] Causin V. Polymers on the crime scene. Switzerland: Springer International Publishing; 2015. Available from: https://doi.org/10.1007/978-3-319-15494-7.

[236] Snyder LR, Dolan JW. Chapter 8 - Liquid-solid chromatography. In: Fanali S, Haddad PR, Poole CF, Riekkola ML, editors. Liquid Chromatography. second edition ed. Elsevier; 2017. p. 191 – 203. Available from: https://doi.org/10.1016/B978-0-12-805393-5.00008-7.

[237] McMaster M. HPLC A Practical User's Guide. vol. 101. Second edition ed. Corradini D, editor. John Wiley & Sons, Inc., Hoboken; 2007.

[238] Sahu PK, Ramisetti NR, Cecchi T, Swain S, Patro CS, Panda J. An overview of experimental designs in HPLC method development and validation. J Pharm Biomed Anal. 2018;147:590 – 611. Review issue 2017. Available from: https://doi.org/10.1016/j.jpba.2017.05.006.

[239] Jandera P. Gradient Elution Mode. In: Corradini D, editor. Handbook of HPLC. Chromatographic Science Series. vol. 101. second edition ed. CRC Press; 2011. p. 119–154.

[240] Morgan NY, Smith PD. HPLC Detectors. In: Corradini D, editor. Handbook of HPLC. Chromatographic Science Series. vol. 101. second edition ed. CRC Press; 2011. p. 207–231.

[241] Mellon FA. Mass spectrometry | Principles and instrumentation. In: Caballero B, editor. Encyclopedia of Food Sciences and Nutrition. second edition ed. Oxford: Academic Press; 2003. p. 3739 – 3749. Available from: https://doi.org/10.1016/B0-12-227055-X/00746-X.

[242] de Hoffmann E, Charette JJ, Stroobant V, Trottier J. Mass Spectrometry: Principles and Applications. Third edition ed. John Wiley Sons Ltd; 2007.

[243] Gross J. Mass Spectrometry-A Textbook. Springer; 2011. Available from: https://doi.org/10.1007/978-3-642-10711-5.

[244] Smith RW. Mass Spectrometry. In: Siegel JA, Saukko PJ, Houck MM, editors. Encyclopedia of Forensic Sciences. second edition ed. Waltham: Academic Press; 2013. p. 603 – 608. Available from: https://doi.org/10.1016/B978-0-12-382165-2.00250-6.

[245] Argenta DF, Martelli SM, Caon T. Dendrimer as a platform for drug delivery in the skin. In: Holban AM, Grumezescu AM, editors. Materials for Biomedical Engineering. Elsevier; 2019. p. 331 – 367. Available from: https://doi.org/10.1016/B978-0-12-818433-2.00010-8.

[246] El-Aneed A, Cohen A, Banoub J. Mass spectrometry, review of the basics: electrospray, MALDI, and commonly used mass analyzers. Appl Spectrosc Rev. 2009;44(3):210–230. Available from: https://doi.org/10.1080/05704920902717872.

[247] Clarke W. In: Nair H, Clarke W, editors. Mass spectrometry in the clinical laboratory: determining the need and avoiding pitfalls. San Diego: Academic Press; 2017. p. 1 – 15. Available from: https://doi.org/10.1016/B978-0-12-800871-3.00001-8.

[248] Haag AM. 7. In: Mirzaei H, Carrasco M, editors. Mass Analyzers and Mass Spectrometers. Cham: Springer International Publishing; 2016. p. 157–169. Available from: https://doi.org/10.1007/978-3-319-41448-5_7.

[249] Pitt J. Principles and applications of liquid chromatography-mass spectrometry in clinical biochemistry. The Clinical biochemist Reviews. 2009;30:19–34.

[250] Ojeda M, Lopez M. 5. In: Faraldos M, Goberna C, editors. Espectrometría de masas. CSIC Consejo Superior de Investigaciones Cientificas; 2011. p. 267–319.

[251] Domon B, Aebersold R. Mass spectrometry and protein analysis. Science. 2006;312(5771):212–217. Available from: https://doi.org/10.1126/science.1124619.

[252] Covey T, Thomson B, Schneider B. Atmospheric Pressure Ion Sources. Mass spectrometry reviews. 2009 11;28:870–97. Available from: https://doi.org/10.1002/mas.20246.

[253] Dona AC. High-Throughput Metabolic Screening. In: Holmes E, Nicholson JK, Darzi AW, Lindon JC, editors. Metabolic Phenotyping in Personalized and Public Healthcare. Boston: Academic Press; 2016. p. 111 – 136. Available from: https://doi.org/10.1016/B978-0-12-800344-2.00005-7.

[254] Hird SJ, Lau BPY, Schuhmacher R, Krska R. Liquid chromatography-mass spectrometry for the determination of chemical contaminants in food. TrAC Trends in Analytical Chemistry. 2014;59:59 – 72. Available from: https://doi.org/10.1016/j.trac.2014.04.005.

[255] Gergov M. Forensic screening with liquid chromatography-mass spectrometry. In: Bogusz MJ, editor. Forensic Science. vol. 6 of Handbook of Analytical Separations. Elsevier Science B.V.; 2008. p. 491 – 511. Available from: https://doi.org/10.1016/S1567-7192(06)06014-1.

[256] Banerjee S, Mazumdar S. Electrospray ionization mass spectrometry: A technique to access the Information beyond the molecular weight of the analyte. Int J Anal Chem. 2012;p. 1–41. Available from: https://doi.org/10.1155/2012/282574.

[257] Mann M, Fenn JB. 1. In: Desiderio DM, editor. Electrospray. Boston, MA: Springer US; 1992. p. 1–35. Available from: https://doi.org/10.1007/978-1-4899-1173-5_1.

[258] Palma P, Pierini E, Cappiello A. 5. In: Anderson JL, Berthod A, Pino V, Stalcup A, editors. LC-MS interfaces. second edition ed. Wiley-VCH Verlag GmbH & Co. KGaA; 2015. p. 87–110. Available from: https://doi.org/10.1002/9783527678129.assep005.

[259] Medhe S. Mass spectrometry: detectors review. Chemical and Biomolecular Engineering. 2018;3(4):51–58. Available from: https://doi.org/10.11648/j.cbe.20180304.11.

[260] de Hoffmann E. In: Mass Spectrometry. American Cancer Society; 2005. Available from: https://doi.org/10.1002/0471238961.1301191913151518.a01.pub2.

[261] Thomas SN. Chapter 10 - Mass spectrometry. In: Clarke W, Marzinke MA, editors. Contemporary Practice in Clinical Chemistry. fourth edition ed. Academic Press; 2019. p. 171–185. Available from: https://doi.org/10.1016/B978-0-12-815499-1.00010-7.

[262] Rockwood AL, Kushnir MM, Clarke NJ. Chapter 2 - Mass Spectrometry. In: Rifai N, Horvath AR, Wittwer CT, editors. Principles and Applications of Clinical Mass Spectrometry. Elsevier; 2018. p. 33 – 65. Available from: https://doi.org/10.1016/B978-0-12-816063-3.00002-5.

[263] Mittal RD. Tandem mass spectroscopy in diagnosis and clinical research. Mittal RD. Indian J Clin Biochem. 2015 Apr;30(2):121-3. doi: 10.1007/s12291-015-0498-9. No abstract available. PMID: 25883417. Indian J Clin Biochem. 2015 04;30:121–123. Available from: https://doi.org/10.1007/s12291-015-0498-9.

[264] Frenich AG, nos PPB, Vidal JLM. Comparison of tandem-in-space and tandem-in-time mass spectrometry in gas chromatography determination of pesticides: Application to simple and complex food samples. J Chromatogr A. 2008;1203(2):229 – 238. Available from: https://doi.org/10.1016/j.chroma.2008.07.041.

[265] Johnson JV, Yost RA, Kelley PE, Bradford DC. Tandem-in-space and tandem-in-time mass spectrometry: triple quadrupoles and quadrupole ion traps. Anal Chem. 1990;62(20):2162–2172. Available from: https://doi.org/10.1021/ac00219a003.

[266] Glish GL, Burinsky DJ. Hybrid Mass Spectrometers for Tandem Mass Spectrometry. J Am Soc Mass Spectrom. 2008;19(2):161 – 172. Available from: https://doi.org/10.1016/j.jasms.2007.11.013.

[267] Hocart CH. Mass Spectrometry: An Essential Tool for Trace Identification and Quantification. In: Liu HWB, Mander L, editors. Comprehensive Natural Products II. Oxford: Elsevier; 2010. p. 327–388. Available from: https://doi.org/10.1016/B978-008045382-8.00187-8.

[268] Twyman RM. Mass spectrometry | multidimensional. In: Worsfold P, Townshend A, Poole C, editors. Encyclopedia of Analytical Science. second edition ed. Oxford: Elsevier; 2005. p. 430 – 438. Available from: https://doi.org/10.1016/B0-12-369397-7/00354-X.

[269] Chiaradia MC, Collins CH, Jardim ICSF. The state of the art of chromatography associated with the tandem mass spectrometry for toxic compound analyses in food. Química Nova. 2008;31:623 – 636. Available from: https://doi.org/10.1590/S0100-40422008000300030.

[270] Payne AH, Glish GL. Tandem Mass Spectrometry in Quadrupole Ion Trap and Ion Cyclotron Resonance Mass Spectrometers. In: Biological Mass Spectrometry. vol. 402 of Methods in Enzymology. Academic Press; 2005. p. 109 – 148. Available from: https://doi.org/10.1016/S0076-6879(05)02004-5.

[271] Chindarkar NS, Park HD, Stone JA, Fitzgerald RL. Comparison of Different Time of Flight-Mass Spectrometry Modes for Small Molecule Quantitative Analysis. J Anal Toxicol. 2015 08;39(9):675–685. Available from: https://doi.org/10.1093/jat/bkv057.

[272] Stock N. Introducing graduate students to high-resolution mass spectrometry (HRMS) using a hands-on approach. J Chem Educ. 2017 11;94. Available from: https://doi.org/10.1021/acs.jchemed.7b00569.

[273] Allen DR, McWhinney BC. Quadrupole time-of-flight mass spectrometry: a paradigm shift in toxicology Screening Applications. The Clinical biochemist Reviews. 2019;40(3):135–146. Available from: https://doi.org/10.33176/AACB-19-00023.

[274] Chernushevich IV, Loboda AV, Thomson BA. An introduction to quadrupole-time-of-flight mass spectrometry. Journal of mass spectrometry. 2001 August;36(8):849–865. Available from: https://doi.org/10.1002/jms.207.

[275] Araujo P. Key aspects of analytical method validation and linearity evaluation. J Chromatogr B. 2009;877(23):2224 – 2234. Available from: https://doi.org/10.1016/j.jchromb.2008.09.030.

[276] Leite M, Freitas A, Silva AS, Barbosa J, Ramos F. Maize (Zea mays L.) and mycotoxins: A review on optimization and validation of analytical methods by liquid chromatography coupled to mass spectrometry. Trends in Food Science & Technology. 2020;99:542 – 565. Available from: https://doi.org/10.1016/j.tifs.2020.03.023.

[277] Peris-Vicente J, Esteve-Romero J, Carda-Broch S. Chapter 13 Validation of Analytical Methods Based on ChromatographicTechniques: An Overview. In: Anderson LJ, Berthod A, Pino EV, Stalcup MA, editors. Analytical Separation Science. vol. 5. first edition ed. Wiley-VCH Verlag GmbH & Co. KGaA; 2015. p. 1757–1808. Available from: https://doi.org/10.1002/9783527678129.assep064.

[278] Raposo F, Ibelli-Bianco C. Performance parameters for analytical method validation: Controversies and discrepancies among numerous guidelines. TrAC Trends in Analytical Chemistry. 2020;129:115913. Available from: https://doi.org/10.1016/j.trac.2020.115913.

[279] Chandran S, Singh R. Comparison of various international guidelines for analytical method validation. Die Pharmazie - An International Journal of Pharmaceutical Sciences. 2006;62(1). Available from: https://doi.org/10.1691/ph2007.1.5064.

[280] Raposo F, Barceló D. Challenges and strategies of matrix effects using chromatography-mass spectrometry: An overview from research versus regulatory viewpoints. TrAC Trends in Analytical Chemistry. 2020;p. 116068. Available from: https://doi.org/10.1016/j.trac.2020.116068.

[281] Kollipara S, Bende G, Agarwal N, Varshney B, Paliwal J. International Guidelines for Bioanalytical Method Validation: A comparison and discussion on current scenario. Chromatographia. 2011;p. 201–217. Available from: https://doi.org/10.1007/s10337-010-1869-2.

[282] Swartz ME, Krull IS. Chapter 1- Introduction to Analytical Method Validation. In: Handbook of Analytical Validation. CRC Press; 2012. .

[283] Ravichandran V, Shalini S, Sundram K, Harish R. Validation of analytical methods - Strategies importance. Int J Pharm Pharm Sci. 2010 07;2:18–22. Available from: https://www.researchgate.net/publication/279892924.

[284] Peters FT, Maurer HH. Bioanalytical method validation and its implications for forensic and clinical toxicology - A review. Accreditation and Quality Assurance. 2002;7(11):441–449. Available from: https://doi.org/10.1007/s00769-002-0516-5.

[285] Dos Reis Duarte JL. Análise crítica do método cromatográfico para quantificação de TCA e soluções para a sua melhoria. Universidade de Porto. 2016;.

[286] Paschoal JAR, Rath S, Airoldi FPdS, Reyes FGR. Validação de métodos cromatográficos para a determinação de resíduos de medicamentos veterinários em alimentos. Quim Nova. 2008;31:1190 – 1198. Available from: https://doi.org/10.1590/S0100-40422008000500048.

[287] Borges B. Verificaço de conformidade. Validação de um método analítico. Universidade de Coimbra. 2014;.

[288] Raposo F. Evaluation of analytical calibration based on least-squares linear regression for instrumental techniques: A tutorial review. TrAC Trends in Analytical Chemistry. 2016;77:167 – 185. Available from: https://doi.org/10.1016/j.trac.2015.12.006.

[289] Barwick V. Preparation of calibration curves: A guide to best practice. LGC/VAM; 2003. 032. Available from: http://www.lgcgroup.com/our-science/national-measurement-laboratory/publications-and-resources/good-practice-guides/preparation-of-calibration-curves-a-guide-to-best/.

[290] Vareli CS, Pizzutti IR, Gebler L, Cardoso CD, Gai DSH, Fontana MEZ. Analytical method validation to evaluate dithiocarbamates degradation in biobeds in South of Brazil. Talanta. 2018;184:202 – 209. Available from: https://doi.org/10.1016/j.talanta.2018.03.009.

[291] Magnusson B, (eds) UO. The Fitness for Purpose of Analytical Methods - A Laboratory Guide to Method Validation and Related Topics; 2014. Available from: https://www.eurachem.org/index.php/publications/guides/mv.

[292] Coelho M, Mendes VM, Lima IS, Martins FO, Fernandes AB, Macedo PM, et al. Direct analysis of [6,6-2H2] glucose and [U-13C6] glucose dry blood spot enrichments by LC-MS/MS B Analytical technologies in the biomedical and life sciences. Journal of chromatography B. 2016;1022:242–248.

[293] Harmonised Tripartite Guideline, Validation of analytical procedures: text and methodology Q2(R1); 2015. Available from: http://www.ich.org/products/guidelines/quality/article/quality-guidelines.html.

[294] Camargo SPS. Development and validation of an analytical methodology for determination of cannabidiol and tetrahydrocanabinol in plasma samples using gas phase chromatografy /mass espectrometry. Universidade de São Paulo. 2008;Available from: https://doi.org/10.11606/D.60.2008.tde-02122008-131214.

[295] Zeng W, Musson DG, Fisher AL, Wang AQ. A new approach for evaluating carryover and its influence on quantitation in high-performance liquid chromatography and tandem mass spectrometry assay. Rapid Commun Mass Spectrom. 2006;20(4):635–640. Available from: https://doi.org/10.1002/rcm.2353.

[296] Hughes NC, Wong EYK, Fan J, Bajaj N. Determination of carryover and contamination for mass spectrometry-based chromatographic assays. The AAPS journal. 2007;9(3):353–360. Available from: https://doi.org/10.1208/aapsj0903042.

[297] Vu DH, Koster RA, Wessels AMA, Greijdanus B, Alffenaar JWC, Uges DRA. Troubleshooting carry-over of LC-MS/MS method for rifampicin, clarithromycin and metabolites in human plasma. J Chromatogr B. 2013;917-918:1 – 4. Available from: https://doi.org/10.1016/j.jchromb.2012.12.023.

[298] Naidis I, Turpeinen S. Guidance for the validation of analytical methodology and calibration of equipment used for testing of illicit drugs in seized materials and biological specimens; 2009.

[299] Zhou W, Yang S, Wang PG. Matrix effects and application of matrix effect factor. Bioanalysis. 2017;9(23):1839–1844. PMID: 29171768. Available from: https://doi.org/10.4155/bio-2017-0214.

[300] Taylor PJ. Matrix effects: the Achilles heel of quantitative high-performance liquid chromatography-electrospray-tandem mass spectrometry. Clinical Biochemistry. 2005;38(4):328 – 334. LC Mass Spectrometry: Recent Developments in Clinical Chemistry. Available from: https://doi.org/10.1016/j.clinbiochem.2004.11.007.

[301] Lister AS. 7 - Validation of HPLC Methods in Pharmaceutical Analysis. In: Ahuja S, Dong MW, editors. Handbook of Pharmaceutical Analysis by HPLC. vol. 6 of Separation Science and Technology. Academic Press; 2005. p. 191–217. Available from: https://www.sciencedirect.com/science/article/pii/S0149639505800510.

[302] Khuri A. Introduction to Linear Regression Analysis, Fifth Edition by Douglas C. Montgomery, Elizabeth A. Peck, G. Geoffrey Vining. International Statistical Review. 2013 08;81.

[303] Mansilha C, Melo A, Rebelo H, Ferreira IMPLVO, Pinho O, Domingues V, et al. Quantification of endocrine disruptors and pesticides in water by gas chromatography - tandem mass spectrometry. Method validation using weighted linear regression schemes. J Chromatogr A. 2010;1217(43):6681–6691. 11th International Symposium on Hyphenated Techniques in Chromatography and Hyphenated Chromatographic Analyzers. Available from: https://www.sciencedirect.com/science/article/pii/S0021967310006291.

[304] Martin J, Adana D, Garcia Asuero A. Chapter 7. In: Fitting Models to Data: Residual Analysis, a Primer; 2017. .

[305] Almeida AM, Castel-Branco MM, ao ACF. Linear regression for calibration lines revisited: weighting schemes for bioanalytical methods. J Chromatogr B. 2002;774(2):215–222. Available from: https://www.sciencedirect.com/science/article/pii/S1570023202002441.

[306] Miller JN, Miller JC. Statistics and Chemometrics for Analytical Chemistry. Fifth edition ed. Pearson Education; 2005.

[307] Moosavi M, Ghassabian S. Chapter 6. In: Linearity of Calibration Curves for Analytical Methods: A Review of Criteria for Assessment of Method Reliability; 2018. .

[308] Van Loco J, Elskens M, Croux C, Beernaert H. Linearity of calibration curves: Use and misuse of the correlation coefficient. Katholieke Universiteit Leuven, Open Access publications from Katholieke Universiteit Leuven. 2002 07;7.

[309] Gu H, Liu G, Wang J, Aubry AF, Arnold ME. Selecting the correct weighting factors for linear and quadratic calibration curves with least-squares regression algorithm in bioanalytical LC-MS/MS assays and impacts of using incorrect weighting factors on curve stability, data quality, and assay performance. Analytical chemistry. 2014 September;86(18):8959–8966. Available from: https://doi.org/10.1021/ac5018265.

[310] Wille S, Peters F, Di Fazio V, Samyn N. Practical aspects concerning validation and quality control for forensic and clinical bioanalytical quantitative methods. Accredit Qual Assur. 2011 06;16:279–292.

[311] Assigning Values to Non-detected/Non-quantified Pesticide Residue in Human Health Food Exposure Assessments; 2000.

[312] Jusko WJ. Use of pharmacokinetic data below lower limit of quantitation values. Pharmaceutical research. 2012;29(9):2628–2631.

[313] Shrivastava A. Methods for the determination of limit of detection and limit of quantitation of the analytical methods. Chronicles of Young Scientists. 2011 06;2:21–25.

[314] Desimoni E, Brunetti B. About Estimating the Limit of Detection by the Signal to Noise Approach. Pharmaceutica Analytica Acta. 2015 Mar;6(3).

[315] Gao F, McDaniel J, Chen E, Rockwell H, Lynes M, Tseng YH, et al. Monoacylglycerol Analysis Using MS/MSALL Quadruple Time of Flight Mass Spectrometry. Metabolites. 2016 08;6:25.

[316] Zhang P, Chan W, Ang I, Wei R, Lam M, Lei K, et al. Revisiting fragmentation reactions of protonated α-amino acids by high-resolution electrospray ionization tandem mass spectrometry with collision-induced dissociation. Sci Rep. 2019 04;9:6453.

[317] Angeles LG, Aga D. Establishing Analytical Performance Criteria for the Global Reconnaissance of Antibiotics and Other Pharmaceutical Residues in the Aquatic Environment Using Liquid Chromatography-Tandem Mass Spectrometry. Journal of Analytical Methods in Chemistry. 2018 06;2018:1–9.

[318] Tan A, Awaiye K. 17. In: Use of Internal Standards in LC-MS Bioanalysis. John Wiley & Sons, Ltd; 2013. p. 217–227. Available from: https://onlinelibrary.wiley.com/doi/abs/10.1002/9781118671276.ch17.

[319] Bunch DR, McShane AJ, Wang S. Investigation of transition ion ratio variation for liquid chromatography-tandem mass spectrometry: A case study approach. Clin Chim Acta. 2018;486:205–208. Available from: https://doi.org/10.1016/j.cca.2018.08.009.

[320] The European Communities,. Implementing council Directive 96/23/EC concerning the performance of Analytical methods and the interpretation of results; 2012. Available from: https://eur-lex.europa.eu/legal-content/EN/ALL/?uri=CELEX:32002D0657.

[321] Stolker AAM, Niesing W, Fuchs R, Vreeken R, Niessen W, Brinkman U. Liquid chromatography with triple-quadrupole and quadrupole-time-of-flight mass spectrometry for the determination of micro-constituents - A comparison. Analytical and bioanalytical chemistry. 2004 05;378:1754–61.

[322] Mol HGJ, Zomer P, López MG, Fussell RJ, Scholten J, de Kok A, et al. Identification in residue analysis based on liquid chromatography with tandem mass spectrometry: Experimental evidence to update performance criteria. Anal Chim Acta. 2015;873:1–13. Available from: https://doi.org/10.1016/j.aca.2015.03.007.

[323] Hertz L. The Glutamate-Glutamine (GABA) Cycle: Importance of Late Postnatal Development and Potential Reciprocal Interactions between Biosynthesis and Degradation. Frontiers in Endocrinology. 2013;4:59. Available from: https://www.frontiersin.org/article/10.3389/fendo.2013.00059.

[324] Madeira C, Alheira FV, Calcia MA, Silva TCS, Tannos FM, Vargas-Lopes C, et al. Blood Levels of Glutamate and Glutamine in Recent Onset and Chronic Schizophrenia. Front Psychiatry. 2018;9:713. Available from: https://www.frontiersin.org/article/10.3389/fpsyt.2018.00713.

[325] Madeira C, Vargas-Lopes C, Brandão CO, Reis T, Laks J, Panizzutti R, et al. Elevated glutamate and glutamine levels in the cerebrospinal fluid of patients with probable alzheimer's disease and depression. Front Psychiatry. 2018;9:561. Available from: https://doi.org/10.3389/fpsyt.2018.00561.

[326] Hashimoto K, Bruno D, Nierenberg J, Marmar C, Zetterberg H, Blennow K, et al. Abnormality in glutamine-glutamate cycle in the cerebrospinal fluid of cognitively intact elderly individuals with major depressive disorder: a 3-year follow-up study. Transl Psychiatry. 2016;6(e744). Available from: https://doi.org/10.1038/tp.2016.8.

[327] Nuzzo T, Mancini A, Miroballo M, Casamassa A, Di Maio A, Donati G, et al. High performance liquid chromatography determination of L-glutamate, L-glutamine and glycine content in brain, cerebrospinal fluid and blood serum of patients affected by Alzheimer's disease. Amino acids. 2021;53(3):435–449. Available from: https://doi.org/10.1007/s00726-021-02943-7.

Appendix A

Appendix

Appendix

A.1 Materials and methods

Table A.1: Additional information about the analytes used in this project.

Compounds	Properties	Solvents	Solubility	Max Conc. mg/mL
Choline chloride				
	M_{mi}: 139.08 g/mol	ethanol	soluble	28 mg/mL
	Polar, XLogP3: -0.4	water	soluble	500 mg/mL
Acetylcholine chloride				
	M_{mi}: 181.09 g/mol	DMSO	soluble	18.17 mg/mL
	XLogP3: 0.2	water	soluble	18.17 mg/mL
L-glutamic acid				
	M_{mi}: 147.05 g/mol	methanol	insoluble	0.35 mg/mL
	XLogP3: -3.7	ethanol	soluble	36 mg/mL
		water	soluble	8.57 mg/mL
L-glutamine				
	M_{mi}: 146.07 g/mol	methanol	insoluble	3.5 mg/100mL
	Polar, XLogP3: -3.1	water	soluble	41.3 mg/mL
		ethanol	insoluble	46 µg/100mL
GABA				
	M_{mi}: 103.06 g/mol	methanol	insoluble	1.2 ug/mL
	Polar, XLogP3: -3.2	water	soluble	20 mg/mL

M_{mi}: Monoisotopic mass; DMSO Dimethyl sulfoxide. Source: PubChem Database

A.2 Results and discussion

A.2.1 Method development

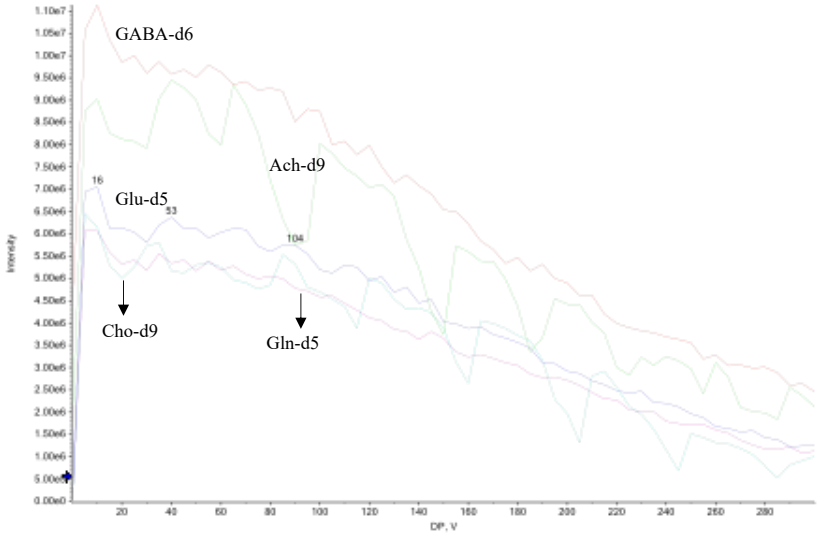

Figure A.1: Declustering potential (DP) ramping from 0-300 V for Glu-d5, Gln-d5, GABA-d6, ACho-d9 and Cho-d9.

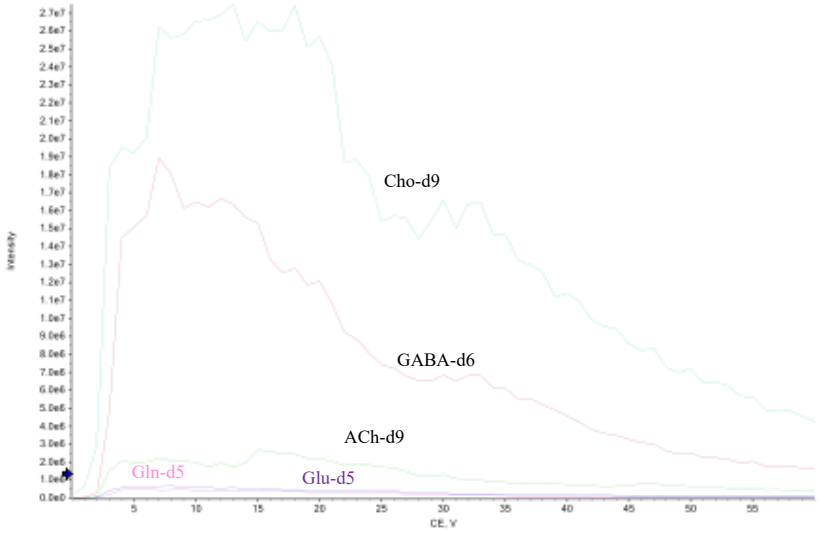

Figure A.2: Collision energy (CE) ramping for Glu-d5, Gln-d5, GABA-d6, ACho-d9 and Cho-d9, in a range of 5 to 45 V.

A.2.2 Compound identification and verification

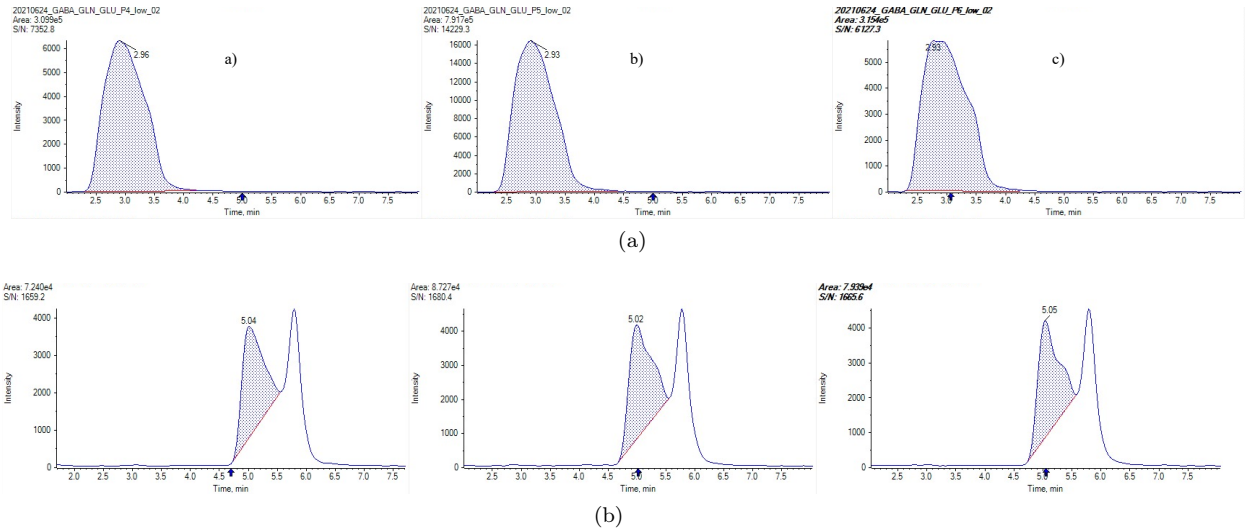

Figure A.3: Non-linear results obtained from a) ACh precursor ion m/z 87.05, and b) Cho m/z 60.08, at 0.07, 0.1 and 0.3 pmol/µL.

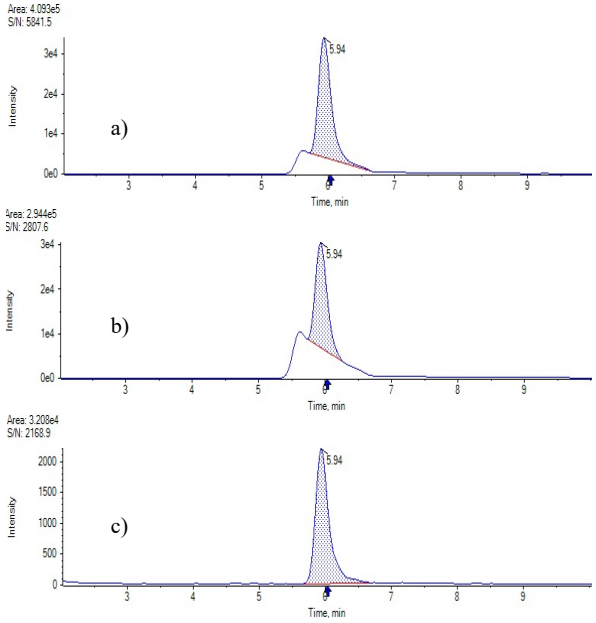

Figure A.4: Representative LC-MS/MS chromatograms of the fragments monitored for glutamine, a) m/z 84.05 b) m/z 130.05 and c) m/z 101.07.

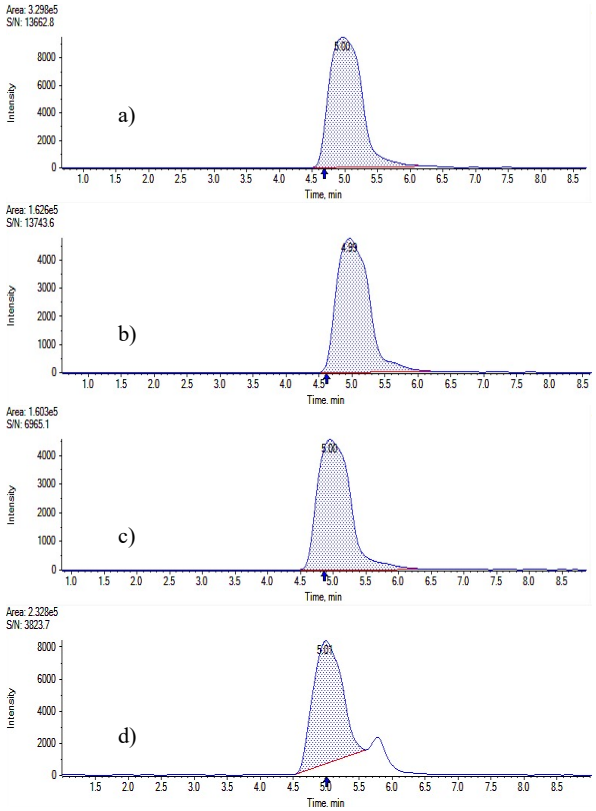

Figure A.5: Representative LC-MS/MS chromatograms of the fragments monitored for GABA, a) m/z 87.05 b) m/z 69.03 c) m/z 45.04 and d) m/z 43.02.

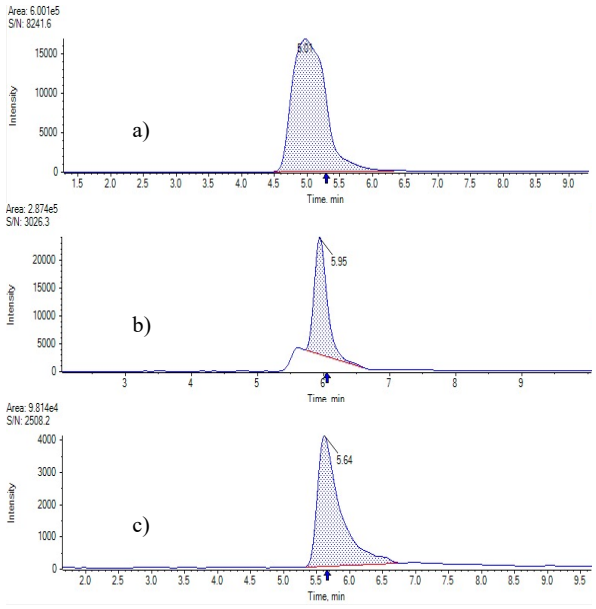

Figure A.6: Representative LC-MS/MS chromatograms of the IS fragments used in quantification for a) GABA-d6 with m/z 93.08 b) Glu-d5 with m/z 107.09 and c) Gln-d5 with m/z 135.08.

A.3 Method validation

A.3.1 Linearity

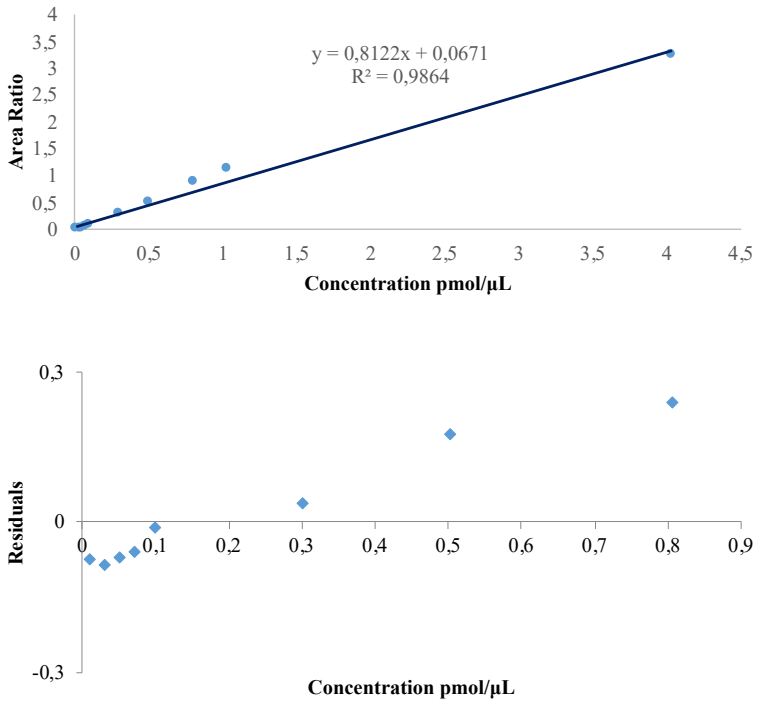

	Coefficients	Standard Error (SE)	t Stat	t. crit	p-value
a	0.067	0.046	1.47	2.31	0.533
b	0.812	0.034	24.11	2.31	0.000
R_2	0.986				
$S_{y/x}$	0.070				

	df	SS	MS	F
Regression	1	1.37	1.36	99.70
Residual	8	0.11	0.014	
Total	9	1.48		

Figure A.7: Example of a linearity analysis of the fragment m/z 87.05 of GABA in the range of 0.01 to 4.003 pmol/µL.

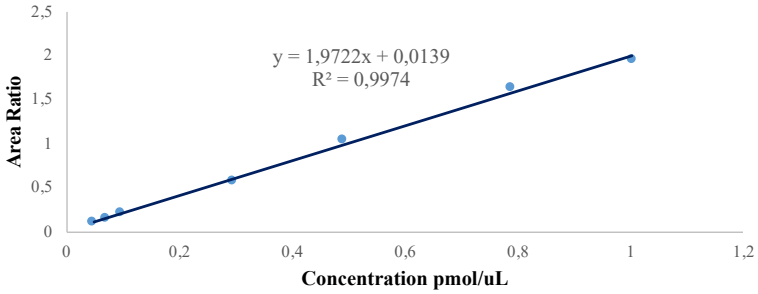

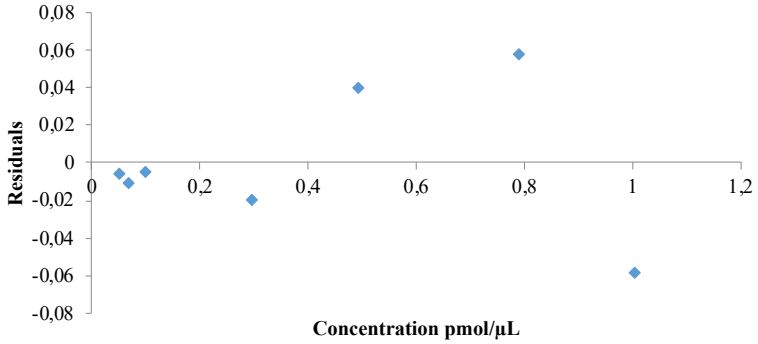

	Coefficients	Standard Error (SE)	t Stat	t. crit	p-value
a	0.0139	0.024	0.58	2.57	0.589
b	1.972	0.045	43.46	2.57	0.000
R_2	0.999				
$S_{y/x}$	0.070				

	df	SS	MS	F
Regression	1	3.34	3.34	1888.81
Residual	5	0.0088	0.0018	
Total	6	3.35		

Figure A.8: Example of a linearity analysis of the quantification fragment m/z 84.05 of Gln in the range of 0.049 to 1.003 pmol/µL.

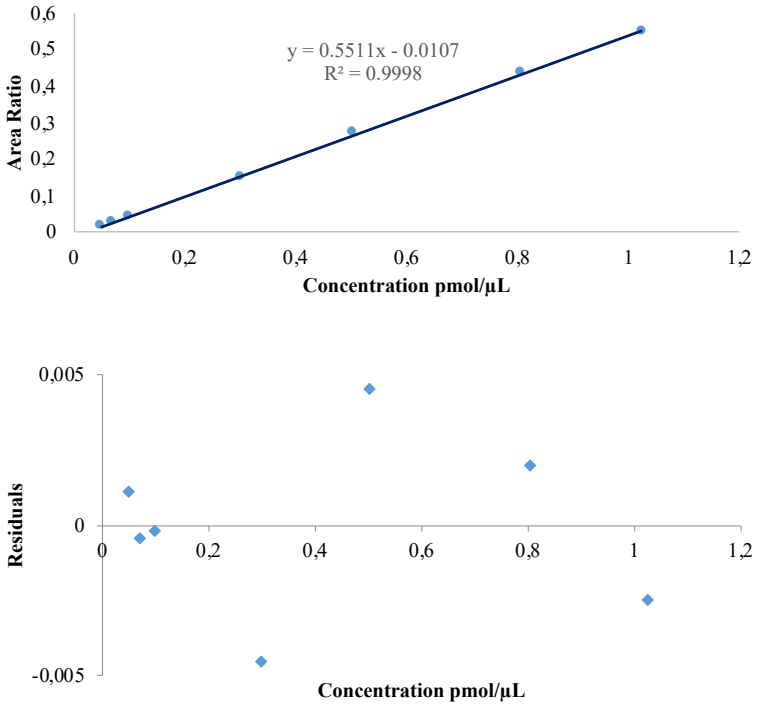

	Coefficients	Standard Error (SE)	t Stat	t crit	p-value
a	-0.011	0.0019	5.77	2.57	0.002
b	0.551	0.0034	161.01	2.57	0.000
R_2	0.999				
$S_{y/x}$	0.0032				

	df	SS	MS	F	F crit	p-value
Regression	1	0.28	0.27	25925.63	6.61	0.000
Residual	5	0.00	0.00			
Total	6	0.27				

Figure A.9: Example of a linearity analysis of the quantification fragment m/z 69.03 of GABA in the range of 0.05 to 1.024 pmol/µL.

A.3.2 Weighted least squares

Table A.2: Nominal concentrations and their respective sum of absolute relative errors calculated using unweighted and weighted models with empirical weights $1/x$, $1/x^2$, $1/y$ and $1/y^2$ for the fragment at m/z 84.05 of GABA.

Nominal concentration (pmol/µL)	Model 1 $1/x^0$ (OLS)	Model 2 $1/x$ (WLS)	Model 3 $1/x^2$ (WLS)	Model 4 $1/y$ (WLS)	Model 5 $1/y^2$ (WLS)
0.05	27.42	19.07	14.14	16.24	9.85
0.07	13.95	12.50	15.34	14.41	17.67
0.1	12.57	11.70	13.00	12.76	13.42
0.3	8.02	8.58	7.88	8.59	7.93
0.503	12.21	11.90	11.32	11.82	12.84
0.805	8.96	8.74	8.98	8.63	9.12
1.024	4.19	4.53	6.39	4.68	8.57
Σ |%RE|	87.32	77.03	77.05	77.13	79.41
Mean R^2	0.9989	0.9995	0.9988	0.9994	0.9983

Table A.3: Nominal concentrations and their respective sum of absolute relative errors calculated using unweighted and weighted models with empirical weights $1/x$, $1/x^2$, $1/y$ and $1/y^2$ for the fragment at m/z 87.05 of Glutamine.

Nominal concentration (pmol/µL)	Model 1 $1/x^0$ (OLS)	Model 2 $1/x$ (WLS)	Model 3 $1/x^2$ (WLS)	Model 4 $1/y$ (WLS)	Model 5 $1/y^2$ (WLS)
0.049	17.19	16.81	14.58	14.17	8.98
0.069	32.60	18.11	18.98	19.78	22.50
0.098	19.88	12.19	11.95	13.54	14.30
0.296	20.72	21.08	20.70	20.70	20.87
0.492	15.64	15.11	14.52	14.97	15.25
0.789	16.60	17.05	17.35	17.37	16.70
1.003	7.46	6.87	6.44	6.61	7.18
Σ |%RE|	130.08	107.22	104.52	107.15	105.78
Mean R^2	0.9973	0.9988	0.9975	0.9989	0.9970

A.4 Method application in CSF samples

A.4.1 CSF samples

Table A.4: Complementary information on the CSF samples analyzed.

Nº	Age	Gender	Grup
#05	50	F	Aβ -
#06	54	F	Aβ -
#07	55	F	Aβ -
#08	58	F	Aβ -
#09	59	F	Aβ -
#10	59	F	Aβ -
#11	60	F	Aβ -
#12	60	F	Aβ -
#13	61	F	Aβ -
#24	60	F	Aβ -
#27	46	M	Aβ -
#28	57	M	Aβ -
#29	57	M	Aβ -
#30	60	M	Aβ -
#31	62	M	Aβ -
#32	63	M	Aβ -
#33	64	M	Aβ -
#34	68	M	Aβ -
#35	68	M	Aβ -
#36	70	M	Aβ -
#38	49	F	Aβ +
#39	54	F	Aβ +
#40	55	F	Aβ +
#41	57	F	Aβ +
#42	60	F	Aβ +
#43	65	F	Aβ +
#44	68	F	Aβ +
#45	70	F	Aβ +
#46	71	F	Aβ +
#47	71	F	Aβ +
#48	71	F	Aβ +
#52	54	M	Aβ +
#53	55	M	Aβ +
#54	58	M	Aβ +
#55	62	M	Aβ +
#56	64	M	Aβ +
#57	69	M	Aβ +
#58	78	M	Aβ +
#59	80	M	Aβ +
#60	64	M	Aβ +

F – female; M – male

Table A.5: Measurement of glutamine and GABA in Aβ- group

Nº	Gln (area ratio)	GABA (area ratio)
#05	2.69	0.03
#06	1.02	0.04
#07	1.26	0.03
#08	1.25	0.11
#09	1.56	0.04
#10	0.81	0.07
#11	0.51	0.06
#12	0.63	0.06
#13	0.87	0.05
#24	1.18	0.08
#27	1.87	0.04
#28	1.43	0.04
#29	1.20	0.04
#30	0.74	0.13
#31	1.68	0.04
#32	1.18	0.03
#33	1.55	0.06
#34	0.76	0.09
#35	1.23	0.06
#36	3.88	0.03

Table A.6: Measurement of glutamine and GABA in Aβ + group

Nº	Gln (area ratio)	GABA (area ratio)
#38	1.04	0.05
#39	1.43	0.04
#40	1.18	0.03
#41	1.72	0.04
#42	1.44	0.04
#43	1.85	0.03
#44	1.88	0.05
#45	2.16	0.06
#46	4.64	0.02
#47	4.51	0.05
#48	1.54	0.02
#52	2.39	0.04
#53	1.24	0.06
#54	1.08	0.07
#55	1.50	0.02
#56	0.80	0.05
#57	1.44	0.04
#58	1.76	0.02
#59	0.63	0.04
#60	1.13	0.03

Table A.7: Analysis of variability in the areas ratios obtained for each ion monitored in glutamine and GABA in the calibration curve. AR: area ratio

Parameters	Gln		GABA	
	AR 130/84	AR 101/84	AR 69/87	AR 43/87
Mean	1.38	7.81	0.48	0.50
Standard deviation	0.06	1.65	0.02	0.03
% RSD	4.01	21.16	5.17	6.69

Table A.8: Statistic analysis of the data acquired for the measurement of glutamine in CSF samples from patients with AD, with studies Aβ+ and Aβ-.

	Median (area ratio)	Average	Standard deviation	% RSD	Fold change	P_{value}
Aβ+	1.47	1.77	1.05	59.57	1.21	0.108
Aβ-	1.21	1.36	0.77	56.70		

Table A.9: Statistic data analysis for the measurement of glutamine comparing females and males from Aβ+ and Aβ-.

Gender	Group	Median (area ratio)	Average	Standard deviation	% RSD	Fold change	P_{value}
Females	Aβ+	1.72	2.12	1.25	58.90	1.57	0.013
	Aβ-	1.10	1.18	0.62	52.54		
Males	Aβ+	1.24	1.33	0.53	39.79	0.87	0.720
	Aβ-	1.43	1.55	0.90	57.76		

Table A.10: Statistic analysis of the data acquired for the measurement of GABA in CSF samples from patients with AD, with studies Aβ+ and Aβ-.

	Median (area ratio)	Average	Standard deviation	% RSD	Fold change	P_{value}
Aβ+	0.04	0.04	0.01	33.86	0.87	0.056
Aβ-	0.05	0.06	0.03	46.98		

Table A.11: Statistic data analysis for the measurement of GABA comparing females and males Aβ+ and Aβ-.

Gender	Group	Median (area ratio)	Average	Standard deviation	% RSD	Fold change	P_{value}
Females	Aβ+	0.04	0.04	0.01	33.01	0.73	0.051
	Aβ-	0.06	0.06	0.02	39.88		
Males	Aβ+	0.04	0.04	0.02	36.52	0.98	0.497
	Aβ-	0.04	0.06	0.03	55.83		

Table A.12: Statistical data analysis for ratios of measurements of GABA/Gln comparing Aβ+ and Aβ- groups.

	Median (area ratio)	Average	Standard deviation	% RSD	P_{value}
Aβ+	0.03	0.03	0.02	0.61	0.070
Aβ-	0.04	0.06	0.04	0.77	

Table A.13: Statistical data analysis for ratios of measurements of GABA/Gln comparing females and males Aβ+ and Aβ-.

Gender	Group	Median (ratio)	Average	Standard deviation	% RSD	P_{value}
Females	Aβ+	0.03	0.02	0.01	0.50	0.038
	Aβ-	0.06	0.06	0.04	0.62	
Males	Aβ+	0.03	0.04	0.02	0.58	0.968
	Aβ-	0.03	0.05	0.05	1.01	

Table A.14: Statistic data analysis for the measurement of glutamine focused on the ages of the patients in the groups Aβ+ and Aβ-.

Ages	Group	Median (area ratio)	Average	Standard deviation	% RSD	Fold change	P_{value}
≥ 60	Aβ+	1.54	1.94	1.24	63.91	1.31	0.189
	Aβ-	1.18	1.29	0.94	72.51		
≤ 60	Aβ+	1.24	1.44	0.48	0.33	0.99	0.918
	Aβ-	1.26	1.45	0.56	0.38		

Table A.15: Statistic data analysis for the measurement of GABA focused on the ages of the patients in the groups Aβ+ and Aβ-.

Ages	Group	Median (area ratio)	Average	Standard deviation	% RSD	Fold change	P_{value}
≥ 60	Aβ+	0.04	0.04	0.01	36.45	0.63	0.006
	Aβ-	0.06	0.06	0.03	44.54		
≤ 60	Aβ+	0.04	0.05	0.01	0.27	1.11	0.536
	Aβ-	0.04	0.05	0.02	0.49		

Table A.16: Statistic data analysis for ratios of measurements of GABA/Gln focused on the ages of the patients in the groups Aβ+ and Aβ-.

Ages	Group	Median (area ratio)	Average	Standard deviation	% RSD	P_{value}
≥ 60	Aβ+	0.02	0.03	0.03	0.78	0.741
	Aβ-	0.04	0.05	0.03	0.61	
≤ 60	Aβ+	0.04	0.04	0.02	0.49	0.164
	Aβ-	0.03	0.04	0.02	0.45	